ARCHITECTURE OF THE TRANSMEMBRANE SIGNALING ARRAYS THAT REGULATE BACTERIAL CHEMOTAXIS

A Dissertation

Presented to the Faculty of the Graduate School

of Cornell University

In Partial Fulfillment of the Requirements for the Degree of

Doctor of Philosophy

by

Xiaoxiao Li

August 2012

ARCHITECTURE OF THE TRANSMEMBRANE SIGNALING ARRAYS THAT REGULATE BACTERIAL CHEMOTAXIS

Xiaoxiao Li, Ph. D.

Cornell University 2012

Bacterial chemotaxis is the behavior of bacteria to swim towards favorable chemical locations, while away from unfavorable ones. The ternary complex, which is comprised of the transmembrane methyl accepting chemotaxis protein (MCP), the coupling protein CheW and the kinase CheA, is essential to the signaling pathway. The regulation of CheA by MCPs determines the rotation bias of the flagella and hence the movement of the cells. The exquisitely high sensitivity and signal amplification of chemotaxis is attributed to the architecture of individual complexes and their assembly into larger arrays.

This dissertation focuses on the study of the ternary complex using various biophysical methods. We determined the first crystal structure of the ternary complex in *Thermotoga maritima*. The components in the complex crystal structure are well conserved among bacteria and therefore we believe this architecture is likely to be commonly preserved. We proposed a model on the assembly of the complex arrays from individual complex based on this crystal structure and the electron cryotomography findings by our collaborators. We also determined a crystallographic dimer structure of the coupling protein CheW. Based on this dimer structure of CheW

as well as a previously determined crystallographic dimer structure of the regulatory domain of CheA, we suggest other possible ways of that the receptor arrays may assembly.

We also designed and obtained cytoplasmic regions of MCPs associated by a trimerization motif. These designed "trimers-of-receptor-dimers" form a stimulatory complex with CheA and CheW. We probed the conformation of the resulted stimulatory complex and compared it with the conformation of the previously characterized inhibitory complex.

BIOGRAPHICAL SKETCH

Xiaoxiao Li was born in Harbin, China and raised up in this northeastern city of ten million people. She is the only child of her parents, but she grew up in a big family, being very close to her grandparents and her extended family. She was a curious kid and found interests particularly in nature. Her favorite classes were science and literature in school. She attended Harbin Number One hundred and thirteen Middle School and first developed an interest for chemistry in middle school. She attended Harbin Number Three High School and deepened her interest in chemistry there. At the age of seventeen, she left her hometown to go to college in Beijing. Xiaoxiao graduated from Peking University with a B.S. from the College of Chemistry and Chemical engineering. In college, she did undergraduate research on growing carbon-nanotubes in Prof. Yan Li's lab. After college, she decided to pursue a career in science and to travel abroad for advanced degrees. She joined the Department of Chemistry at Duke University. She learned more biochemistry at Duke and worked in the lab of Prof. Barbara Shaw on applying borano-modified DNA/RNA as potential antiviral agents. She graduated with a M.S. from Duke and transferred to Cornell University two years later. She joined Prof. Brian Crane's lab at Cornell University and worked on the signaling complex that regulate the bacterial chemotaxis. Xiaoxiao married Yi Wu in Ithaca, NY where Cornell is located.

Dedicated to my grandparents

ACKNOWLEDGMENTS

Xiaoxiao is grateful to her family, not just her parents and her husband, but her whole extended family. Three of her grandparents do not live up to this day to see her getting her Ph.D. degree, but they all knew that she was a bright kid and would achieve her goal despite of great effort. She would like to thank her grandparents, for giving her great love, trust and support, most importantly, that they passed on the wisdom of learning to be open minded and grateful.

Xiaoxiao thanks her parents for everything, especially for giving her freedom and encouraging her to think independently since she was very little. They give advices but do not intervene with her choices. They have been the most loving and supportive parents all along.

Xiaoxiao thanks her husband for loving her, tolerating her bad temper every time she has it. She thanks him also for believing in her, even at moments when she doubts herself.

Xiaoxiao would like to thank her longtime friends, especially Xiaoyu, without whose encouragement her morality could be much lower during the hard times, in graduate school particularly, without whose perspective she would not be practical.

Five years at Cornell has been a memorable experience for Xiaoxiao. Among all the aspects, she cherishes the interactions with the people she met at Cornell the most. She was with a group of very kind and caring people. Her advisor, Brian Crane, is an understanding and intelligent man. She wishes she could have learned more from him. Alex, Brian's wife, has been a patient, whimsical teacher. Joanne Widom, who is

at her grandma's age and still actively contributes to science, is a model for her. Ria, Bee, Camille and Anna are her everyday company, who shared every bit of these years' surprises and wonders with her. Anand has been a great friend, who she trusts a lot and has fun conversations with quite often. Tom and Ken have shared laughter with her throughout the years. Sarah and Karen are great scientists who are currently postdocs in the lab. They are not only good experimenters, but also excellent presenters. They both devoted time on proof reading Xiaoxiao's thesis. Xiaoxiao is very grateful for their help. Greg and Craig, Dipanjan are the cheerful juniors in the lab. Talking with them has been a pleasure for Xiaoxiao. Bhumit, Mike, Abiola and Sudhamsu, her former labmates, shared their knowledge in science with her and their secrets on how to enjoy graduate school. She would also like to thank her former labmates Jaya, Gaby and Brian Z because in Xiaoxiao's early days in the lab, they all offered suggestions and advices to her.

Xiaoxiao acquainted with a few people outside the lab and became good friends with many of them. She would like to thank Yang, for sharing amusing stories, accompanying her to movies and lunches. She would like to thank the group of friend who dine with her weekly: Zihui, Qi, Xiaoyang, Mingshu, Zhaoyin, Zhao, Xiaonan and Guozhang, Yading, Yibei, Yao, Zhen, and Weishan. Every week's gathering time had been very enjoyable to her.

Her friends in and out the lab had been with her through the ups and downs. They are there at her wedding in Ithaca, whose smiles she would look over and over again whenever she looks at her wedding pictures. Everyday life can be trivial and sometimes tiring. But when she looks back, the tiring part surely will be blurred. She

will only remember that she was there laughing and having a good time. She had people she could chat with. A small conversation, a warm smile, a pointless argument shall be all that she will remember.

Xiaoxiao would like to thank her committee members, Prof. Steve Ealick and Prof. Rick Cerione. They both have been very nice to her and offered her advice and support generously whenever needed. She would also like to thank people who offered help on her experiments. Peter Borbat from the Freed group has taught her a lot and helped her greatly on her EPR experiments. It was always lighthearted for her to have a conversation with Peter. Peter is not only knowledgeable and intelligent, but also has a good sense of humor. Prof. Holger Sondermann and his student Laura Byrnes have assisted her on MALS. Prof. Chris Fromme taught her how to set up the robotic tray. Prof. Peng Chen and his student Aaron Keller have assisted her in doing FRET experiments. Aaron is very patient and is the most organized person Xiaoxiao has ever known. She would like to thank Cynthia Kinsland, whose lab she visited numerous times for all sorts of experiments.

Xiaoxiao also has regrets for the past five years. She wishes she had spent more time with her husband, her parents and her friends. She wishes she had made more friends in Ithaca and hanged out more with them. Nevertheless, she is fine leaving Cornell with these regrets. She will embrace the nature of great imperfection of her life and a new era of life that might come with more regrets.

TABLE OF CONTENTS

LIST OF FIGURES

LIST OF TABLES

Table

LIST OF ABBREVIATIONS

ADP adenosine 5'-diphosphate

ATP adenosine 5'-triphosphate

BME β-mercaptoethanol

DEER Double Electron Electron Resonance

DTT dithiothreitol

DNA deoxy nucleic acid

DQC Double-quantum coherence

Ec or *E. coli Escherichia coli*

ECT electron cryotomography

EM Electron Microscopy

EPR Electron Paramagnetic Resonance

FPLC Fast Protein Liquid Chromatography

HAMP Histidine kinase, Adenylyl cyclase, Methyl-accepting protein, and Phosphatase

IPTG β-D-thiogalactopyranosidase

MALS Multi-Angle Light Scattering

MCP Methyl-accepting Chemotaxis Protein

MS Mass Spectrometry

MTSL *S*-(2,2,5,5-tetramethyl-2,5-dihydro-1H-pyrrol-3-yl)methyl

methanesulfonothioate

NADH β-Nicotinamide Adenine Dinucleotide

Ni-NTA Nickel-Nitriloacetic Acid

NMR Nuclear Magnetic Resonance

PAGE polyacrylamide gel electrophoresis

PMSF phenylmethanesulfonylfluoride

SDS sodium dodecyl sulfate

Tm or T. maritima Thermotoga maritima

TMEA thio-specific agent Tris-(2-maleimidoethyl)amine

CHAPTER ONE

INTRODUCTION ON BACTERIAL CHEMOTAXIS

1.1 Overview of chemotaxis

Chemotaxis describes the ability of bacteria to modulate their movement in response to chemicals sensed in their environment. In the absence of chemical stimuli, bacteria cells spend more time smooth swimming than tumbling. In the presence of a concentration gradient of attractants, bacteria lengthen the time for smooth swimming to swim up the gradient; on the other hand, in the presence of repellents, bacteria tumble more in order to reorient themselves and move away from the repellent source.

The bacterial chemotaxis signaling pathway bears remarkable sensitivity, dynamic sensing range, and high signal gain. Bacteria (e.g. *Escherichia coli)* can sense ligands (either repellent or attractant) on a significantly broad concentration range, from the concentration of 10 μM to 1 M. Moreover, bacteria are very sensitive to environmental changes. Specifically, *E. coli* cells respond to a < 1% change of the ligand occupancy of aspartates (Jasuja et al. 11346-51) . A fraction of changes in ligand binding can induce fraction changes up to 14 times in the kinase activity, and changes in the flagella rotation bias (Segall, Block and Berg 8987-91) . To date, there is vast information, both experimental and theoretical, on the distinct features of the chemotaxis signaling system (Wadhams and Armitage 1024-37; Hazelbauer and Lai 124-132; Sourjik and Armitage 2724-2733; Sourjik 569-576) . Molecular components of the signaling cascades have been identified and characterized (Parkinson 857-71) . Interactions among those components have been probed (Wadhams and Armitage 1024-37) . Localizations

and dynamics of the components have been visualized and measured (Sourjik and Armitage 2724-2733) . Models for the sensing and responding networks have been built (Falke and Erbse 1149-51; Hazelbauer and Lai 124-132; Sourjik 569-576; Park et al. 400-407; Bhatnagar et al. 3824-41) . Because the signaling pathway of bacterial chemotaxis has been heavily investigated, and because it is a relatively simple system compared to other signaling pathways, bacterial chemotaxis has become a prototype for transmembrane signaling pathways. Thanks to much research undertaken for the last forty years, we now have a good overall understanding of this signaling pathway on the molecular level (Wadhams and Armitage 1024-37).

The bacterial chemotaxis signaling pathway is a typical two-component system. Two component signaling pathways typically involve a transmembrane histidine kinase that senses the signal and a response regulator to relay the signal to downstream effectors. In bacterial chemotaxis the first component is substituted by a transmembrane receptor with a bound cytoplasmic histidine kinase.

The signaling pathway responsible for bacterial chemotaxis involves two transmembrane macromolecular complexes. One complex located at the cell poles senses the signal and regulates downstream signaling cascades. The other complex either resides on the lateral membrane (e.g. *E. coli)* or at the cell pole (e.g. *Thermotoga maritima*) and responds to the signal by changing the rotation bias of the flagella and hence the movement of the cell. Both complexes involve a delicate assembly of multiple proteins.

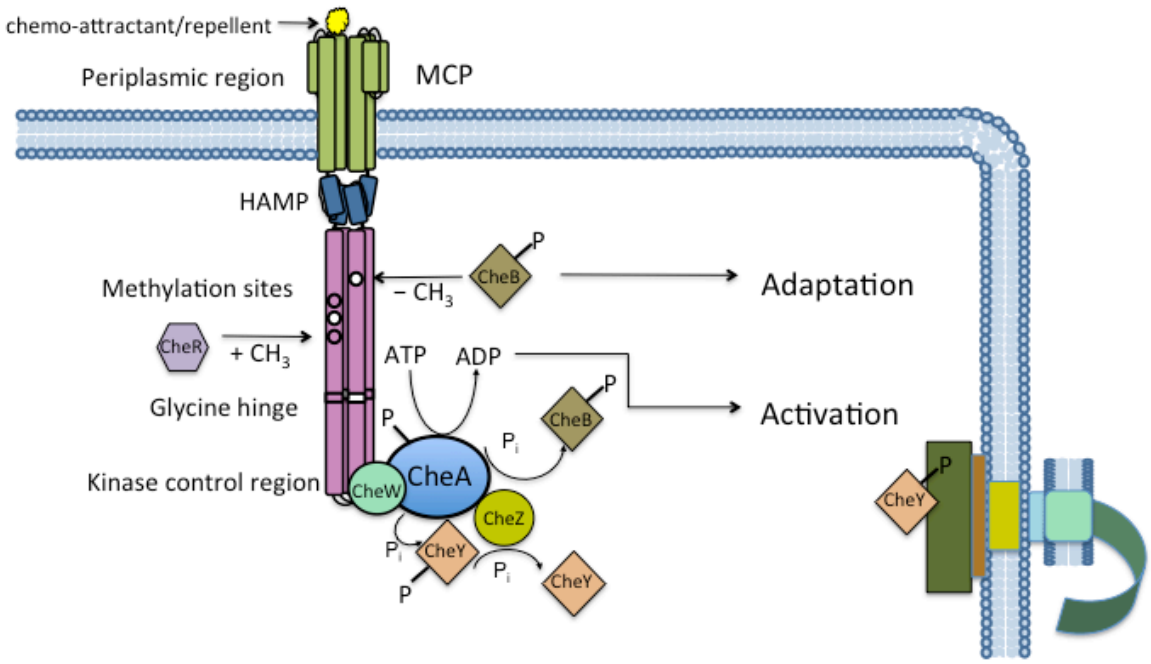

Fig. 1-1 Schematic of bacterial chemotaxis signaling pathway. Each chemotaxis protein is represented with shapes of solid colors except for the MCP, which is segmented in three parts: the periplasmic domain together with the transmembrane domain, the HAMP domain and the cytoplasmic domain. Phosphoryl groups are denoted as capitalized P on the schematic. Auto-phosphorylation, phosphor-transfer, methylation, demethylation and deamidation reactions are depicted with arrows.

The signaling complex, which assembles into extended arrays across the membrane, is composed of transmembrane methyl accepting chemotaxis proteins (MCPs), coupling proteins CheW, and auto-kinases CheA. Additional proteins such as CheZ and CheY also co-localize with the complex (Sourjik and Armitage 2724-2733) . The ternary complex made of MCPs, CheA and CheW is stable, showing low exchange rate with newly expressed proteins or free cytoplasmic proteins *in vivo*(Schulmeister et

al. 6403-6408). The motor complex, also known as the flagella complex, comprises more molecular components than the signaling complex (Wadhams and Armitage 1024-37) . It is the result of tightly regulated expression of about 50 genes and very much resembles a real motor (Blair 489-522) . The torque is generated with the aid of a stator part of the complex that sits through cytoplasm, periplasm, inner membrane and the peptidoglycan layer. The C-ring, a cytoplasmic region of the flagella complex, controls the direction of flagella rotation. The C-ring is composed of multiple copies of the proteins FliM, FliG and FliN. The signal messenger regulated by the signaling complex is the response regulator protein CheY. CheY binds to the FliM/FliN portion of the motor complex to convey the signal (Lee et al. 52-6; Dyer et al. 71-84; Sarkar, Paul and Blair 9370-5) .

1.2 Sensing and responding to the signal

This thesis is focused on the signaling complex. As mentioned earlier, the signaling complex localizes at the cell poles and forms a stable complex. The exchange time of the MCPs with newly expressed MCPs is longer than a cell cycle. The kinase and coupling protein also exchange slowly with their unbound counterparts (Schulmeister et al. 6403-6408). *In vitro*, the ternary complex can be reconstituted without losing its functions and is found to be stable even under harsh conditions (Erbse and Falke 6975-6987).

When the periplasmic domain of the MCP binds ligands, a signal is propagated downward through the membrane to the membrane distal signaling region of the MCP. When the ligands bound are chemo-repellents (such as heavy metal ions), the kinase CheA that is bound to MCPs, via the coupling protein CheW, auto-phosphorylates on a conserved His residue. Phosphorylated CheA can transfer this signal by phosphorylating

the response regulator CheY. Phosphorylated CheY diffuses to the motor complex and binds to FliM. This binding induces the rotation of the motor complex to switch direction, and results in the flagellum having a more biased clockwise rotation. In most bacteria, the flagellum is a left-handed coiled coil, the hardness and wavelength of which can be altered depending on the direction of the rotation. A clockwise rotation shortens the length of the flagellum and causes the once bundled flagella to come apart. As a result, the bacterium starts to tumble and as a result reorients itself. Phosphorylated CheY has enhanced binding affinity over unphosphorylated CheY for binding FliM. Therefore, by controlling the level of phosphorylated CheY, the kinase that is regulated by the MCP exerts control over the movement of the cell. When ligands bound are chemo-attractants (such as amino acids), the kinase activity of CheA is suppressed, causing a lower steady state concentration of phosphorylated CheY. As a result, the flagella have a biased counter-clockwise rotation. The bundle of flagella re-forms and propels the bacteria to swim smoothly.

CheY dephosphorylates itself on the time scale of 10s, which is a relatively high rate (Segall, Manson and Berg 855-7) . The phosphatase CheZ accelerates the process to the time scale of 0.1 s (Segall, Manson and Berg 855-7) . CheZ is also localized at the poles with the ternary complex (Vaknin and Berg 1416-1423) and will be discussed in further detail in chapter two. Interestingly, CheZ can accelerate the phospho-transfer from CheA to CheY when CheY is bound to CheZ (Guhaniyogi et al. 1419-28; Schuster, Silversmith and Bourret 6003-8) . Given that the phosphorylation and dephosphorylation reactions both happen within 20-30s and 0.1s, respectively (Levit, Liu and Stock 6651-8;

Sourjik and Berg 12669-74) , the response time to signal is short, as observed in the behavioral studies.

1.3 Adaption to the signal

In order to move up the concentration gradient further, bacteria in their current environment have to be able to reset themselves to the pre-stimulus level. MCP can undergo reversible methylation and demethylation at specific conserved glutamate residues (Chao et al. 561-571; Kehry and Dahlquist 761-72; Springer and Koshland DE 533-7) . The modification state of the MCP determines its activity: methylation increases its activity while demethylation lowers it (Sourjik and Berg 437-41; Borkovich, Alex and Simon 6756-60) . Because the kinase activity is coupled to the states of the MCPs, methylation/demethylation indirectly affect the activity of the kinase. In *E. coli,* adaptation requires two enzymes, the methyl-esterase CheB and the methyltransferase CheR (Springer and Koshland DE 533-7) . CheB can deamidate and demethylate the MCPs; the activity of MCP is modulated by the kinase activity of CheA through its response regulator domain, which CheA phosphorylates (Kehry, Doak and Dahlquist 983-90; Kehry et al. 3599-603). The adaptation pathway can reset the kinase activity to a pre-stimulus level and allow the bacteria to respond to changes in the environment. The time scale of adaptation is longer than that of sensing and responding. It is on the time scale of minutes, which allows the bacteria to compare its current conditions with those of minutes ago.

1.4 Cooperativity in sensing and adaption

In *E. coli*, there are five types of MCP homo-dimers with distinctive periplasmic ligand binding domains. MCPs that are located at the cell poles can form mixed trimer-

of-dimers and further cluster into higher order arrays (Sourjik 569-576; Hazelbauer and Lai 124-132) . Mixed clusters of different MCPs can incorporate different signals and perform cooperative sensing (Hansen, Sourjik and Wingreen 17170-5; Gestwicki and Kiessling 81-4) . Deactivation of the MCPs is also highly cooperative (Gestwicki and Kiessling 81-4) . A team model for MCP signaling can account for the observed cooperativity, in which a group of mixed MCPs with finite coupling strength can switch on/off simultaneously based on the initial activity of the coupled MCPs (Sourjik and Berg 437-41; Sourjik 569-576; Hansen, Sourjik and Wingreen 17170-5; Sourjik and Wingreen 262-8) . For inactive MCPs, binding to a few attractants stabilizes the inactive form of all the coupled MCPs. For active MCPs, the transition to the inactive form only happens when the majority of the coupled MCPs are bound with attractants. The sensitivity of the signaling pathway increases as the number of coupled MCPs increases. In terms of adaptation, CheR and CheB can act on 4-6 adjacent MCPs when bound to one MCP (Li and Hazelbauer 1617-1626) . Methyl-transfer among MCPs enables the adaptation enzymes to exert control over a broad range of MCPs and affect the sensitivity of the coupled MCPs (Kim et al. 119-35; Sourjik and Berg 437-41) .

1.5 Individual components of the pathway

1.5.1 MCP

The key to the transmembrane signaling apparatus is the MCP. In *E. coli*, there are five types of MCPs: high abundance receptors Tsr and Tar, and low abundance receptors Trg, Tap and Aer (Hazelbauer and Lai 124-132) . Tsr is responsible for serine and redox level sensing; Tar is responsible for aspartate and maltose sensing; Trg is

responsible for ribose, galactose and thermo sensing; Tap is responsible for peptide and thermo sensing; Aer is responsible for sensing redox level sensing.

The MCP is a naturally homo-dimer, regardless of its ligand occupancy. MCPs consist of a periplasmic domain, a transmembrane domain, and a cytoplasmic domain that forms a four-stranded antiparallel helical coiled-coil (Pollard, Bilwes and Crane 1936-44) . MCPs cluster into patches that contain thousands of MCPs at one or both cell poles, with only few clustering at the lateral positions. Different types of MCPs are believed to form mixed arrays at the cell poles (Ames and Parkinson 9292-9297) and perform cooperatively to regulate the kinase activity. It will be discussed in chapter two how the high sensitivity of MCPs is a result of clustering.

1.5.1.1 Different signaling modules of the MCPs

MCP signaling is first triggered upon ligand binding to the MCP periplasmic domain. The signal is propagated through the membrane, and along the 300 Å long cytoplasmic region to the membrane distal tip region to which the kinase is bound (for a schematic of the MCP, see Fig. 1-1). All five types of MCP dimers in *E. coli* span the membrane with four helices. A HAMP domain follows on the cytoplasmic side of the membrane. HAMP domains are common signal-transducing protein motifs named after proteins in which this motif was found: Histidine kinase, Adenylyl cyclase, Methyl-accepting protein, and Phosphatase. Flanking the HAMP domain is the methylation region (or adaptation region) where the conserved Glu/Gln residues that undergo reversible methylation/demethylation are found followed by a glycine hinge. The most membrane distal region is the conserved kinase control tip region, which is the region responsible for regulating the kinase activity (this domain is also known as the signaling

domain) (Alexander and Zhulin 2885-90; Le Moual and Koshland DE 568-85). Each signaling module transduces the signal presumably through conformational changes. Changes occurring at different modules are correlated with each other in a manner that is not yet fully understood.

Periplasmic module of MCP

Four types of MCPs (Tsr, Tar, Trg and Tap) have periplasmic modules that bind to various ligands such as amino acids, metal ions, and carbohydrates. The sequence conservation of the periplasmic ligand binding module is low and the structures determined on the different periplasmic domains elucidate the specificity of the ligand binding to different periplasmic domains (Lacal et al. 2873-2884; Jancarik et al. 31-4; Spurlino, Lu and Quiocho 5202-19; Vyas, Vyas and Quiocho 5226-37; Mowbray and Petsko 7991-7; Milburn et al. 1342-7) . This variety within the module allows the bacteria to sense different environmental cues. Although each MCP has two symmetrical ligand binding sites on two subunits, in the crystal structure of Tar specifically, only one subunit is occupied presumably due to negative cooperativity (Milburn et al. 1342-7; Tatsuno et al. 423-5) .

Transmembrane module of MCP

The transmembrane module of the MCP has been the subject of fewer studies. However, by probing the regions proximal to the membrane spanning helices, a piston displacement of a membrane spanning helix is predicted to transduce the signal (Falke and Erbse 1149-51; Falke and Hazelbauer 257-65) . Structure comparison of apo- and attractant- bound MCPs revealed a piston movement of the C-terminal helix towards the cytoplasm (Milburn et al. 1342-7) . Because the C-terminal helix is believed to be

continuous with the transmembrane part of MCP, such a movement is predicted to be propagated downwards through the membrane. This piston displacement was detected with Electron Paramagnetic Resonance (EPR) spectroscopy (Ottemann et al. 1751-4) . Furthermore, modifications on the anchors of the membrane spanning helices can trap the helices in different positions across the membrane, which could mimic the helix movement during signal transduction (Miller and Falke 1763-70; Draheim et al. 1268-1277) .

HAMP of MCP

In *E. coli* MCPs, immediately below the transmembrane module is the HAMP domain. The HAMP domain is a commonly found signaling module between the transmembrane region and the cytoplasmic region in bacteria. This domain plays a crucial important role in converting transmembrane signals into downstream output signals.

The first HAMP structure was determined with nuclear magnetic resonance (NMR) (Hulko et al. 929-940) . This HAMP domain is part of an archaeal, hyperthermophilic transmembrane protein of unknown function in *Archaeoglobus fulgidus* (Hulko et al. 929-940). Each monomer of this dimeric HAMP domain is composed of two parallel helices that are connected with a non-helical linker. Upon dimerization the two monomers form a tight parallel four-helix bundle, with the two linkers wrapped around the two monomers. Later, the structure of three concatenated HAMP domains from the *P.aeruginosa* aerotaxis protein Aer2 was determined with X-ray crystallography (Airola et al. 436-48). In this structure, the first and the third HAMP domains have similar conformations with that of the "canonical" NMR structure. By

contrast, the second HAMP domain is different from the "canonical" HAMP. While still folding as a parallel four-helix bundle, this HAMP is more loosely packed, with the two monomers more splayed apart. In addition, the interactions that stabilize the packing in the second HAMP domain are different from those observed in the "canonical" HAMP structure. The two different types of HAMP conformations may represent different signaling states of the HAMP domain and may induce different conformational changes of downstream modules.

Adaptation module of MCP

About 140 to 195 Å away from the MCP tip are the conserved Glu/Gln residues that can undergo reversible methylation/demethylation reactions. The reversible methylation/ demethylation reactions modulate the overall charge of the MCPs, and presumably affect the packing and the density of the MCP clusters. MCP density seems to coincide with the level of kinase activity of MCPs-associated CheA. High density MCPs stimulate the kinase activity, while low density MCPs inhibit the kinase activity (Besschetnova et al. 12289-12294).

Glycine Hinge of MCP

The residue glycine provides more flexibility to the protein backbone than any other amino acid. In MCPs, there is a glycine hinge which comprises three conserved glycine residues forming a ring around the four-helix bundle (for *S. typhimurium* Tar, G338, G339, and G437) below the adaptation region, which is thought to facilitate the inter-conversion between MCP's functional states or to allow more functional fluctuations regarding the different states (Coleman et al. 7687-7695). Mutations to any of the highly conserved glycine residues at the glycine hinge module, even to alanine, a

comparatively subtle substitute, caused the cells to experience defective chemotaxis and phenotypes corresponding to either inactivation of the kinase or failure on the part of the MCP to modulate the kinase activity upon addition of attractant (Coleman et al. 7687-7695). The three essential glycine residues reside on the same plane horizontally at the boundary between the adaptation and signaling modules and they could allow for a bend that is either important for inter-dimer packing or has a mechanistic role in on-off switching (Coleman et al. 7687-7695) .

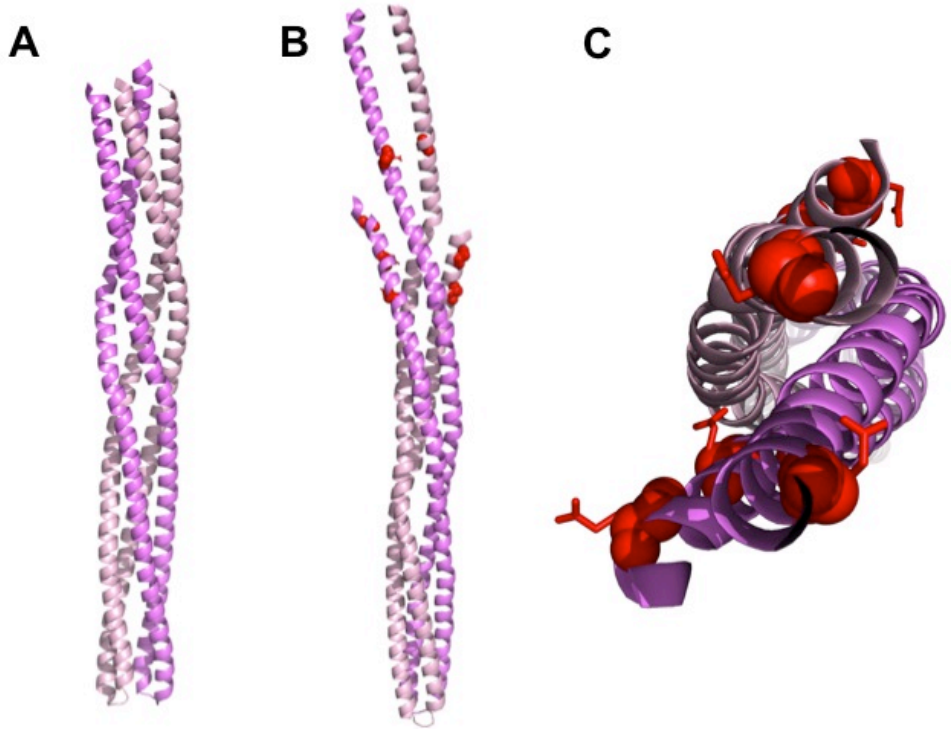

Fig. 1-2 The helical coiled-coil cytoplasmic domain of MCP. The cytoplasmic region of two homo-dimers of MCPs from two distant families of bacteria *T. maritima* and *E. coli* share overall structural similarity. The two subunits are colored with different shades of pink. A. Cytosolic pseudo MCP Tm14. PDB: 3G67. B. EcMCP Tsr. PDB:

1QU7. C. Top view of the EcMCP Tsr with methylation sites depicted as red balls. The side chains of conserved glutamine in this structure are denoted in stick model.

Signaling module of MCP

The cytoplasmic region of the MCP beyond the HAMP domain is composed of repeated helical heptads. The crystal structures of three MCPs cytoplasmic fragments − one from *E.* coli and two from *T.* maritima, an archaea very phylogenetically distant from *E. coli* − display very similar coiled coil structures (Fig. 1-2)(Kim, Yokota and Kim 787-92; Pollard, Bilwes and Crane 1936-44; Park et al. 400-407). Comparative genomic analyses of over 2000 MCPs from 152 species groups the MCPs into 7 major classes according to the number of heptads spanning the cytoplasmic region (Alexander and Zhulin 2885-90). This study also revealed that 10 of the 11 trimer contact residues, which were predicted in the trimer-of-dimer crystal structure of the serine sensing MCP, are highly conserved among all classes. The high conservation of the signaling module is believed to allow for mixed MCP clustering and evolutionarily preserved CheA/CheW binding. Biochemical data also supports the binding of CheA and CheW at this module (Bhatnagar et al. 3824-41; Park et al. 400-407; Boukhvalova, Dahlquist and Stewart 22251-9) .

NWETF motif

The MCP C-terminal penta-peptide NWETF, which is linked by a long linker to the cytoplasmic domain of MCP, is conserved in the two high abundance *E. coli* MCPs Tar and Tsr. This penta-peptide is the docking site for the methylesterase CheR, and is required for CheR to localize *in vivo* (Shiomi et al. 42325-33).

1.5.1.2 Signal transduction along the modules of the MCP

It was proposed that the adaptation module and the signaling module are anti-symmetrically coupled (Swain, Gonzalez and Falke 9266-9277). Mutations that disrupt or loosen the helix-helix packing in either the adaptation or the signaling modules were probed with kinase activation and methylation assays, respectively. It was found that 54% of the mutations in the adaptation module lead to the kinase lock-on state while 62% of the mutations in the signaling module lead to kinase lock-off state. The authors proposed that strong helix packing in the adaption region stabilizes a kinase on-state, while at the same time the signaling module is more mobile and loosely packed. The off-state is proposed to have reverse packing in the two modules.

1.5.2 CheA

CheA is a homo-dimer auto-kinase, an essential chemotaxis protein. CheA is a multi-domain protein; the individual domain structure of CheA and the multiple domain structure have already been determined (Bilwes et al. 131-41; Bilwes et al. 353-60; Quezada et al. 1283-94; Park et al. 11646-51).

1.5.2.1 Domains of CheA and their structures

CheA has five domains with distinct functions. P1 is the histidine phospho-transfer (Hpt) domain, where the conserved His phosphorylation site is located (His 45 in *Thermotoga maritima,* His 48 in *Escherichia coli*). P2 is the response regulator binding domain to which CheY and CheB bind. P3 is the dimerization domain, composed of dimeric antiparallel helical coiled coils. P4 is the catalytic/kinase domain, which has an ATP binding pocket. P5 is the regulatory domain that is a homolog to the coupling protein CheW.

P1 domain

P1 is a four-helix bundle with the conserved histidine side chain facing towards the solvent or its binding partners (Quezada et al. 1283-94; Quezada et al. 30581-5). In *E. coli*, CheA has an allele protein $CheA_s$, which lacks the first four helices of P1. The remaining helix of P1 on $CheA_s$ binds to the phosphatase CheZ (Hao et al. 5842-4) . CheA does not bind to CheZ as the last helix in P1 on CheA is not accessible for binding.

P2 domain

P2 binds to the response regulators CheY and CheB. Connecting P2 to P1, and P3 are two long, flexible linkers (25-45 residues) (Zhou et al. 433-43) . The P2 domain is the least conserved among all domains of CheA. The *Myxococcus xanthus* FrzE protein, a CheA homologue, does not have a P2 domain. Instead, it has a proline and alanine rich linker of 130 residues tethering domains P1 and P3-P4 (McCleary and Zusman 6661-8; Acuna et al. 31-3) .

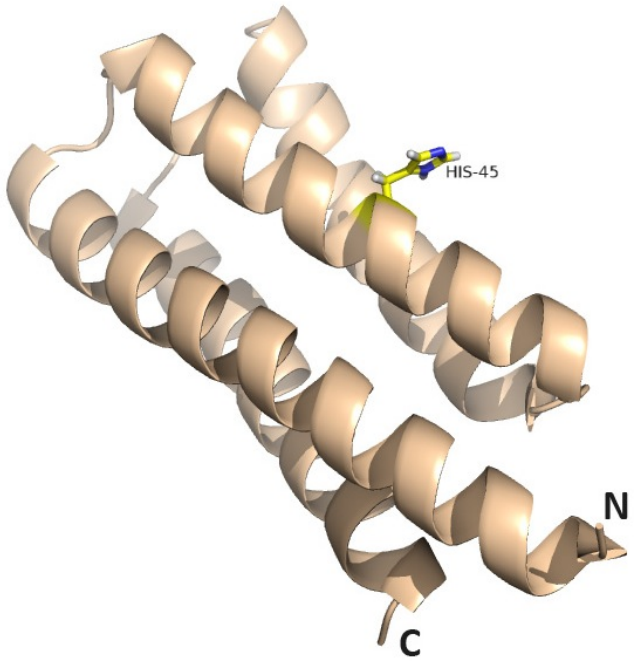

Fig. 1-3 The Hpt (P1) domain of CheA of the thermophilic bacteria *Thermotoga maritima* (TmCheA). Only the first four helices out of five helices of CheA are shown

in this figure. The conserved His residue resides (stick model in yellow with N atoms in blue) at the second helix of the four-helix bundle and is exposed to solvent. The N-termini is at the bottom right corner. This figure is adapted from PDB molecule: 1TQG.

P2 deletion constructs (referred to as CheADP2) were generated for P2 functional studies and demonstrated that CheADP2 retains auto-phosphorylation activity, with a two fold increase compared to wild type (*wt*) CheA (Jahreis et al. 2664-2672). Moreover, CheADP2 appear to be regulated by the MCPs to the same degree as *wt* CheA, namely a ~150 fold activation with membrane-bound Tsr and deactivation in the presence of attractant. As expected, CheADP2 has a slower phosphor-transfer rate to both CheY and CheB under physiological conditions. CheADP2 also exhibits defective chemotactic behaviors on swarm plates.

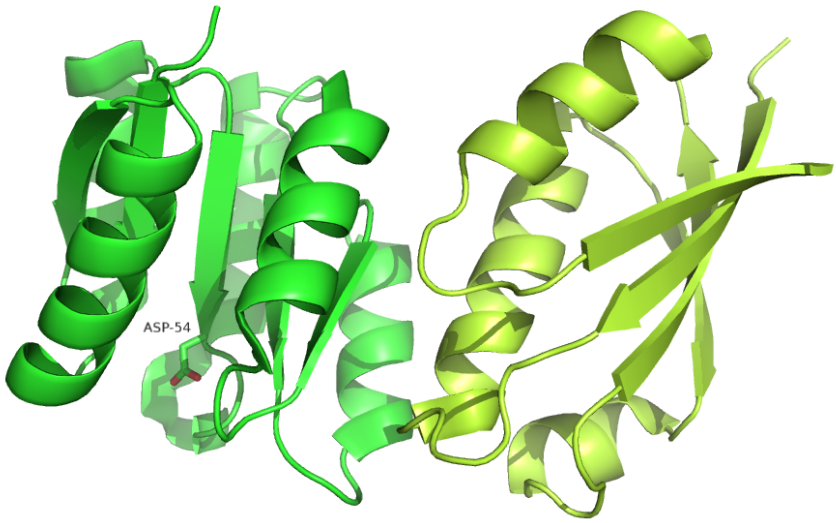

Fig. 1-4 TmCheY with TmCheA response regulator binding domain (P2). CheY is shown in green with the conserved Asp residue shown in stick model (O atoms in red). CheA P2 domain is shown in yellow. Two different modes of binding between CheY with the CheA domain P2 have been observed in complex crystal structures despite sequence conservation for both domains. This figure is adapted from PDB molecule: 1U0S.

As mentioned earlier, in *E. coli* and *T. maritima* CheA, the P2 domain is flanked by two long linkers (25 to 45 residues). These flexible linkers enable P2 to move independently with regards to other domains. Double Electron Electron Resonance (DEER) measurements to determine the P2-P2 intra-dimer distances proved that the movement of P2 is rather unrestricted and independent of other domains (Bhatnagar et al. 3824-41).

P3 domain

CheA dimerize through its P3 domain, the dimerization domain. Upon dimerization, P3 forms a four-helix bundle structurally (Fig. 1-5) where each monomer contributes two antiparallel helices. Dimerization is essential to CheA function (Surette et al. 939-45) .

P4 domain

P4 is the kinase/catalytic domain to which ATP binds. The structure of P4 is a two-layered α/β sandwich, which resembles the ATP binding domain of a class of ATPases, the GHL family (Bilwes et al. 131-41; Bilwes et al. 353-60). In P4, the four-stranded β sheet forms the wall of the ATP binding pocket, which is flanked by α helices

(Fig. 1-6). The structure of the isolated P4 domain with ATP analogs suggests that the γ-phosphate of ATP is positioned at the surface of the binding pocket, which is accessible to interact with P1 (Bilwes et al. 353-60) . This structural study also emphasizes the role of an ATP lid that is composed of a α-helix tethered to the rest of the domain by two flexible linkers. The mobility of the ATP lid may be associated with ATP binding.

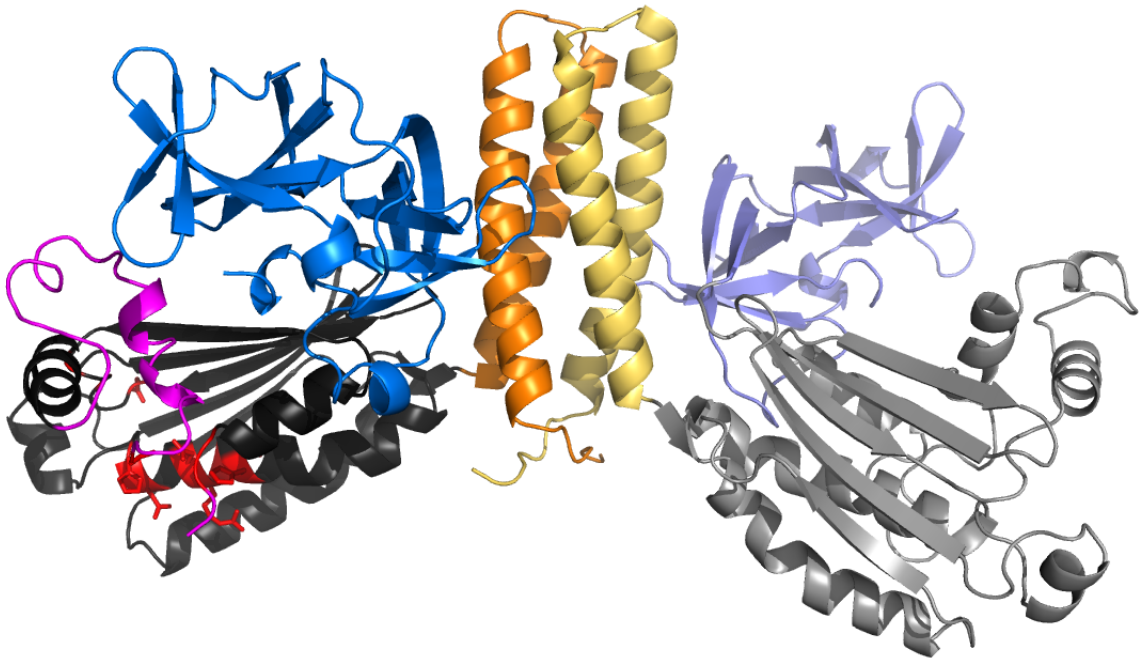

Fig. 1-5 Dimer of TmCheA dimerization, kinase, and coupling (P3P4P5) domains. The dimerization domain is colored in orange; kinase domain in grey; regulatory domain in blue. Different shades of each of the colors above are applied for different subunit. The ATP binding cavity in one of the kinase domains is highlighted with residues involved in binding colored in red. The side chains of residues that coordinate the binding are shown with stick model. The ATP lid, which includes a α-

helix, and the loops connecting it is shown in magenta. This figure is adapted from PDB molecule: 1B3Q.

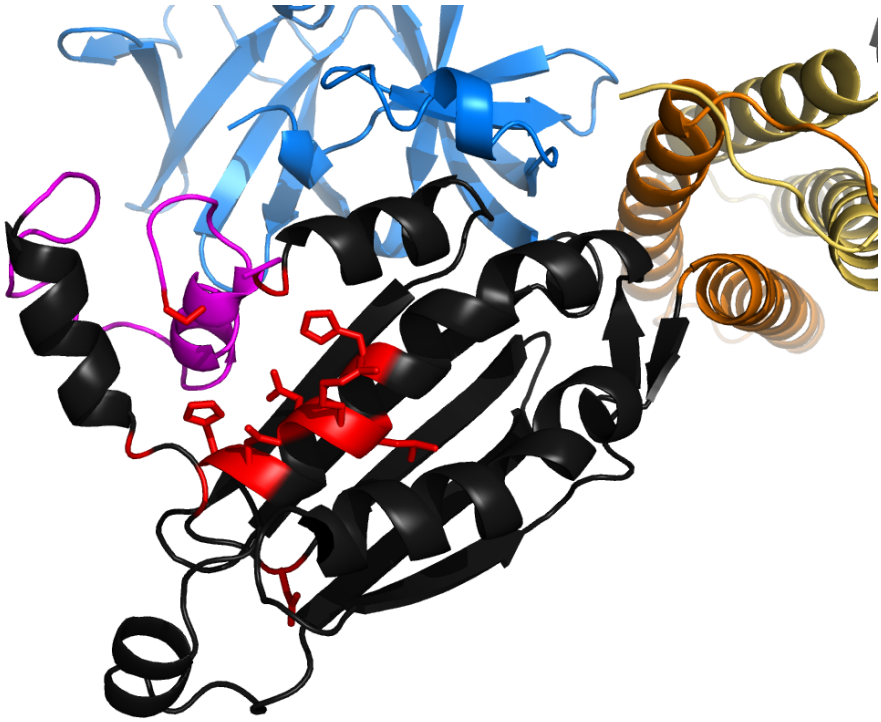

Fig. 1-6 Close-up view of the kinase (P4) domain and the ATP binding pocket. The same color codes are applied in this figure as in Fig. 1-4. This figure is adapted from PDB molecule: 1B3Q.

P5 domain

The regulatory domain (P5) of CheA shows the same structural fold as the coupling protein CheW (Fig. 3-1). It has two β barrels, each of which bears a hydrophobic core and the two almost perpendicular β barrels sandwich another hydrophobic core between them.

1.5.2.2 Trans-phosphorylation of CheA

As histidine kinases only exist in prokaryotes and a few plants, they are potential targets for antibiotics. It is important to understand the phosphorylation mechanism in order to advance drug design for the histidine kinase. However, the initiation of the phosphorylation reaction and the interaction between P1 and P4 domains during phosphorylation still remain unclear. Because P1 and P4 are separated from each other by two other domains and two long linkers, the conformations the two domains adopt can be very dynamic.

First evidence of a trans-phosphorylation mechanism came from the finding that CheA dimer is required for its kinase function (Surette et al. 939-45) and from subsequent rescuing experiments (Levit et al. 32057-63) . Homo-dimers that bear either a defective P1 or P4 domain were defective in kinase activation, but upon the formation of a heterodimer, the kinase activity was rescued. Later it was found that although CheA exists naturally as a dimer, the two ATP binding sites of CheA bind ATP independently with different affinities (Eaton and Stewart 6412-22) . P1 of one subunit cross-links with the P4 of the other subunit (Miller et al. 8699-711) . Chemical shift perturbation on P1-P4 binding also proved that P1 of one subunit interacts with P4 of the other subunit of the dimer (Hamel et al. 9509-9517) . The full-length CheA crystal structure is not available, but the multi-domain CheA (P3P4P5) structure (Bilwes et al. 131-41) shows a hinge at the end of the P3 domain, which could direct the connecting P1 towards the P4 of the other subunit.

The P1-P4 interaction is known to be transient. Since both domains sample a broad range in space, it is enigmatic how the two domains catalyze the phospho-transfer with high efficiency. Because CheA autophosphorylation is the step during which the

spatial changes along the MCP occur and within the ternary complex is first converted to a chemical change, understanding the P1-P4 interaction is the key to not only understanding how signals are relayed and amplified, but also to understanding how signals are coupled between spatial changes with chemical changes.

1.5.2.3 Localization of CheA

CheA co-localizes with the MCP at the cell poles (Sourjik and Berg 740-751). The characteristic exchange time of MCP-bound CheA with free cytoplasmic CheA is 12 min (Schulmeister et al. 6403-6408), which indicates the MCP-bound CheA is stable within the complex.

1.5.3 CheW

CheW is the adaptor/coupling protein in the ternary complex. However, its role has been expanded beyond just tethering the MCP and the kinase. More detailed information on CheW, including its structure, localization, and physiological role will be discussed in chapter three.

1.6 Regulation of CheA by MCP

MCPs can activate the kinase up to 100-fold compared to its basal activation level both with membrane-embedded MCPs and chimera MCP proteins that lack the transmembrane domain (Hazelbauer and Lai 124-132; Wolanin et al. 14313-14318) . *In vivo* fluorescence resonance energy transfer (FRET) showed that a single MCP can affect up to 36 kinases (Sourjik and Berg 123-127) . Attractant binding to MCPs can deactivate the kinase activity. How MCPs regulate CheA activity is an essential question still unanswered.

REFERENCES

Acuna, G., et al. "The 'CheA' and 'CheY' Domains of Myxococcus Xanthus FrzE Function Independently in Vitro as an Autokinase and a Phosphate Acceptor, Respectively.." *FEBS letters* 358.1 (1995): 31-.

Airola, M. V., et al. "Structure of Concatenated HAMP Domains Provides a Mechanism for Signal Transduction.." *Structure (London, England : 1993)* 18.4 (2010): 436-8.

Alexander, R. P., and I. B. Zhulin. "Evolutionary Genomics Reveals Conserved Structural Determinants of Signaling and Adaptation in Microbial Chemoreceptors.." *Proceedings of the National Academy of Sciences of the United States of America* 104.8 (2007): 2885-90.

Ames, P., and J. S. Parkinson. "Conformational Suppression of Inter-Receptor Signaling Defects." *Proceedings of the National Academy of Sciences of the United States of America* 103.24 (2006): 9292-7.

Besschetnova, T. Y., et al. "Receptor Density Balances Signal Stimulation and Attenuation in Membrane-Assembled Complexes of Bacterial Chemotaxis Signaling Proteins." *Proceedings of the National Academy of Sciences of the United States of America* 105.34 (2008): 12289-94.

Bhatnagar, J., et al. "Structure of the Ternary Complex Formed by a Chemotaxis Receptor Signaling Domain, the CheA Histidine Kinase, and the Coupling Protein CheW as Determined by Pulsed Dipolar ESR Spectroscopy.." *Biochemistry* 49.18 (2010): 3824-41.

Bilwes, A. M., et al. "Nucleotide Binding by the Histidine Kinase CheA.." *Nature structural biology* 8.4 (2001): 353-60.

Bilwes A.M., et al. "Structure of CheA, a Signal-Transducing Histidine Kinase.." *Cell* 96.1 (1999): 131-41.

Blair, D. F. "How Bacteria Sense and Swim.." *Annual review of microbiology* 49 (1995): 489-522.

Borkovich, K. A., L. A. Alex, and M. I. Simon. "Attenuation of Sensory Receptor Signaling by Covalent Modification.." *Proceedings of the National Academy of Sciences of the United States of America* 89.15 (1992): 6756-60.

Boukhvalova, M. S., F. W. Dahlquist, and R. C. Stewart. "CheW Binding Interactions with CheA and Tar. Importance for Chemotaxis Signaling in Escherichia Coli.." *The Journal of biological chemistry* 277.25 (2002): 22251-9.

Chao, X., et al. "A Receptor-Modifying Deamidase in Complex with a Signaling Phosphatase Reveals Reciprocal Regulation." *Cell* 124.3 (2006): 561-7.

Coleman, M. D., et al. "Conserved Glycine Residues in the Cytoplasmic Domain of the Aspartate Receptor Play Essential Roles in Kinase Coupling and on-Off Switching." *Biochemistry* 44.21 (2005): 7687-95.

Draheim, R. R., et al. "Tryptophan Residues Flanking the Second Transmembrane Helix (TM2) Set the Signaling State of the Tar Chemoreceptor." *Biochemistry* 44.4 (2005): 1268-77.

Dyer, C. M., et al. "A Molecular Mechanism of Bacterial Flagellar Motor Switching.." *Journal of molecular biology* 388.1 (2009): 71-84.

Eaton, A. K., and R. C. Stewart. "The Two Active Sites of Thermotoga Maritima CheA Dimers Bind ATP with Dramatically Different Affinities.." *Biochemistry* 48.27 (2009): 6412-22.

Erbse, A. H., and J. J. Falke. "The Core Signaling Proteins of Bacterial Chemotaxis Assemble to Form an Ultrastable Complex." *Biochemistry* 48.29 (2009): 6975-87.

Falke, J. J., and A. H. Erbse. "The Piston Rises again.." *Structure (London, England : 1993)* 17.9 (2009): 1149-51.

Falke, J. J., and Hazelbauer G. L. "Transmembrane Signaling in Bacterial Chemoreceptors.." *Trends in biochemical sciences* 26.4 (2001): 257-6.

Gestwicki, J. E., and L. L. Kiessling. "Inter-Receptor Communication through Arrays of Bacterial Chemoreceptors.." *Nature* 415.6867 (2002): 81-4.

Guhaniyogi, J., et al. "Interaction of CheY with the C-Terminal Peptide of CheZ.." *Journal of bacteriology* 190.4 (2008): 1419-28.

Hamel, D. J., et al. "Chemical-Shift-Perturbation Mapping of the Phosphotransfer and Catalytic Domain Interaction in the Histidine Autokinase CheA from Thermotoga Maritima." *Biochemistry* 45.31 (2006): 9509-17.

Hansen, C. H., V. Sourjik, and N. S. Wingreen. "A Dynamic-Signaling-Team Model for Chemotaxis Receptors in Escherichia Coli.." *Proceedings of the National Academy of Sciences of the United States of America* 107.40 (2010): 17170-5.

Hao, S., et al. "Structural Basis for the Localization of the Chemotaxis Phosphatase CheZ by CheAS.." *Journal of bacteriology* 191.18 (2009): 5842-4.

Hazelbauer, G. L., and W. C. Lai. "Bacterial Chemoreceptors: Providing Enhanced Features to Two-Component Signaling." *Current opinion in microbiology* 13.2 (2010): 124-32.

Hulko, M., et al. "The HAMP Domain Structure Implies Helix Rotation in Transmembrane Signaling." *Cell* 126.5 (2006): 929-40.

Jahreis, Knut, et al. "Chemotactic Signaling by an Escherichia Coli CheA Mutant that Lacks the Binding Domain for Phosphoacceptor Partners." *The Journal of Bacteriology* 186.9 (2004): 2664-72.

Jancarik, J., et al. "Crystallization and Preliminary X-Ray Diffraction Study of the Ligand-Binding Domain of the Bacterial Chemotaxis-Mediating Aspartate Receptor of Salmonella Typhimurium.." *Journal of molecular biology* 221.1 (1991): 31-4.

Jasuja, R., et al. "Response Tuning in Bacterial Chemotaxis.." *Proceedings of the National Academy of Sciences of the United States of America* 96.20 (1999): 11346-51.

Kehry, M. R., and F. W. Dahlquist. "Adaptation in Bacterial Chemotaxis: CheB-Dependent Modification Permits Additional Methylations of Sensory Transducer Proteins.." *Cell* 29.3 (1982): 761-2.

Kehry, M.R., et al. "Enzymatic Deamidation of Methyl-Accepting Chemotaxis Proteins in Escherichia Coli Catalyzed by the cheB Gene Product.." *Proceedings of the National Academy of Sciences of the United States of America* 80.12 (1983): 3599-603.

Kehry, M.R., et al. "Sensory Adaptation in Bacterial Chemotaxis: Regulation of Demethylation.." *Journal of bacteriology* 163.3 (1985): 983-0.

Kim, C., et al. "Determinants of Chemotactic Signal Amplification in Escherichia Coli.." *Journal of molecular biology* 307.1 (2001): 119-35.

Kim, K. K., H. Yokota, and S. H. Kim. "Four-Helical-Bundle Structure of the Cytoplasmic Domain of a Serine Chemotaxis Receptor.." *Nature* 400.6746 (1999): 787-92.

Lacal, J., et al. "Sensing of Environmental Signals: Classification of Chemoreceptors According to the Size of their Ligand Binding Regions." *Environmental microbiology* 12.11 (2010): 2873-84.

Le Moual, H., and Jr Koshland DE. "Molecular Evolution of the C-Terminal Cytoplasmic Domain of a Superfamily of Bacterial Receptors Involved in Taxis.." *Journal of molecular biology* 261.4 (1996): 568-85.

Lee, S. Y., et al. "Crystal Structure of an Activated Response Regulator Bound to its Target.." *Nature structural biology* 8.1 (2001): 52-6.

Levit, M. N., Y. Liu, and J. B. Stock. "Mechanism of CheA Protein Kinase Activation in Receptor Signaling Complexes.." *Biochemistry* 38.20 (1999): 6651-8.

Levit, M., et al. "Active Site Interference and Asymmetric Activation in the Chemotaxis Protein Histidine Kinase CheA.." *The Journal of biological chemistry* 271.50 (1996): 32057-63.

Li, M., and G. L. Hazelbauer. "Adaptational Assistance in Clusters of Bacterial Chemoreceptors." *Molecular microbiology* 56.6 (2005): 1617-26.

McCleary, W. R., and D. R. Zusman. "Purification and Characterization of the Myxococcus Xanthus FrzE Protein shows that it has Autophosphorylation Activity.." *Journal of bacteriology* 172.12 (1990): 6661-8.

Milburn, M. V., et al. "Three-Dimensional Structures of the Ligand-Binding Domain of the Bacterial Aspartate Receptor with and without a Ligand.." *Science (New York, N.Y.)* 254.5036 (1991): 1342-7.

Miller, A. S., et al. "CheA Kinase of Bacterial Chemotaxis: Chemical Mapping of Four Essential Docking Sites.." *Biochemistry* 45.29 (2006): 8699-711.

Miller, A. S., et al. "Side Chains at the Membrane-Water Interface Modulate the Signaling State of a Transmembrane Receptor.." *Biochemistry* 43.7 (2004): 1763-70.

Mowbray, S. L., and G. A. Petsko. "The X-Ray Structure of the Periplasmic Galactose Binding Protein from Salmonella Typhimurium at 3.0-A Resolution.." *The Journal of biological chemistry* 258.13 (1983): 7991-7.

Ottemann, K. M., et al. "A Piston Model for Transmembrane Signaling of the Aspartate Receptor.." *Science (New York, N.Y.)* 285.5434 (1999): 1751-4.

Park, S. Y., et al. "Reconstruction of the Chemotaxis Receptor-Kinase Assembly." *Nature structural & molecular biology* 13.5 (2006): 400-7.

Park, S. Y., et al. "In Different Organisms, the Mode of Interaction between Two Signaling Proteins is Not Necessarily Conserved.." *Proceedings of the National Academy of Sciences of the United States of America* 101.32 (2004): 11646-51.

Parkinson, J. S. "Signal Transduction Schemes of Bacteria.." *Cell* 73.5 (1993): 857-71.

Pollard, A. M., A. M. Bilwes, and B. R. Crane. "The Structure of a Soluble Chemoreceptor Suggests a Mechanism for Propagating Conformational Signals.." *Biochemistry* 48.9 (2009): 1936-44.

Quezada, C. M., et al. "Helical Shifts Generate Two Distinct Conformers in the Atomic Resolution Structure of the CheA Phosphotransferase Domain from Thermotoga Maritima.." *Journal of molecular biology* 341.5 (2004): 1283-94.

Quezada, C. M., et al. "Structural and Chemical Requirements for Histidine Phosphorylation by the Chemotaxis Kinase CheA.." *The Journal of biological chemistry* 280.34 (2005): 30581-5.

Sarkar, M. K., K. Paul, and D. Blair. "Chemotaxis Signaling Protein CheY Binds to the Rotor Protein FliN to Control the Direction of Flagellar Rotation in Escherichia Coli.." *Proceedings of the National Academy of Sciences of the United States of America* 107.20 (2010): 9370-5.

Schulmeister, S., et al. "Protein Exchange Dynamics at Chemoreceptor Clusters in Escherichia Coli." *Proceedings of the National Academy of Sciences of the United States of America* 105.17 (2008): 6403-8.

Schuster, M., R. E. Silversmith, and R. B. Bourret. "Conformational Coupling in the Chemotaxis Response Regulator CheY.." *Proceedings of the National Academy of Sciences of the United States of America* 98.11 (2001): 6003-8.

Segall, J. E., M. D. Manson, and H. C. Berg. "Signal Processing Times in Bacterial Chemotaxis.." *Nature* 296.5860 (1982): 855-7.

Segall, J.E. et al. "Temporal Comparisons in Bacterial Chemotaxis.." *Proceedings of the National Academy of Sciences of the United States of America* 83.23 (1986): 8987-91.

Shiomi, D., et al. "Dual Recognition of the Bacterial Chemoreceptor by Chemotaxis-Specific Domains of the CheR Methyltransferase.." *The Journal of biological chemistry* 277.44 (2002): 42325-33.

Sourjik, V. "Receptor Clustering and Signal Processing in E. Coli Chemotaxis." *Trends in microbiology* 12.12 (2004): 569-76.

Sourjik, V. "Spatial Organization in Bacterial Chemotaxis." *The EMBO journal* 29.16 (2010): 2724-33.

Sourjik, V., and H. C. Berg. "Binding of the Escherichia Coli Response Regulator CheY to its Target Measured in Vivo by Fluorescence Resonance Energy Transfer.." *Proceedings of the National Academy of Sciences of the United States of America* 99.20 (2002a): 12669-74.

Sourjik, V., et al. "Functional Interactions between Receptors in Bacterial Chemotaxis.." *Nature* 428.6981 (2004): 437-1.

Sourjik, Victor. "Responding to Chemical Gradients: Bacterial Chemotaxis.." *Current opinion in cell biology* 24.2 (2012): 262-8.

Sourjik, Victor, and Howard C. Berg. "Localization of Components of the Chemotaxis Machinery of Escherichia Coli using Fluorescent Protein Fusions." *Molecular microbiology* 37.4 (2000): 740-51.

Sourjik, V. "Receptor Sensitivity in Bacterial Chemotaxis." *Proceedings of the National Academy of Sciences* 99.1 (2002b): 123-7.

Springer, W. R., and Jr Koshland DE. "Identification of a Protein Methyltransferase as the cheR Gene Product in the Bacterial Sensing System.." *Proceedings of the National Academy of Sciences of the United States of America* 74.2 (1977): 533-7.

Spurlino, J. C., G. Y. Lu, and F. A. Quiocho. "The 2.3-A Resolution Structure of the Maltose- Or Maltodextrin-Binding Protein, a Primary Receptor of Bacterial Active Transport and Chemotaxis.." *The Journal of biological chemistry* 266.8 (1991): 5202-19.

Surette, M. G., et al. "Dimerization is Required for the Activity of the Protein Histidine Kinase CheA that Mediates Signal Transduction in Bacterial Chemotaxis.." *The Journal of biological chemistry* 271.2 (1996): 939-45.

Swain, K. E., M. A. Gonzalez, and J. J. Falke. "Engineered Socket Study of Signaling through a Four-Helix Bundle: Evidence for a Yin-Yang Mechanism in the Kinase Control Module of the Aspartate Receptor." *Biochemistry* 48.39 (2009): 9266-77.

Tatsuno, I., et al. "Signaling by the Escherichia Coli Aspartate Chemoreceptor Tar with a Single Cytoplasmic Domain Per Dimer.." *Science (New York, N.Y.)* 274.5286 (1996): 423-5.

Vaknin, A., and H. C. Berg. "Physical Responses of Bacterial Chemoreceptors." *Journal of Molecular Biology* 366.5 (2007): 1416-23.

Vyas, N. K., M. N. Vyas, and F. A. Quiocho. "Comparison of the Periplasmic Receptors for L-Arabinose, D-Glucose/D-Galactose, and D-Ribose. Structural and Functional Similarity.." *The Journal of biological chemistry* 266.8 (1991): 5226-37.

Wadhams, G. H., and J. P. Armitage. "Making Sense of it all: Bacterial Chemotaxis.." *Nature reviews.Molecular cell biology* 5.12 (2004): 1024-37.

Wolanin, P. M., et al. "Self-Assembly of Receptor/Signaling Complexes in Bacterial Chemotaxis." *Proceedings of the National Academy of Sciences of the United States of America* 103.39 (2006): 14313-8.

Zhou, H., et al. "Phosphotransfer and CheY-Binding Domains of the Histidine Autokinase CheA are Joined by a Flexible Linker.." *Biochemistry* 35.2 (1996): 433-.

CHAPTER TWO

HEXAGONALLY-PACKED CHEMORECEPTOR ARRAYS NETWORKED BY RINGS OF KINASE AND COUPLING PROTEINS[**]

2.1 INTRODUCTION

2.1.1 Higher-order receptor arrays

The assembly of Mehthyl Accepting Chemoreceptor Proteins (MCPs) in high-ordered arrays has been the focus of much research in the last twenty years. MCPs span the cytoplasmic membrane as homo-dimers and associate into much larger clusters. Electron Microscopy allows scientists to directly visualize the MCP patches in intact cells. From the EM images, the MCPs appear as striations almost orthogonal to the cytoplasmic membrane and are mainly locating at the cell poles. In *E. coli,* MCPs form circular or ellipsoidal patches of ~250 nm^2 area(Zhang et al. 3777-3781). An estimate of ~6500 MCPs is needed to form a cluster of that size. A subsequent Electron Cryo Tomography (ECT) study suggested a smaller number of MCPs per patch in *C. crescentus* (in the range of thousands per patch). The tight clustering of MCPs into patches and the polar pattern of localization of MCPs are also found in other bacteria and Archaea (Gestwicki et al. 6499-502; Briegel et al. 17181-17186) .

The clustering of receptors invokes a number of questions: How do the receptors assemble into such arrays? Is there an order to the assembly? Is the assembly architecture conserved among bacteria and Archea? How does the assembly contribute to the sensitivity and dynamic range of signaling? Do CheA, CheW and other chemotaxis proteins co-localize in the MCP patches and do they contribute to the clustering?

Immuno-EM with gold-labeled antibodies revealed a basic arrangement of CheA molecules at the base of the receptors. Later, *in vivo* fluorescence microscopy and high resolution Photo-Activated Localization Microscopy (PALM) (Greenfield et al. e1000137) techniques were used to document the co-localization with MCPs of CheW, CheA and other chemotaxis proteins and to determine the dynamics of the associations. Strong clustering of MCPs requires CheA and CheW (Skidmore et al. 967-73) : however CheA- or CheW- independent clustering can be observed, but is more diffusive than CheA/CheW dependent clustering (Skidmore et al. 967-73; Sourjik and Berg 740-751) . *In vivo* crosslinking experiments demonstrated that the cross-linking of different types of MCPs was CheA/CheW independent, but did not indicate the degree of the CheA/CheW independent assembly (Ames et al. 7060-7065) . Following those experiments, the role of CheA and CheW in the clustering of MCPs remained unclear.

Recent progress in EM and ECT studies of the chemoreceptor arrays provided more insights on the architecture of the chemoreceptor arrays. Various labeling and imaging techniques confirmed that the patches observed at the cell poles are MCP clusters (Briegel et al. 30-41) . The cryo-ECT study on *C. crescentus* MCP arrays with fluorescently tagged MCPs (Briegel et al. 30-41) also revealed a striking order in the arrays: the MCPs are arranged in a honey-comb fashion, with groups of MCPs residing at the vertices of the hexagons. This observation was made possible by significant improvement in the level of resolution obtained by reducing noises with filters, averaging sub-volumes with hexagonal arrangement and applying six-fold rotational symmetry to the average. Besides the density accounted for by MCPs, the authors also observed two density plates, one at the base of the MCPs that can be attributed to the bound CheA and

CheW, and the other 10 nm below the cytoplasmic membrane that can be partially attributed to the adaptation enzymes CheR and CheB. The honey-comb arrangement was beyond people's expectation on the degree of order, but it should be noted here that the long-range order of the hexagonal arrangement is imperfect(Khursigara, Wu and Subramaniam 6805-6810). Not only they have overall disordered packing, they exhibit a decreased order approaching the membrane. How is this honey-comb arrangement is achieved and what interactions are contributing to it are still intriguing questions.

2.1.2 Regulation of the kinase by receptor clusters

The clustering of receptors is believed to contribute to the sensitivity of the bacteria (Bray, Levin and Morton-Firth 85-8; Duke and Bray 10104-8) . Also because of the conserved cytoplasmic domain of the receptors(Alexander and Zhulin 2885-90), different types of MCPs could couple to each other, and as a direct result, different signals could be integrated and sensed with parity. For example, stabilizing the low abundance MCP Trg (150 copies per cell, (Hazelbauer and Engstrom 35-42)) with a synthetic multivalent ligand can enhance the output of the high abundance MCP Tsr (3000 copies per cell, (Slocum and Parkinson 565-77), which responds to serine. (Gestwicki and Kiessling 81-4). Not only activation is believed to be cooperative, but also deactivation, because the deletion or mutation of one type of MCP would lower or deplete the response of another type of MCP(Gestwicki and Kiessling 81-4; Ames et al. 7060-7065). Modeling studies have supported this view of cooperative sensing among MCPs to amplify the responses (Bray, Levin and Morton-Firth 85-8; Duke and Bray 10104-8). Moreover, the inter-receptor communication also involves the adaptation mechanism of the sensory system(Li and Hazelbauer 1617-1626; Endres and Wingreen

13040-13044; Li and Weis 357-65) where methyl-transfer happens among MCPs and provides a precise feedback control. The different "states" of the MCPs vary by the kinase activity of associated CheA molecules, therefore in order to understand the cooperativity among MCPs, it is crucial to learn not only how MCPs communicate, but also how the MCP, CheA and CheW associate to form the ternary complex, and how CheA activity is regulated by MCPs within the complex.

2.1.3 The conformation of the ternary complex

Small unit of complexes are capable of transmitting a signal and of regulating kinase activity (Li and Hazelbauer 9390-9395). Many of the *in vitro* reconstituted signaling complexes do not bear the membrane embedded MCP clusters but are still able to modulate the kinase activity in a manner comparable with membrane embedded clusters. For example, the nanodisk incorporated MCPs can activate the kinase activity by ~100 folds (Li and Hazelbauer 9390-9395). In order to elucidate how MCPs regulate the kinases, again, it is necessary to determine the interactions between CheA, CheW and MCPs within the ternary complex.

There has been considerable progress made on the determination of the ternary complex structure, based on genetic, biochemical, and structural information (Hazelbauer and Lai 124-132). Basing on these studies, a few models were proposed (Park et al. 400-407; Bhatnagar et al. 3824-41; Endres, Falke and Wingreen e150; Erbse and Falke 6975-6987; Shimizu and Le Novere 5-9) . It is important to note, however, that the composition and conformation of the ternary complex as well as its assembly into clusters still remain controversial. The determination of the ternary complex structure has benefited a lot from available protein structures of individual components (or domains of individual

components) of the ternary complex (Bilwes et al. 131-41; Bilwes et al. 353-60; Quezada et al. 30581-5; Quezada et al. 1283-94; Griswold et al. 121-5; Park et al. 400-407; Kim, Yokota and Kim 787-92; Pollard, Bilwes and Crane 1936-44; Alexander et al. 494-503) . Many of these structures were determined in the Crane research group. These structures provided useful information on possible interfaces within the complex, but a complex structure with all three components was missing.

This chapter describes our work on determining the crystal structure of the ternary complex, the modeling of the high-order clusters based on our ternary complex crystal structure and based on the EM tomography studies carried out by our collaborator Ariane Briegel in Grant Jensen's lab in Caltech.

2.2 MATERIALS AND METHODS

2.2.1 Cell Growth and Sample Preparation for Electron Cryo-Tomography (ECT)

TH17261 is a mini-cell-producing strain of *Salmonella enterica Serovar Typhimurium* that overexpresses flagellar structures. TH17261 carries a second copy of the ftsZ+ gene expressed from an arabinose promoter (DaraBAD1091::ftsz+). This strain was constructed by first replacing the araBAD structural genes with the tetracycline-resistance cassette or tetRA element from transposon Tn10 and then replacing the tetRA element with the ftsZ + gene as described (Karlinsey 199-209). Induction of excess FtsZ by arabinose results in minicell formation. The lhrA, ydiV, and ecnR genes encode negative regulators of the flagellar master operon, flhDC (Erhardt and Hughes 376-93; Wozniak, Lee and Hughes 1498 -1508). The lhrA and ecnR gene mutants were constructed by

insertion of the tetRA cassette and oligonucleotide-directed replacement resulting in gene deletion leaving the first and last 15 base pairs of the coding regions as described (Karlinsey 199-209). The construction of the ecnR deletion mutant (DecnR::FKF, where FKF represents the Flp recombinase target cassette) was previously described(Wozniak, Lee and Hughes 1498 -1508). The strain also carries promoter-up mutations in the flagellar flhDC master operon as described (Erhardt and Hughes 376-93). The various alleles were moved into a single strain by bacteriophage P22-mediated transduction(Wozniak, Lee and Hughes 1498 -1508).

Sample preparation. *S. enterica* strain 17261 minicells were grown overnight shaking in LB medium at 37 °C. The culture was then diluted 1⁄100 into fresh LB containing 0.1% L-Arabinose and grown for an additional 3 hrs. One milliliter aliquots were centrifuged at 3;000 × g for 5 min to remove large cells and then the supernatant was centrifuged at 18;000 × g to collect minicells. The resulting pellets were then resuspended in 50 μL LB.

B. subtilis subsp. *subtilis* strain 168 was grown overnight shaking in LB at 37 °C. The culture was diluted in fresh LB medium and grown to log phase. One milliliter culture was spun down for 5 min at 4;000 × g and resuspended in protoplast preparation medium (250 mL containing 6.25 g LB, 20 mM MgCl2, and 20 mM sucrose). Lysozyme was added to a final concentration of 100 μg⁄mL, and 5 mL were incubated without shaking in a 125-mL Erlenmeyer flask until protoplasts were formed.

H. hepaticus American Type Culture Collection strain 51449 was grown and E. coli strain MG1655 was grown and lysed as described previously(Briegel et al. 17181-

17186).

Electron Cryotomography. Right before plunge freezing, the different cell preparations (*S. enterica* minicells, lysed *E. coli* and *B. subtilis* cells, and intact *H. hepaticus* cells) were each mixed with colloidal gold pretreated with BSA to avoid particle aggregation (Iancu et al. 375-9). Four microliters of cell-and-gold solution were applied to R2/2 copper/Rhodium Quantifoil gridsTM (Quantifoil Micro Tools), blotted, and plunged in liquid ethane or ethane/propane mixture(Iancu et al. 375-9) 51. Images were collected using an FEI PolaraTM (FEI), 300 kV field emission gun transmission electron microscope equipped with a Gatan energy filter and a lens-coupled 4;000 × 4;000 Ultracam (Gatan). Tilt series from up to −70° to 70° with an increment of 1°, an underfocus of −8 to −10 μm, and a pixel size on the specimen level of 6.3 Å were recorded using Leginon (Suloway et al. 11-8). A cumulative dose of 200 electrons⁄Å2 or less was used for each tilt series.

Tilt series were aligned and contrast transfer function corrected using the IMOD software package(Mastronarde 36-51). Three-dimensional reconstructions were calculated using IMOD or TOMO3D (Mastronarde 36-51; Agulleiro and Fernandez 582-3). Subvolume averaging and symmetrizing was done using PEET(Nicastro et al. 944-8).

2.2.2 Protein Preparation for Crystallography

A gene fragment encoding residues 107–191 of *T. maritima* receptor Tm14s (Pollard, Bilwes and Crane 1936-44) was PCR cloned into vector pET28a (Novagen) and expressed as a protein fragment flanked by an N-terminal Histidine6 tag in *E. coli* strain BL21 (RIL DE3) (Novagen) after induction with IPTG at 18 °C and overnight growth for

21 h. Tm14s was purified first with Ni-nitrilotriacetate affinity chromatography, followed by overnight thrombin digestion, and size-exclusion chromatography (Superdex 75 Hi-load FPLC column in 50 mM NaCl, 100 mM Tris 7.5, 10% glycerol). *T. maritima* CheW and CheA Δ354 (P4P5 domain, residues 355–671) were expressed and purified as described previously(Park et al. 400-407).

2.2.3 Crystallization and Data Collection

Cubic-shaped crystals ($50 \times 50 \times 50\ \mu m^3$) were grown from a mixture of 520 μM Tm14s (107–191), 457 μM CheA Δ354, and 121 μM CheW after 1 mo by vapor diffusion from a 2-μL drop [1∶1 mixture of protein and reservoir: 500 μL reservoir of 0.2 M sodium acetate trihydrate, 0.1 M Tris (pH 8.5), 15% w*t*/vol polyethylene glycol 4,000]. SDS-PAGE analysis with mass spectrometry identification confirmed all components in the crystals. Most crystals diffracted to <8 Å resolution; however, after extensive screening, several crystals diffracting to higher resolution were found. Crystals were soaked briefly in cryoprotectant consisting of 85⁄15 (vol⁄vol) reservoir solution with glycerol prior to data collection in an N_2 cold stream. Diffraction data (Table 1) were collected at 100 K with synchrotron radiation at beamline A1 at the Cornell High Energy Synchrotron Source.

2.2.4 Crystal Structure Determination and Refinement

Diffraction data were processed with HKL2000 (Otwinowski and Minor 307-326). Initial phases were obtained by molecular replacement with PHASER (McCoy et al. 658-674) using one subunit of the CheA Δ354-CheW complex [Protein Data Bank (PDB) 2CH4 chain A and chain W] as a search model. The truncated receptor dimer (PDB 3G67) was

manually built into the resulting electron density maps with XFIT(McRee and Israel 208-13). The model was refined to 4.5-Å resolution with the deformable elastic network (DEN) method (Schroder, Brunger and Levitt 1630-41; Schroder, Levitt and Brunger 1218-22), as implemented in CNS (Brunger 2728-33). Although not well-resolved, electron density for the core β-sheet of the P4 domain was evident below the connection to P5. Refinement of three different orientations of P4 centered on this density showed little discrimination in R_{free}. Electron density at the very tip of the receptors was also weak, and thus the helix register was set by packing constraints at the distal end.

2.2.5 Electron Cryotomography Modeling

An all-atom model of a Tsr cytoplasmic trimer-of-dimers containing three complete four-helix bundles to the level of the HAMP domain was constructed based on the crystal structures of Tsr (PDB code 1QU7) and Tm1143 (PDB code 2CH7) and then built into ECT density symmetrized about the sixfold axis relating trimer-of-dimers. The model was refined in reciprocal space to 20 Å resolution against vector structure factors from the volume of a single trimer placed in a P1 unit cell, first by rigid body refinement of the three subunits, then by rigid body refinement of nine individual helical sections (three from each dimer) that comprised the signaling tip, stalk to the glycine hinge, and adaptation regions. The three- fold symmetry relating the dimers within trimers was not enforced on the ECT maps nor the all-atom model. Geometry optimization in CNS (Brunger 2728-33) was performed to correct stereochemistry at junctions of the helical segments. Cross-validation methods were applied to monitor the course of refinement. The helical segments were adjusted to difference Fourier maps amidst cycles of refinement. DEN refinement (Schroder, Brunger and Levitt 1630-41; Schroder, Levitt

and Brunger 1218-22) to 20 Å resolution was applied, but produced little improvement in cross-validated refinement statistics. Refined trimers were then related by sixfold symmetry and rigid body refined into a volume composing an entire honeycomb hexameric assembly of receptor trimers. The P5-CheW ring was placed in the residual density. To extend the lattice beyond one ring structure, each subunit from the model of dimeric CheA:CheW (Bhatnagar et al. 3824-41) was superimposed on P5 domains of adjacent rings, which were positioned in the tomography maps according to the observable density and the receptor trimer positions. This action superimposed the associated CheW domains perfectly and projected the P4 domains down below the receptors. Relative to the model of dimeric CheA:CheW derived from spin-labeling studies, the P4–P5-CheW units have rotated about the hinges to P3 so that they lie in the same plane (Fig. 2-8). The superposition also placed an associated P3 in the center of the hexagon edges, between the two-facing-two receptor dimers. P3 was then rotated to complete appropriate linkages with each P4. P4 was adjusted slightly about the P4P5 linkage to optimize overlap with the tomography density.

Table 1. Data Collection and Refinement Statistics for Ternary Complex

Wavelength (Å)	0.97700
Space group	R32
Cell Parameters	a = 213.99, b = 213.99, c = 208.19
Resolution (Å)	30 – 4.5 (4.58 – 4.50)
No. of observations	59703
No. of unique reflections	10933
Completeness (%)	98.3 (96.6)
R_{sym} [a]	0.108 (0.65)
I/σ(I)	15.7 (1.9)

Refinement statistics	
Resolution range	50-4.5 (4.66 – 4.50 Å)
R factor, %	24.5 (32.5)
R_{free}, %	29.6 (35.7)
Molecules / Asym unit	1 P4-P5, 1 CheW, 2 Tm14s
Residues / Asym unit	572
Atoms	
Protein	4497
Solvent Content (%)	84
Mean B-values (Å^2)	
CheA P5	185 Å^2
CheW	197 Å^2
Tm14	206 Å^2
CheA P4	345 Å^2
Rmsd from ideal geometry	
Bonds	0.002 Å
Angles	0.8°
Ramachandran plot, %	
Most favored	67.6
Additionally allowed	29.3
Generously allowed	3.1
Disallowed	0.0
Missing residues	P4 Residues 451-507 (ATP-lid)

Data for outermost resolution shell are given in parenthesis.
[a] $R_{sym} = \Sigma\Sigma_j |I_j - \langle I \rangle| / \Sigma\Sigma_j I_j$

2.2.6 Crystal contacts and optimization of crystals

Upon getting the initial 4.5Å resolution crystal structure, we attempted various means of optimizing the crystals and increasing their diffraction resolution, including the use of different types of crystallization and additive screens. Because the crystals took about one month to grow, we also tried micro- and macro- seeding hoping to accelerate crystal nucleation and to obtain better quality crystals. However, none of our efforts to optimize produced better crystals. Because of the crystal contact involves a receptor dimer stacked with another inverted receptor dimer and the fact that the helical density is not disrupted at the junction (Fig. 2-1), we attempted to optimize crystal formation by varying the residues at the receptor's termini. Various constructs with different end truncations of the Tm14s were cloned. Among the ten new constructs we made (Tm14s (106-191, 107-192, 107-193, 107-194, 108-191,109-191), a few of them co-crystalized with CheA P4P5 and CheW in screen conditions similar to initial crystallization conditions. One construct 107-192 yielded new complex crystals that diffracted to 3.5Å resolution. Surprisingly, this new construct is only longer by one residue compared to the receptor (107-191) that yielded the earlier 4.5Å complex.

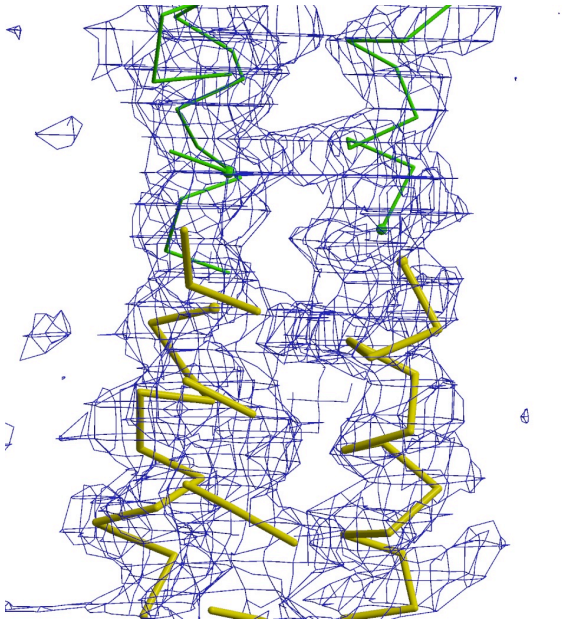

Fig. 2-1 Continuous electron density at the crystal contact region formed by end-to-end MCPs in the crystal. The yellow helices and the green helices are from two different MCP dimers.

Determination of the receptor registry

Even in the 3.5Å data set, it is challenging to determine the registry of the receptor in the complex structure, because the helical density can be well fit with shifts of the registry. We incorporated selenomethionine residues in the receptor protein (three of them in the shorter constructs), but were not able to obtain crystals. We therefore manually manipulated the positions of the receptor dimer in the asymmetric unit to allow the receptors to form continuous helices with symmetric receptors.

2.2.7 Purification and spin-labeling of receptor tips

Proteins with site-directed cysteine mutations were expressed as described before.

Because the shorter construct of Tm14 is not as stable as other proteins, these proteins were expressed in 18 °C cultures for 12 hrs. Cells were harvested and stored at -20 °C.

Cell pellets were thawed right before purification, lysed and spun down as previously described (lysis buffer containing 10% glycerol). Glycerol is added as the cryoprotectant since the protein sample is to be flash frozen prior to the ESR experiment. The cell lysate was then loaded onto the Ni^{2+} NTA column. The resin was washed one time with three times column volume wash buffer (containing 10% glycerol) to reduce non-specific binding. His-tagged receptor fragments immobilized onto the column were then spin-labeld by adding a solution containing 5 mg of MTSSL (Toronto Research) dissolved in 150 µl acetonitrile and 2.85 ml wash buffer (10% glycerol). Resin was shaken on a rocker at room temperature for 4 hrs followed by another 12 hr at 4 °C was carried out. After labeling, the protein was eluted with 10 ml elution buffer (10% glycerol). Samples were then further purified by size exclusion chromatography on FPLC. The buffer used (50 mM Tris pH 7.5, 150 mM NaCl) also contains 10% glycerol. Chromatography fractions that contain the intact spin labeled protein were combined and concentrated down to desired concentration. Protein was kept frozen at -80 °C until used in experiments.

2.3 RESULTS AND DISCUSSION

Electron cryotomography has previously shown that MCPs form extended hexagonal lattices at the poles of cells linked at their cytoplasmic tips by a CheA/W "baseplate" (Briegel et al. 30-41; Khursigara, Wu and Subramaniam 6805-6810). Moreover, a recent cryotomographic study showed that the basic architecture of the

lattice is universally conserved throughout chemotactic bacteria(Briegel et al. 17181-17186). By correcting tilt series for the contrast transfer function of the microscope before 3D reconstruction, Dr. Briegel substantially increased the resolution of the tomograms so that individual MCP dimers are now clearly visible in subtomogram averages (Fig.2-2). In all cases imaged so far, including both Gram-negative (*E. coli, Helicobacter hepaticus, and Salmonella enterica*) and Gram-positive (*Bacillus subtilis*) cells, trimers of receptor dimers are located at the vertices of the hexagonal lattice facing their three neighboring trimers in a "two-on-two" orientation. As seen previously in *Caulobacter crescentus*(Briegel et al. 30-41), the higher resolution tomograms confirm that the arrays are well-ordered near the CheA/W baseplate, but become less so in the HAMP, transmembrane, and periplasmic domains.

Based upon the new tomography images, we set out to model the receptor conformations using crystal structures of cytoplasmic domains as a starting point. The shape of the MCP complexes in the EM maps resembles the "trimer-of-dimers" crystal structure of the truncated cytoplasmic region of the *E. coli* serine receptor Tsr (Kim, Yokota and Kim 787-92). The cryo-tomograms show, however, that the receptor dimers retain their four- helix-bundle quaternary structure all the way from the CheA/W baseplate to the HAMP domains, and therefore allow a more complete modeling of the cytoplasmic domains (Fig. 2-3). In addition, the stalks of the receptor dimers appear straighter adjacent to the baseplate and diverge to a lesser extent than those of the crystal structure. A bend is seen, however, near a conserved glycine hinge that is known to be important for proper receptor function (Coleman et al. 7687-7695). Baseplate densities are also clear, but none of the existing crystal structures, including the dimer of three

subdomains of CheA (P3, P4, and P5) (Bilwes et al. 131-41) or the complex of two CheA subdomains (P4 and P5) and CheW (Park et al. 400-407) could be unambiguously fit into the EM maps.

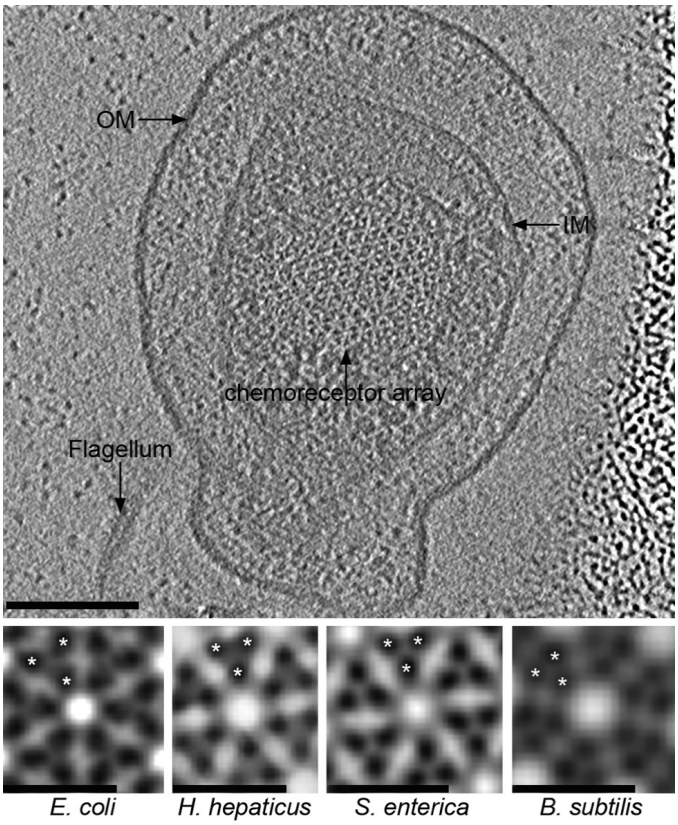

Fig. 2-2 Architecture of native chemoreceptor arrays as seen by electron cryo-tomography. (Upper) Tomographic slice through the top of a *S. enterica* mini- cell. OM, outer membrane; IM, inner membrane. (Scale bar: 100 nm.) (Lower) Subtomogram averages of *E. coli*, *H. hepaticus*, *S. enterica*, and *B. subtilis* (from left to right) chemoreceptor arrays after application of sixfold symme- try. In all cases, the individual receptor dimers (asterisks) are clearly resolved, revealing a two-facing-two packing arrangement: A pair of dimers faces another pair of dimers at each interface around the ring, or to describe it in another way, trimers are oriented such

that one receptor dimer points to- ward the center of each hexagon. The conserved architecture also shows that the cell lysis used to thin the *E. coli* and *B. subtilis* samples for high-resolution ECT did not perturb the arrays. (Scale bars: 12 nm.)

To define the interactions among the receptors, CheA and CheW at higher resolution, crystals were therefore grown of a ternary complex of *Thermotoga maritima* proteins. The ternary complex crystals contain the CheA kinase (P4) and regulatory (P5) domains, CheW, and the highly conserved signaling domain of a *Thermotoga* MCP(Pollard, Bilwes and Crane 1936-44). Although the crystals diffract to only 4.5 Å resolution and have a large unit cell (Table 1), their high solvent content and relatively simple asymmetric unit allowed for an unambiguous placement of the secondary structure elements in each component, whose high-resolution structures have all been previously determined (Park et al. 400-407; Pollard, Bilwes and Crane 1936-44).

CheW and the CheA regulatory domain (P5) are paralogs, each composed of two intertwined β-barrels known as subdomains 1 and 2 (Griswold et al. 121-5). Up until now, the significance of this relationship has not been fully appreciated. Within the asymmetric unit, P5 subdomain 1 binds CheW subdomain 2 in a pseudosymmetric interaction previously characterized (Fig. 2-4 A, Left) (Park et al. 400-407; Zhao and Parkinson 3299-3307) 32. The receptor tip binds alongside CheW at the junction between the two β-barrels with a configuration consistent with previous structural (Bhatnagar et al. 3824-41) and other studies (Boukhvalova, VanBruggen and Stewart 23596-23603; Underbakke, Zhu and Kiessling 483-95) (Fig. 2-3A, Right). CheW primarily contacts the receptor on the helix N-terminal to the hairpin tip. Due to the dimeric nature of the receptor, the symmetry-related helix on the adjacent subunit faces

the receptor trimer interface. Competition for binding the same N-terminal helix may explain why overexpression of CheW interferes with receptor trimer formation (36).

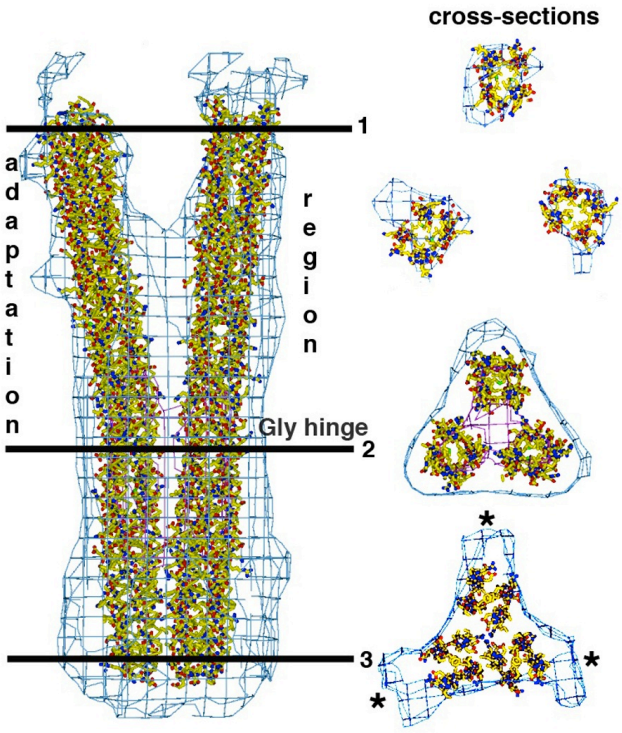

Fig. 2-3 Model of a receptor trimer within the EM map. Two isosurfaces of the receptor region of the EM map are shown as blue and magenta grids (low and higher density, respectively) with an all-atom model of a receptor trimer fit to the map, seen from the side (Left, with back dimer removed for clarity) and in cross-section at three different positions (Right). The atomic model is based on a crystal structure of a truncated E. coli Tsr MCP which crystallized in a similar configuration(Kim, Yokota and Kim 787-92). To fit that structure into the EM map, the four- helix coiled-coil was extended (based on the crystal structure of receptor Tm1143 (Park et al. 400-407)) to the junction of the HAMP domain (residues 264–514), separated slightly at the tips to better fit the electron density, and then refined

against the EM data in reciprocal space (see Materials and Methods). The density clearly confirms the trimers-of-dimers architecture in vivo, but compared to the crystal structure, the receptors bend in the glycine hinge region and the four-helix coiled-coil extends to the level of the HAMP domain. The hexagonal order decreases toward the membrane. The additional density seen around the receptor tips (asterisks) is where the receptor bundle connects with the CheA/W baseplate.

Not anticipated, the crystallographic symmetry reveals a remarkable extended assembly state for the ternary complex (Fig. 2-4B). The crystallographic threefold axis generates a ring structure of the CheW and CheA regulatory domains wherein subdomain 2 of the regulatory domain binds to subdomain 1 of CheW in a contact that mimics the associations made by the analogous surfaces of the opposing β-barrels (Fig. 2-4A, Center). Furthermore, the distal ends of the receptor helix bundles interact with the regulatory domains in a manner that mimics that of the receptor tip with CheW (Fig. 2-4B and Fig. 2-5). Together, these associations generate a large double- ring structure of pseudo-sixfold symmetry with receptors binding alternatively to the CheW and P5 units around the ring (Fig. 2-4B).

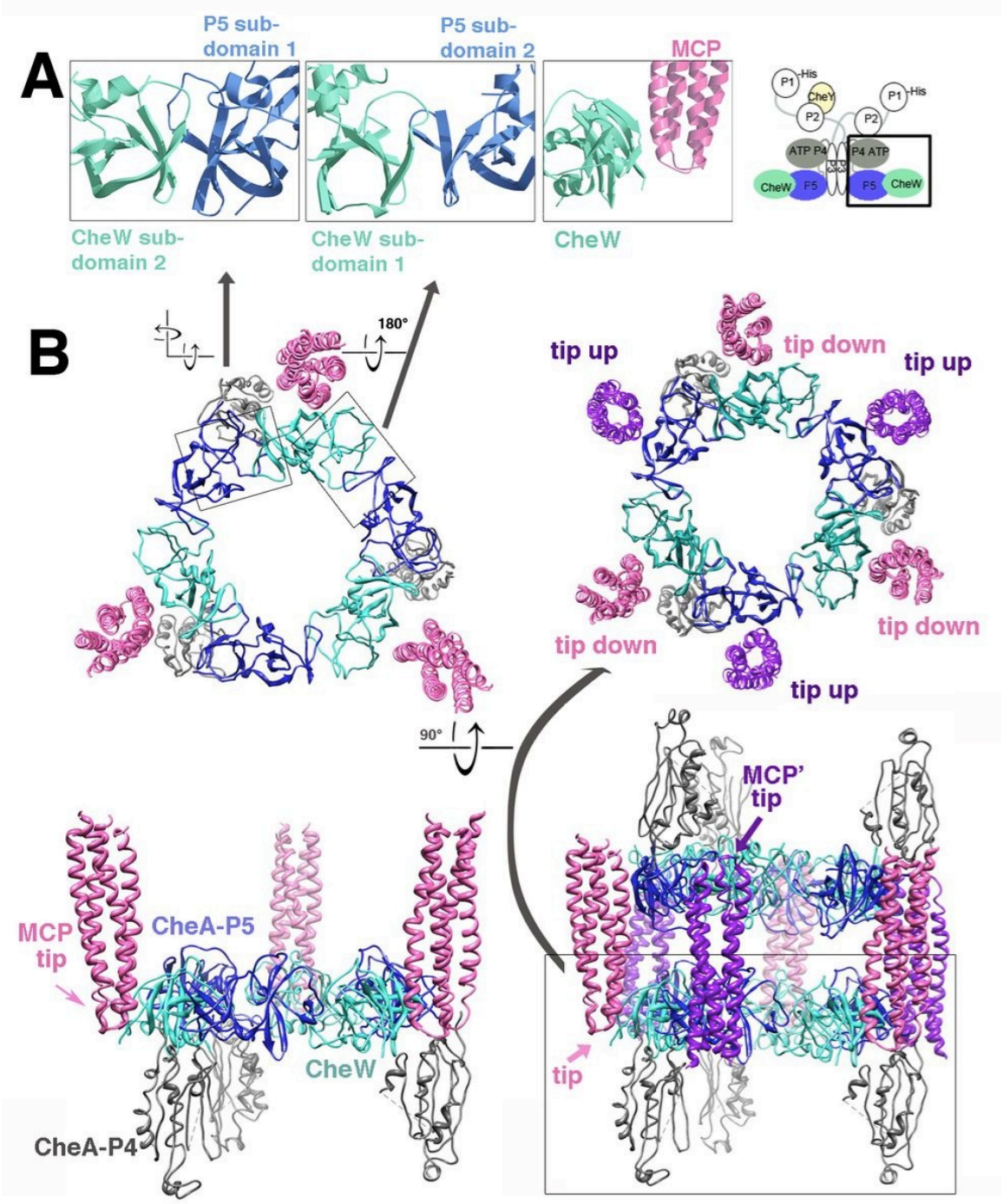

Fig. 2-4 Ternary complex crystal structure of T. maritima chemotaxis proteins. (A) Close-ups of the pseudosymmetric interactions made by the opposite ends of CheW (green ribbons) and P5 (blue ribbons), and the interaction between the receptor tip (magenta ribbons) and CheW. Inset shows a schematic of dimeric CheA:CheW, with

the crystallized unit boxed. (B) Ring structure formed by the ternary complex crystals. Three CheW domains and three P5 domains generate a ring, and each CheW binds one receptor tip (pink) between subdomains 1 and 2 (Left). Similar interactions between P5 with the distal end of receptors (purple) link rings "head-to-head" in the unit cell (Right). The P4 domains (gray), of which only the core elements are visible, project above and below the double-ring structure at the junction to P5.

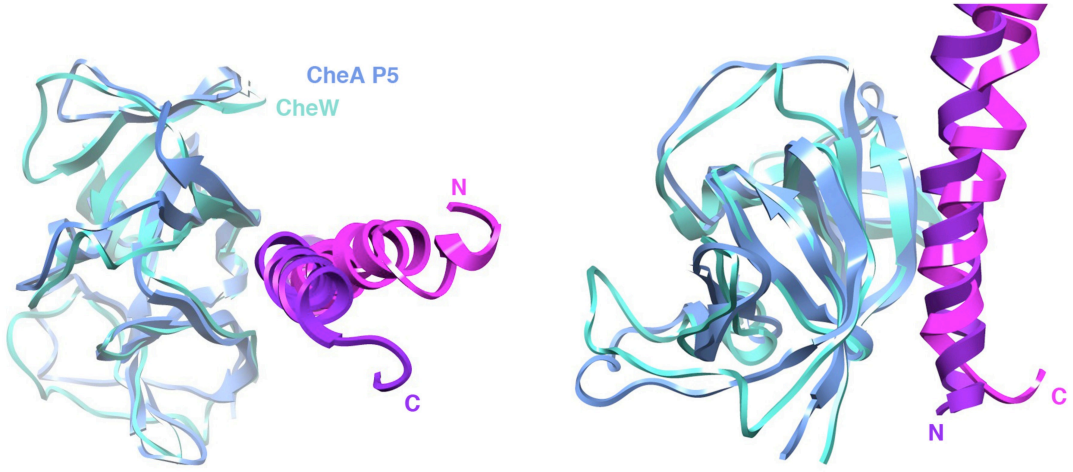

Fig. 2-5 Similarity of receptor helix binding by CheW and P5. Superposition of CheW (green ribbons) and P5 (blue ribbons) with their associated receptor helices (pink and purple ribbons, respectively) as seen in the crystal structure. In the case of CheW, the receptor helix N-terminal to the hairpin tip binds into the groove formed between subdomain 1 and 2. The analogous groove in P5 binds the N-terminal end of the same receptor helix running in the opposite direction.

Although alternating receptor bundles around the ring are antiparallel, each of the receptor dimers docks a helix into a groove that is conserved between the two β-barrels of

either CheW or the CheA regulatory domain P5 (Fig. 2-4). The interaction between the regulatory domain and the receptor as found in the crystal is likely nonnative because it would require adjacent receptors around the ring to be oriented in opposite directions, which is implausible because they all traverse the membrane. However, given the residue conservation of P5 and CheW in the binding groove and the similarity in helix side-chain interactions indicated by the two different receptor associations, it is likely that P5 can also bind a receptor tip in the same orientation as CheW does. In support of this important inference, CheA is known to bind receptors without CheW (Bhatnagar et al. 3824-41; Levit, Grebe and Stock 36748-54), isolated P5 domains are recruited to receptor clusters independent of CheW(Kentner et al. 407-417), and CheA and CheW compete for the same or overlapping binding determinants on receptors (Levit, Grebe and Stock 36748-54; Asinas and Weis 30512-30523). The P4 kinase domains are not well defined in the crystal structure, but density for the central β-sheet and some peripheral helices is observed projecting above and below the rings at the junction to P5 (Fig. 2-4B and Fig. 2-5).

One ring of the crystal structure with its six associated receptors holds a striking relationship in symmetry, dimension, and shape to the CheA/W baseplate density in the cellular tomograms. Superimposing the three receptor bundles associated with one ring of the crystal structure with those fit to the EM maps (Fig. 2) accommodates the CheA P5-CheW ring well within the honeycomb lattice (Fig. 4A). A corresponding ring of density can be seen in the EM maps, although at lower contour levels than the receptor density (Fig. 2-7A). Thus, the P5-CheW ring is present in cells, but with either lower occupancy or higher disorder than the receptor trimers. Superposition of the P5-CheW unit with one

subunit of the dimeric-CheA-bound-to-CheW model from crystallographic and spin-labeling studies(Bhatnagar et al. 3824-41) places the second P5 subunit within the neighboring hexagon, and rotating about the P3–P4 junction to bring the CheA P5 subunits into planarity aligns CheW and P5 with their expected receptor contacts in the neighboring hexagon (Fig. 2-8) Without additional manipulation, the kinase domains now project below the rings and be- tween the hexamers in a region of the EM maps that also shows substantial density (Fig. 2-7B). If the CheA dimerization domain (P3) remains connected to one of either CheA subunit, these manipulations place the dimerization domain in the space between the two-facing-two receptor dimers (Fig. 2-7C). Rotation about the center of P3 provides reasonable connections to the kinase domains of both subunits and aligns the dimeric axes of P3 with those of the receptors (Fig. 2-7C and Fig. 2-8), as indicated by prior studies(Bhatnagar et al. 3824-41; Miller et al. 8699-711). However, there is little density in this location in the EM maps, which suggests that the dimerization domain does not assume a fixed position against the receptors.

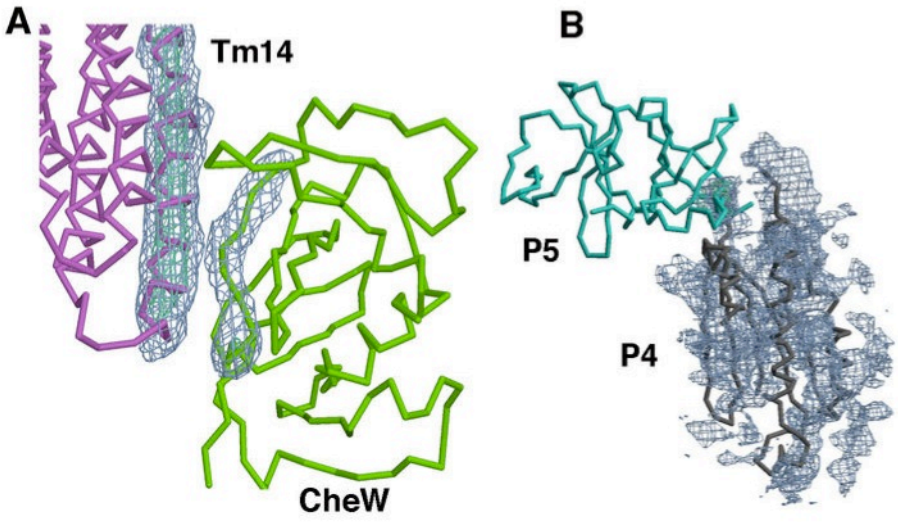

Fig. 2-6 Unbiased 4.5 Å resolution electron density for the CheA:Tm14s:CheW

ternary complex. (A) Simulated-annealed Fo-Fc omit electron density (blue mesh 3 σ; cyan mesh 5 σ) for an interacting helix (magenta trace) of Tm14 and β-strand of CheW (green trace). (B) Fo-Fc electron density (blue mesh 1.5 σ) in the region of the CheA P4 domain (grey trace) where it connects to P5 (top, blue trace). The P4 domain was not included in the Fc calculation. The P4 model does not contain the ATP lid region.

The structure of the array precludes CheA, however, from being present in three copies in every ring of the lattice (Fig. 4D). Thus the lattice has P6 point symmetry (Fig. 2-6D) and in terms of CheA/CheW content comprises one empty hexagon surrounded by six occupied hexagons, each containing three CheA and three CheW subunits.

The position of the CheA/W complex bridging two trimers of receptor dimers is consistent with the stoichiometry found in the activating complex: 2 receptor trimers of dimers, 1 $CheA_2$, and 2 CheWs (Li and Hazelbauer 9390-9395). With this ratio, the nanodisk incorporated full-length receptor Tar can activate the kinase to the similar level of membrane vesicle embedded receptors activates the kinase.

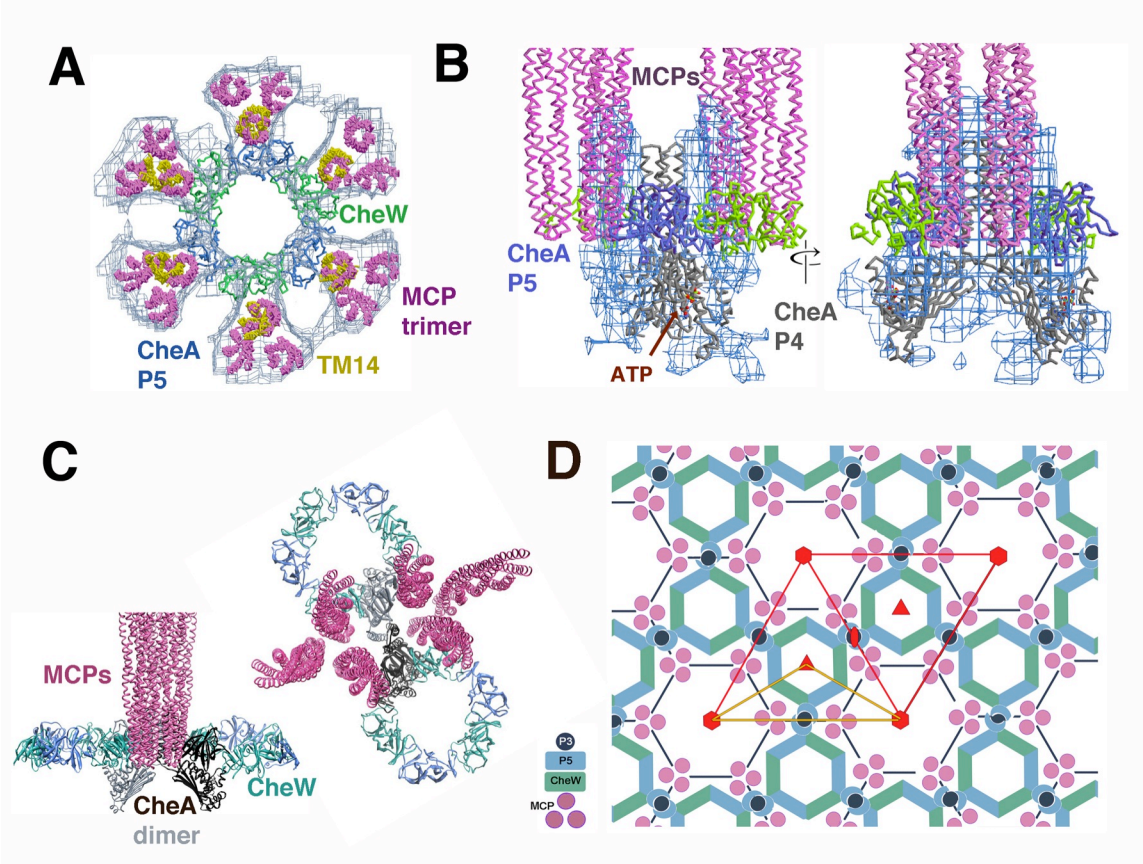

Fig. 2-7 Structure of native chemoreceptor arrays. (A) Superposition of one ring of the crystal structure (P5 blue, CheW green) with its six receptor dimers (yellow helices) on the EM map (blue mesh) with its previously fit 18 receptor dimers (pink). The EM density in the CheA/W ring is only about half as intense as within the receptors, suggesting either lower occupancy or higher disorder. (B) Side view of the EM density (blue mesh) in the region of the CheA-P4 kinase domain (gray). (C) The CheA dimer links CheW/P5 rings. The two subunits of the CheA dimer (black and gray) provide one P5 to each of two neighboring rings. The P3 dimerization domain resides between the receptor bundles at the center of one hexagonal edge and the P4 domains reside beneath the interlocked rings. Views shown are in the plane of the rings (Left) and looking down from the membrane (Right). (D) The

arrangement of components within the receptor array produces P6 point symmetry (P6 unit cell boxed in red, with the asymmetric unit in yellow; six-, three-, and twofold symmetry axes are designated in red). The lattice gives a CheA:CheW:MCP subunit stoichiometry of 1:1:6. If the "empty" hexagons instead contain six CheW proteins, the ratio would become 1:2:6.

This arrangement produces a $CheA_2$:CheW:$(MCP_2)_3$ subunit stoichiometry of 1:2:2. Not all CheA or CheW nodes in the lattice need be filled to produce an extended, stable structure, however, which may explain the lower density of the rings in the EM maps. In the past literatures, there have been different, and very controversial CheA:CheW:MCPs subunit ratios published, varying among 1:4:6(Levit, Grebe and Stock 36748-54); 1:0.8:6.8(Li and Hazelbauer 3687-3694); and 1:3:6–9(Erbse and Falke 6975-6987). People have contributed this discrepancy to sample preparation and Greater than 1:1 CheW to CheA ratios may be due to CheW substituting for CheA at certain positions within the lattice or even composing complete rings. If six CheW proteins were to fill the empty hexagon of the lattice, the subunit stoichiometry becomes 1:2:2. The completeness of the native arrays may also vary under different conditions, thereby leading to a range of measured ratios. This could also explain the observations that excessive amount of CheW can inhibit chemotaxis. If CheW is in excess than CheA, CheW molecules could replace CheA in the ring and lower the copies of CheA in the lattice and hereby the kinase activity measured.

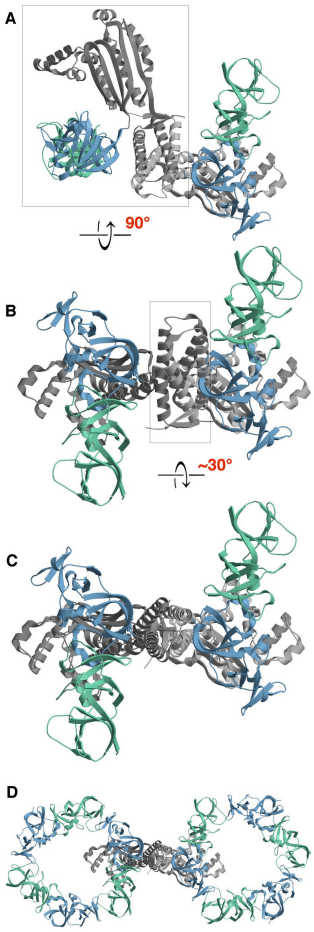

Fig. 2-8 Domain manipulations for modeling the CheA dimer into the chemoreceptor arrays. (A) Domain orientations in the dimeric CheA:CheW model derived from crystallography and ESR-spin labeling (P3-P4, grey; P5, blue, CheW, green; the two copies of P3-P4 within the dimer are distinguished by different shades of grey). (B) A ~90° rotation about the P3-P4 linkage of the right subunit brings the second P5-CheW unit of the ESR model into the same plane as the first. The boxed domains of the left subunit shown in (A), which include the P4 domain and the entire P3 domain, were transformed as a rigid body. (C) The P3 domain (boxed in (B)) was then rotated by ~30 ° to align it with the receptor helices and optimize connections to the two P4 domains. (D) Expansion of the two P5-CheW

units of the CheA dimer into the connected rings found in the crystal structure. The dimensions of the CheA dimer positions the planar P5:CheW units perfectly for anchoring the CheW:P5 rings inside the hexagonal lattice of receptor trimer-of-dimers defined by electron cryo-tomography.

Previous work supports the notion that different CheW/ P5-type domains can compete for similar positions within the arrays. CheA and CheW recognize overlapping sites on receptors with comparable dissociation constants (within a factor of approximately 10), but they also bind synergistically and in a manner that depends on the receptor stoichiometry (Levit, Grebe and Stock 36748-54; Asinas and Weis 30512-30523; Erbse and Falke 6975-6987). This competitive, yet cooperative behavior is consistent with a lattice structure where interactions among CheA and CheW subunits organize receptor binding surfaces that are similar on the two proteins. Furthermore, CheW and the P5 regulatory domain may substitute for each other within the rings, with different compositions producing different aggregate levels of kinase activity. Structural data have demonstrated that the P5 domains can self-associate through a symmetric contact that mimics the interaction observed with CheW in the ternary crystal structure(Bilwes et al. 131-41; Park et al. 400-407). Many bacteria also contain CheV, which is a fusion between a CheW and a CheY domain, the latter of which can be phosphorylated by CheA(Alexander et al. 494-503). The function of CheV varies among organisms, but generally overlaps with that of CheW(Alexander et al. 494-503). It follows that CheV proteins may also replace CheA P5 and/or CheW within the hexagonal lattice and thereby influence coupling between receptor and kinase.

Thus, the precise composition of the rings in terms of CheW, CheA, and CheV

may vary in different signaling states, while still maintaining the interlocking nature of the baseplate, which would explain the ultra-stability of the arrays(Erbse and Falke 6975-6987) and provide the structural connections needed for highly cooperative responses. This model is also consistent with the idea that signal amplification derives from kinase coupling within the extended lattice(Goldman, Levin and Bray 1853-1859); however, interactions among receptors, CheW, and CheA all may contribute to cooperativity. Finally, because the cells imaged here had adapted to their surrounding conditions, they are expected to contain both active and inactive CheA; hence, the modeled network likely reflects a mixture of these two states(Briegel et al. 748-57).

Conformation of the ternary complex

The CheW/receptor distance in the crystal structure matches well with the PDS distance measured in solution(Bhatnagar et al. 3824-41). For example, the distance between S80 of CheW and E167 of the receptor in the crystal structure is 21 Å while the R_{max} in the PDS study is also 21 Å. The K9 of CheW to E149 of the receptor is 22 Å while the R_{max} in the PDS study is 28 Å. Given that the PDS distances were derived from an inhibitory complex in solution and the same type of MCP was applied in both studies, it is possible that the crystal structure we obtained correspond to that of the inhibitory state.

Pairwise interfaces within the ternary complex

MCP interface with CheW

It was confirmed by the NMR study of the Tm14/CheW interface that the shorter

construct of Tm14 retains the native structure of Tm14 and binds to CheW with the same manner as full length Tm14 (Vu et al. 759-67). Also because of the remarkably reserved receptor tip sequence (Alexander and Zhulin 2885-90) , we believe the binding mode is commonly preserved.

In the crystal structure, the receptor homo-dimer binds to CheW almost exclusively with the N-terminal side of the tip. Residues Leu138, Ile142, Glu143 and Arg146 are the ones most close to CheW. This binding interface is in good agreement with the NMR chemical shift study on Tm14/CheW binding interface (Vu et al. 759-67) . On the C-terminal side of the MCP tip, the crystal structure shows the residues 152, 153 of are on the binding interface, which may be the residues on the C-terminal side of the tip to undergo chemical shifts upon CheW binding in the NMR study.

Interestingly, a previously identified residue in Tsr R366 (correspond to R146 in Tm14) whose mutation to any other residue caused chemotaxis defects as well as failure to form the ternary complex (Mowery, Ostler and Parkinson 8065-8074) is found to have its side-chain in close proximity with Val27 and Asp28 of CheW (Val27 was measured to have the biggest methyl chemical shift on receptor binding). Although the side chain of R146 cannot be determined without ambiguity because of its position near the tip region, it could adopt a conformation to form hydrogen bonds with both the side chains of Glu12, Asp28 and the main chain carbonyl of Val27 (Fig. 2-9). Furthermore, R146 in this conformation also forms salt bridges with Glu12 and Asp28. The authors of the biochemical study favored the interpretation that mutation of R146 disrupts the trimer-of-dimers and hereby lead to defective chemotaxis. However, based on the crystal structure we believed that simply because this residue is important for receptor/CheW interaction,

and that its mutation will disrupt the ternary complex. There is no alternative residue that can satisfy the formation of three hydrogen bonds with nearby CheW residues. This rationale can explain why any mutation of this residue leads to chemotaxis defects.

It is noteworthy that reasonable area of the hydrophobic surfaces from both the MCP side and CheW side are buried in the binding interface. For example, I142 (MCP) with V101 (CheW), L138 (MCP) with Gly100 (CheW), Ile135 (MCP) with Val98 (CheW) are all neighboring residues at the interface (Fig. 2-10). The exclusion of the once solvent-exposed hydrophobic residues likely favors the binding of the CheW to MCP.

CheW interface with MCP

In our crystal structure, CheW binds to the receptor with a groove formed by β strands 1,3 and 8. The groove is located between the two β barrels and hosts quite a few hydrophobic residues. The binding interface agrees well with previous biochemical studies including the findings of the genetic suppressor screens (Vu et al. 759-67; Boukhvalova, VanBruggen and Stewart 23596-23603; Boukhvalova, Dahlquist and Stewart 22251-9) . Among the residues on CheW with the largest chemical shift of the methyl side chain upon adding receptors, Val27 and Val98 are closest to the receptor, also in close proximity with Ile42 and Ile135 of the MCP, respectively. The large perturbation in environment from the solvent exposed one to a buried binding interface surrounded by hydrophobic residues can explain the observation of the big chemical shifts. The residues with moderate chemical shifts Leu14, Ile30 and Leu99 also reside close to the receptor. Besides these residues identified before, we believe Met32, Val33,

Val98, Leu99, and Val101 are also important residues for binding because of their positions at the interface.

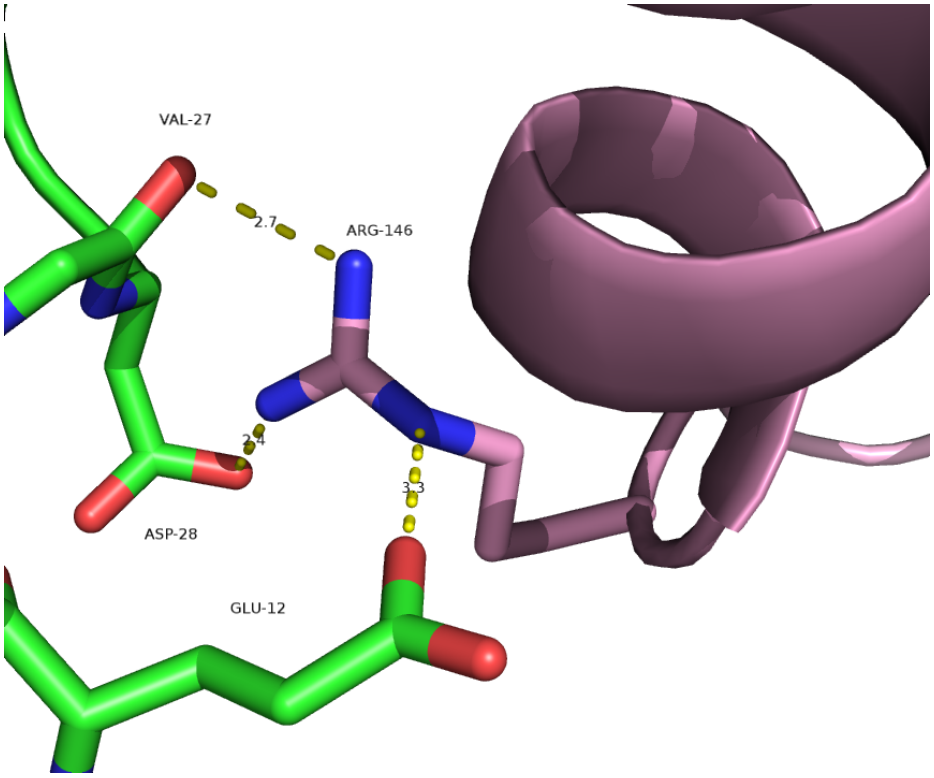

Fig. 2-9 The role of R146 of MCP on interface formation. R146 is involved in forming H-bonds with three residues of CheW. The mainchain and the carbon atoms of MCP are shown in pink wheras the mainchain and the carbon atoms of CheW are shown in green. Oxygen atoms are color-coded in red and nitrogen atoms are in blue. Hydrogen bonds are denoted as yellow dashed lines.

Previously identified mutant of residue EcCheW V36 (correspond to TmCheW I30), which totally abolished chemotaxis (Boukhvalova, Dahlquist and Stewart 22251-9) , resides at the interface of CheW and MCP. Interestingly, this mutant not only caused binding deficiency of CheW to MCP, but also caused lower CheW/CheA binding affinity,

which could imply that the signal is propagated on CheW from the MCP binding side to the CheA binding side. All other mutants identified to hamper MCP/CheW binding also weakened CheA/CheW binding (Boukhvalova, VanBruggen and Stewart 23596-23603) , but mutations that affected CheA/CheW binding did not necessarily affect MCP/CheW binidng.

The only exception is 154o CheW, which has a deletion of the C-terminus helix (last 13 residues) (Boukhvalova, VanBruggen and Stewart 23596-23603) . The C-terminus helix has weak interaction with P5 as seen in the crystal structure. While this construct decreased the binding of CheW to CheA, its deletion increased the binding affinity of CheW to MCP by 3 fold, producing a K_d value of 3.6 μM (*wt* K_d = 11 μM). We tested 154ocr in our crystallization studies, but unfortunately we did not obtain crystals of this variant. We will discuss the role of CheW C-terminal helix in the next chapter with more detail.

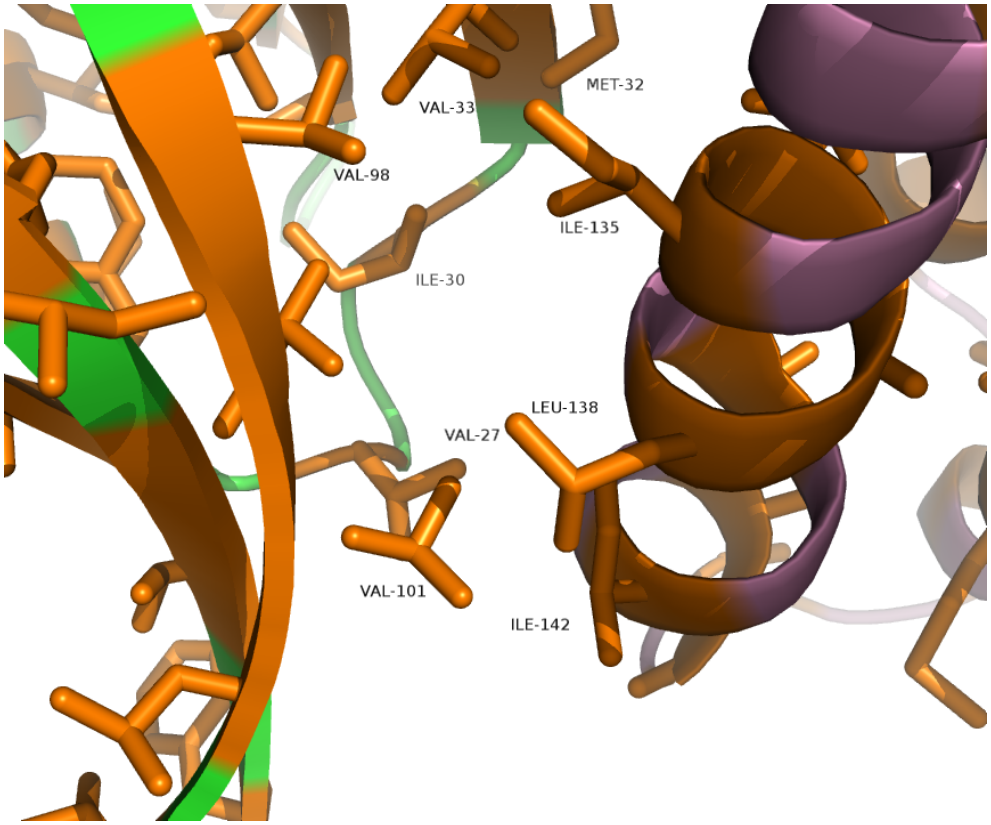

Fig. 2-10 Hydrophobic residues at the MCP/CheW interface. The side chains of the hydrophobic residues on MCP and CheW at the interface are indicated in orange stick model. The main chain is also colored in orange on the ribbon model. A good number of hydrophobic residues reside at the interface and hereby be buried.

CheW interface with CheA P5

In the ring formed with alternating CheW and CheA P5, CheW interact with P5 through both β barrels. Subunit 2 of CheW interacts with subunit 1 of CheA P5 as previously observed in the crystal structure of CheW with CheA P4P5. The binding site on this end of CheW involves β4, β5 and the loop between β3 and β4. The short C-terminal helix of CheW also interacts with P5 on this end. This agrees well with the prediction of the binding interface by mutagenesis studies and NMR dynamics (Griswold

et al. 121-5; Boukhvalova, VanBruggen and Stewart 23596-23603; Boukhvalova, Dahlquist and Stewart 22251-9) , although not all the predicted residues are directly at the interface (Boukhvalova, VanBruggen and Stewart 23596-23603) . For example, two glycine residues, EcCheW G57 (correspond to TmCheW G51), EcCheW G133 (correspond to TmCheW G124) do not reside directly at the interface. This indicates the mutations of these residues can trigger conformation changes at the binding interface, which is another circumstantial evidence that conformational signals may be propagated towards the CheA/CheW binding interface from the MCP/CheW side.

The binding interface at the other end of CheW on the other end involves subunit 1 of CheW and subunit 2 of CheA P5. This binding interface was a novel observation, which was not identified for the first time. On CheW, the contact mainly involves the two flexible loops linking β8 and β9, β9 and β10, as well as part of β10. The mutagenesis study found residues at this interface that affected binding and chemotaxis (Boukhvalova, VanBruggen and Stewart 23596-23603) . However, in the previous NMR study, this interface was not recognized (Griswold et al. 121-5) .

P5 interface with MCP

The first interface involving subunit 1 on P5 includes β9, part of β10, loops between β8 and β9, β9 and β10. The second interface on P5 involves β4, part of β5 and the loops linking β3 and β4, β4 and β5. As mentioned earlier, the P5 domain of CheA is homologous to CheW. A superposition of CheW and P5 can be found in the next chapter. One noticeable difference between the two is the C-terminus helix besides the loop regions. CheW has a longer C-terminus helix

Flexible turn at the tip of the receptors

As mentioned earlier, the receptor cytoplasmic module is composed of two helical hairpins. Each subunit folds back on itself to form a two-stranded anti-parallel coiled coils that then dimerize into a four-helix bundle. The membrane-distal tip of the receptor is located at the hairpin turn.

In our higher resolution (3.5 Å) structure, there is still no density for the tip region. We believe it is due to the high mobility of the tip region. In the crystal structure, the ensemble of all different conformations represented within the crystal degrades the quality of the electron density. This result is in agreement with the NMR study of receptor Tm14, where the backbone assignment of the tip residue E149 was not possible because of conformational heterogeneity or the solvent-exchange effects(Vu et al. 759-67). We believe it is the former reason that the tip is too flexible to be nailed. To test this hypothesis (i.e. dynamics), we labeled the Tm14 tip residue E149 with nitroxyl label and measured the intra-dimer distance between the tip residues by DEER. As we expected, the intra-dimer distance of the tip residues is broadly distributed in solution (Fig.2-11). Furthermore, even in the presence of CheA and CheW, the distance profile doesn't vary from that of the receptor alone, which indicates that the space the tip residue samples is independent of CheA/CheW binding or complex formation. The PDS measurements also indirectly confirm the binding of CheW to Tm14 is above the tip as observed in the crystal structure. Another piece of evidence came from the cross-linking data(Bhatnagar et al. 3824-41) where readily crosslinked product of K9C of CheW and R149C of tm14 were obtained. If the tip of the receptors extended straight down from the upper part, the R149 of receptor and K9 of CheW would be on the same plane orthogonal to the receptor

stalk, but about 22 Å apart from each other. In order for the cross-linking to happen, the receptor has to swing across the plane.

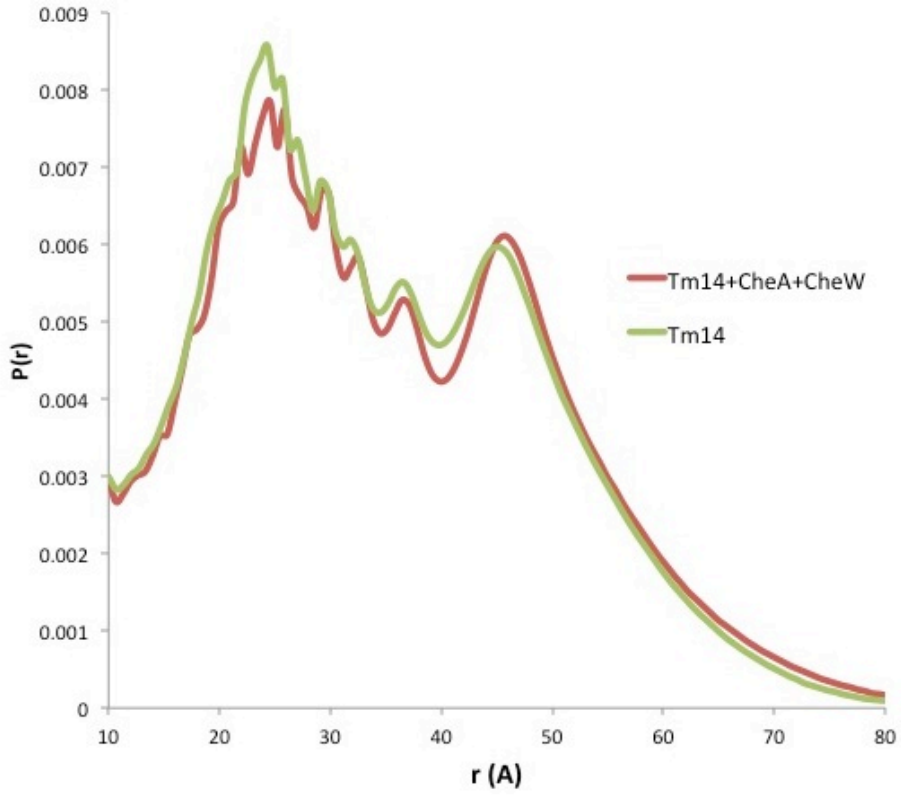

Fig. 2-11 Tm14 E149 intra-dimer distance distribution resolved from spin-label dipolar coupling in the absence and presence of CheA and CheW. The distance is broadly distributed in the detectable range of DEER from 10 to 80 Å. The distribution doesn't change in the presence (red curve) and in the absence (green curve) of CheA and CheW.

The Glu149 residue at the very tip region is highly conserved among chemoreceptors and may play crucial role in the signaling. In a previous study, Mowery

et. al constructed mutants at the corresponding site E391 in *E. coli* Tsr receptors and found that all bulky mutants (e.g. E391F, E391W, E391Y) impaired chemotaxis, but did not the localization of receptor/CheA/CheW or receptor trimer-of-dimers formation(Mowery, Ostler and Parkinson 8065-8074). This result indicates that such mutations at the tip only jeopardize the signal transduction in the receptor homodimer, but not the ternary complex formation, the trimer-of-dimers or the clustering of receptors. As we also observed in the crystal structure and the DEER experiments, the movement of the tips is not restraint with the ternary complex formation and is extensive in both the isolated receptors and when the receptors are in the ternary complex. We believe that substitution to bulky residue likely cause collisions, which prevents the tips to move freely and thereby causes defective chemotaxis. It is possible that the movement of the tips is required for signal transduction, more specifically that the tip flexibility contributes to the recognition of the correct binding site for CheW or CheA P5.

Further complication of the signaling complex

In other organisms other than *E. coli* paralogs of the same chemotaxis proteins and a variety of chemotaxis proteins greatly complicates the system (Wadhams and Armitage 1024-37; Sourjik and Armitage 2724-2733) . Even within the *E. coli* system, other players in the signaling pathway whose impact has yet to be determined, especially those that co-localize with the ternary complex at the cell poles are still awaiting further study.

Below are a few examples of such players. Among them, $CheA_s$ and CheZ are co-localized at the poles with the ternary complex.

$CheA_s$

$CheA_s$ is an alternately processed version of CheA that encoded on the same reading frame(Smith and Parkinson 5370-4). It lacks the first 97 residues of CheA, while only retains its last helix of the five helices. $CheA_s$ presumably dimerize with both itself and full-length CheA (Wolfe, McNamara and Stewart 4483-91) . Because it does not have the histidine residue in the Hpt domain, a $CheA_s$ homodimer is not able to auto-phosphorylate. However, a heterodimer of $CheA_s$/CheA can carry out auto-phosphorylation. Even a heterodimer of $CheA_s$ and CheA with a defective ATP binding domain is functional, consistent with the fact CheA auto-phosphorylation is of trans-mechanism(Wolfe, McNamara and Stewart 4483-91).

CheZ

CheZ, the CheY phosphatase of *E.* coli, is localized at the cell pole together with the other 3 proteins that compose the ternary complex(Vaknin and Berg 17072-17077). A protein exchange dynamics study by fluorescent recovery after photobleaching (FRAP) showed that clustered CheZ at the pole has a low exchange rate with cytoplasmic CheZ (~8 mins), on the scale comparable with CheA and CheW(12 mins) while CheR/CheB (~15 s) and CheY exhibit faster exchange rate(Schulmeister et al. 6403-6408). This study suggested that CheZ can be considered as "a further part of the stable cluster core".

It was revealed by structural studies that CheZ bind to $CheA_s$ on the truncated P1 domain, which is the last helix of full-length CheA (Hao et al. 5842-4; Cantwell et al. 2354-61; O'Connor, Matsumura and Campos 5845-8). With regards to CheZ, it binds to its substrate CheY through its C-terminus(Guhaniyogi, Robinson and Stock 624-45; Guhaniyogi et al. 1419-28).

CheY has inherit phosphatase activity, but CheZ reduces the life time of the phosphorylated CheY from ~10s to ~0.1s(Segall, Manson and Berg 855-7). *In vivo* FRET between CheY and CheZ confirmed the dephosphorylation also happens at the pole cluster(Vaknin and Berg 17072-17077). Although phosphorylated CheY ($CheY_p$) and unphosphorylated CheY bind to CheZ and CheA respectively, CheZ determines the localization of CheY more profoundly. With the phosphatase localizing at the pole next to the kinase, the cell experiences a more uniformly distributed $CheY_p$ concentration compared to a CheZ mutant that doesn't bind to the cluster. Uniformed p-CheY concentration is especially important for the flagella motors. What is more fascinating about this study is that CheZ may contribute to the sensitivity of the signaling pathway. It was found that delocalization of CheZ caused the cells to reduce the chemotactic response to ligand. In the presence of the adaptation proteins (CheR and CheB), the effect was even more pronounced.

CheY

CheY, despite its ability to diffuse within the cell, is in highest concentration at the poles as well (Vaknin and Berg 17072-17077) . Despite its constant association and disassociation from the ternary complex (Schulmeister et al. 6403-6408) , it can be regarded as a member of the polar clusters and may possibly bind to CheZ and CheA simultaneously.

CheY binding to CheA domain P2 recruits CheY to CheA and increases the phospho-transfer rate. It was found that the Asp phosphorylation site in *E. coli* CheY is more open in P2-bound CheY than in CheY alone. Interaction with P2 increases the solvent accessible area of the active site Asp, which is partially mediated through Phe14

adopting a more open conformation(McEvoy et al. 7333-8; Volz and Matsumura 15511-9). There are several other complex structures available containing the *E. coli* P2 domain and CheY. They share common binding interface, but the specific hydrogen bonding sites vary, which implies the plasticity of CheY when it binds to CheA(McEvoy et al. 7333-8). In the complex crystal structure of *T. maritima* P2 and CheY, more drastically different binding was found even though *E. coli* and *T. maritima* P2 and CheY share structural and sequence similarity (Park et al. 11646-51). The CheY in the *T. maritima* complex flipped almost 90° relative to the *E. coli* one. All these findings may be due to the versatility of CheY/P2 binding mode, or because there is another binding partner contributing to the interaction. CheZ could be a potential third binding parter with CheY and CheA in *E. coli.* In *T. maritima,* instead of CheZ, there are the CheC/CheD and CheX phosphatases, which could explain the different interaction modes of P2 and CheY in the two organisms. An NMR study of the interaction between CheY and a CheZ C-terminal peptide found that CheY binds CheZ with a face similar to the one that mediates binding to P2. However, this difference could be due to the fact only a fragment of CheZ was used in this study. The binding of a fragment of CheZ to CheY could be drastically different than binding a full-length CheZ. Also, the mutagenesis study of the CheY binding site of CheZ predicted different binding sites than the NMR study.

It is also a very intriguing fact that CheY binds to P2 with its C-terminal region, which is not conserved with CheB, the other binding partner of the CheA P2 domain. This is surprising because CheB shares overall sequence similarity with CheY in the P2 binding domain (McEvoy et al. 7333-8).

Summary

Chemoreceptor arrays are super-molecular transmembrane machines that allow bacteria to sense their surroundings and respond by chemotaxis. We have combined X-ray crystallography of purified proteins with electron cryo-tomography of native arrays inside cells to reveal the arrangement of the component transmembrane receptors, histidine kinases (CheA) and couplers (CheW). Trimers of receptor dimers lie at the vertices of a hexagonal lattice in a 'two-facing-two' configuration surrounding a ring of CheA regulatory domains (P5) and CheWs. Whereas the CheA kinase domains (P4) project downward below the ring, the CheA dimerization domains (P3) link neighboring rings to form an extended, stable array. This highly interconnected protein architecture underlies the remarkable sensitivity and cooperative nature of transmembrane signaling in bacterial chemotaxis. From the crystal structure of the ternary complex, we also identified the residues important for interactions between proteins and compared the findings with published biochemical studies. Future directions include understanding the regulation mechanism of the kinases by the MCPs, determining the conformation changes upon activation and taking into consideration other binding partners.

** Partial content of this chapter is from the published paper of "Bacterial chemoreceptor arrays are hexagonally-packed trimers of receptor dimers networked by rings of kinase and coupling proteins" on Proc Natl Acad Sci U S A. 2012 Mar 6;109 (10): 3766-71.

Xiaoxiao Li has performed experiments on the crystallography part of the work. Ariane Briegel has performed the experiments on the EM tomography part of the work. Ariane Briegel, Xiaoxiao Li, Grant Jensen, and Brian Crane designed research; Kelly Hughes

contributed new reagents/analytic tools; Ariane Briegel, Xiaoxiao Li, Alexandrine Bilwes, and Brian Crane analyzed data; Ariane Briegel, Xiaoxiao Li, Alexandrine Bilwes, Grant Jensen, and Brian Crane wrote the paper.

REFERENCES

Agulleiro, J. I., and J. J. Fernandez. "Fast Tomographic Reconstruction on Multicore Computers.." *Bioinformatics (Oxford, England)* 27.4 (2011): 582-3.

Alexander, R. P., et al. "CheV: CheW-Like Coupling Proteins at the Core of the Chemotaxis Signaling Network.." *Trends in microbiology* 18.11 (2010): 494-503.

Alexander, R. P., et al. "Evolutionary Genomics Reveals Conserved Structural Determinants of Signaling and Adaptation in Microbial Chemoreceptors.." *Proceedings of the National Academy of Sciences of the United States of America* 104.8 (2007): 2885-90.

Ames, Peter, et al. "Collaborative Signaling by Mixed Chemoreceptor Teams in Escherichia Coli." *Proceedings of the National Academy of Sciences* 99.10 (2002): 7060-5.

Asinas, A. E., and R. M. Weis. "Competitive and Cooperative Interactions in Receptor Signaling Complexes." *The Journal of biological chemistry* 281.41 (2006): 30512-23.

Bhatnagar, J., et al. "Structure of the Ternary Complex Formed by a Chemotaxis Receptor Signaling Domain, the CheA Histidine Kinase, and the Coupling Protein CheW

as Determined by Pulsed Dipolar ESR Spectroscopy.." *Biochemistry* 49.18 (2010): 3824-41.

Bilwes, A. M., et al. "Nucleotide Binding by the Histidine Kinase CheA.." *Nature structural biology* 8.4 (2001): 353-60.

Bilwes, A.M., et al. "Structure of CheA, a Signal-Transducing Histidine Kinase.." *Cell* 96.1 (1999): 131-41.

Boukhvalova, M. S., F. W. Dahlquist, and R. C. Stewart. "CheW Binding Interactions with CheA and Tar. Importance for Chemotaxis Signaling in Escherichia Coli.." *The Journal of biological chemistry* 277.25 (2002): 22251-9.

Boukhvalova, Marina, Ricaele VanBruggen, and Richard C. Stewart. "CheA Kinase and Chemoreceptor Interaction Surfaces on CheW." *Journal of Biological Chemistry* 277.26 (2002): 23596-603.

Bray, D., M. D. Levin, and C. J. Morton-Firth. "Receptor Clustering as a Cellular Mechanism to Control Sensitivity.." *Nature* 393.6680 (1998): 85-.

Briegel, A., et al. "Universal Architecture of Bacterial Chemoreceptor Arrays." *Proceedings of the National Academy of Sciences of the United States of America* 106.40 (2009): 17181-6.

Briegel, A., et al. "Activated Chemoreceptor Arrays Remain Intact and Hexagonally Packed.." *Molecular microbiology* 82.3 (2011): 748-57.

Briegel, A., et al. "Location and Architecture of the Caulobacter Crescentus Chemoreceptor Array.." *Molecular microbiology* 69.1 (2008): 30-41.

Brunger, A. T. "Version 1.2 of the Crystallography and NMR System.." *Nature protocols* 2.11 (2007): 2728-33.

Cantwell, B. J., et al. "CheZ Phosphatase Localizes to Chemoreceptor Patches Via CheA-Short.." *Journal of bacteriology* 185.7 (2003): 2354-61.

Coleman, M. D., et al. "Conserved Glycine Residues in the Cytoplasmic Domain of the Aspartate Receptor Play Essential Roles in Kinase Coupling and on-Off Switching." *Biochemistry* 44.21 (2005): 7687-95.

Duke, T. A., and D. Bray. "Heightened Sensitivity of a Lattice of Membrane Receptors.." *Proceedings of the National Academy of Sciences of the United States of America* 96.18 (1999): 10104-8.

Endres, R. G., J. J. Falke, and N. S. Wingreen. "Chemotaxis Receptor Complexes: From Signaling to Assembly." *PLoS computational biology* 3.7 (2007): e150.

Endres R. G., et al. "Precise Adaptation in Bacterial Chemotaxis through "Assistance Neighborhoods"." *Proceedings of the National Academy of Sciences of the United States of America* 103.35 (2006): 13040-4.

Erbse, A. H., and J. J. Falke. "The Core Signaling Proteins of Bacterial Chemotaxis Assemble to Form an Ultrastable Complex." *Biochemistry* 48.29 (2009): 6975-87.

Erhardt, M., and K. T. Hughes. "C-Ring Requirement in Flagellar Type III Secretion is Bypassed by FlhDC Upregulation.." *Molecular microbiology* 75.2 (2010): 376-93.

Gestwicki, J. E., et al. "Evolutionary Conservation of Methyl-Accepting Chemotaxis Protein Location in Bacteria and Archaea.." *Journal of bacteriology* 182.22 (2000): 6499-502.

Gestwicki, J.E., et al. "Inter-Receptor Communication through Arrays of Bacterial Chemoreceptors.." *Nature* 415.6867 (2002): 81-4.

Goldman, J. P., M. D. Levin, and D. Bray. "Signal Amplification in a Lattice of Coupled Protein Kinases." *Molecular bioSystems* 5.12 (2009): 1853-9.

Greenfield, D., et al. "Self-Organization of the Escherichia Coli Chemotaxis Network Imaged with Super-Resolution Light Microscopy." *PLoS biology* 7.6 (2009): e1000137.

Griswold, I. J., et al. "The Solution Structure and Interactions of CheW from Thermotoga Maritima.." *Nature structural biology* 9.2 (2002): 121-5.

Guhaniyogi, J., V. L. Robinson, and A. M. Stock. "Crystal Structures of Beryllium Fluoride-Free and Beryllium Fluoride-Bound CheY in Complex with the Conserved C-Terminal Peptide of CheZ Reveal Dual Binding Modes Specific to CheY Conformation.." *Journal of molecular biology* 359.3 (2006): 624-45.

Guhaniyogi J., et al. "Interaction of CheY with the C-Terminal Peptide of CheZ.." *Journal of bacteriology* 190.4 (2008): 1419-28.

Hao, S., et al. "Structural Basis for the Localization of the Chemotaxis Phosphatase CheZ by CheAS.." *Journal of bacteriology* 191.18 (2009): 5842-4.

Hazelbauer, G. L., and W. C. Lai. "Bacterial Chemoreceptors: Providing Enhanced Features to Two-Component Signaling." *Current opinion in microbiology* 13.2 (2010): 124-32.

Hazelbauer, G. L., and P. Engstrom. "Multiple Forms of Methyl-Accepting Chemotaxis Proteins Distinguished by a Factor in Addition to Multiple Methylation.." *Journal of bacteriology* 145.1 (1981): 35-42.

Iancu, Cristina,V., et al. "Electron Cryotomography Sample Preparation using the Vitrobot; an Improved Cryogen for Plunge Freezing.." *Microscopy and microanalysis : the official journal of Microscopy Society of America, Microbeam Analysis Society, Microscopical Society of Canada* 14.5 (2008): 375-9.

Karlinsey, J. E. "Lambda-Red Genetic Engineering in Salmonella Enterica Serovar Typhimurium.." *Methods in enzymology* 421 (2007): 199-209.

Kentner, D., et al. "Determinants of Chemoreceptor Cluster Formation in Escherichia Coli." *Molecular microbiology* 61.2 (2006): 407-1.

Khursigara, C. M., X. Wu, and S. Subramaniam. "Chemoreceptors in Caulobacter Crescentus: Trimers of Receptor Dimers in a Partially Ordered Hexagonally Packed Array." *Journal of Bacteriology* 190.20 (2008): 6805-10.

Kim, K. K., H. Yokota, and S. H. Kim. "Four-Helical-Bundle Structure of the Cytoplasmic Domain of a Serine Chemotaxis Receptor.." *Nature* 400.6746 (1999): 787-92.

Levit, M. N., T. W. Grebe, and J. B. Stock. "Organization of the Receptor-Kinase Signaling Array that Regulates Escherichia Coli Chemotaxis.." *The Journal of biological chemistry* 277.39 (2002): 36748-54.

Li, G., and R. M. Weis. "Covalent Modification Regulates Ligand Binding to Receptor Complexes in the Chemosensory System of Escherichia Coli.." *Cell* 100.3 (2000): 357-6.

Li, M., and G. L. Hazelbauer. "Adaptational Assistance in Clusters of Bacterial Chemoreceptors." *Molecular microbiology* 56.6 (2005): 1617-26.

Li, M., and G.L. Hazelbauer. "Cellular Stoichiometry of the Components of the Chemotaxis Signaling Complex." *Journal of Bacteriology* 186.12 (2004): 3687-94.

Li, M., and G. L. Hazelbauer "Core Unit of Chemotaxis Signaling Complexes." *Proceedings of the National Academy of Sciences of the United States of America* 108.23 (2011): 9390-5.

Mastronarde, D. N. "Automated Electron Microscope Tomography using Robust Prediction of Specimen Movements.." *Journal of structural biology* 152.1 (2005): 36-51.

McCoy, A. J., et al. "Phaser Crystallographic Software.." *Journal of applied crystallography* 40.Pt 4 (2007): 658-674.

McEvoy, M. M., et al. "Two Binding Modes Reveal Flexibility in Kinase/Response Regulator Interactions in the Bacterial Chemotaxis Pathway.." *Proceedings of the National Academy of Sciences of the United States of America* 95.13 (1998): 7333-8.

McRee, D. E., and M. Israel. "XtalView, Protein Structure Solution and Protein Graphics, a Short History.." *Journal of structural biology* 163.3 (2008): 208-13.

Miller, A. S., et al. "CheA Kinase of Bacterial Chemotaxis: Chemical Mapping of Four Essential Docking Sites.." *Biochemistry* 45.29 (2006): 8699-711.

Mowery, Patricia, Jeffery B. Ostler, and John S. Parkinson. "Different Signaling Roles of Two Conserved Residues in the Cytoplasmic Hairpin Tip of Tsr, the Escherichia Coli Serine Chemoreceptor." *Journal of Bacteriology* 190.24 (December 15, 2008): 8065-74.

Nicastro, D., et al. "The Molecular Architecture of Axonemes Revealed by Cryoelectron Tomography.." *Science (New York, N.Y.)* 313.5789 (2006): 944-8.

O'Connor, C., P. Matsumura, and A. Campos. "The CheZ Binding Interface of CheAS is Located in Alpha-Helix E.." *Journal of bacteriology* 191.18 (2009): 5845-8.

Otwinowski, Zbyszek, and Wladek Minor. "[20] Processing of X-Ray Diffraction Data Collected in Oscillation Mode." *Methods in Enzymology*. Volume 276 Vol. Academic Press307-326. Macromolecular Crystallography Part A .

Park, S. Y., et al. "Reconstruction of the Chemotaxis Receptor-Kinase Assembly." *Nature structural & molecular biology* 13.5 (2006): 400-7.

Park, S. Y., et al. "In Different Organisms, the Mode of Interaction between Two Signaling Proteins is Not Necessarily Conserved.." *Proceedings of the National Academy of Sciences of the United States of America* 101.32 (2004): 11646-51.

Pollard, A. M., A. M. Bilwes, and B. R. Crane. "The Structure of a Soluble Chemoreceptor Suggests a Mechanism for Propagating Conformational Signals.." *Biochemistry* 48.9 (2009): 1936-44.

Quezada, C. M., et al. "Helical Shifts Generate Two Distinct Conformers in the Atomic Resolution Structure of the CheA Phosphotransferase Domain from Thermotoga Maritima.." *Journal of molecular biology* 341.5 (2004): 1283-94.

Quezada, C. M., et al. "Structural and Chemical Requirements for Histidine Phosphorylation by the Chemotaxis Kinase CheA.." *The Journal of biological chemistry* 280.34 (2005): 30581-5.

Schroder, G. F., A. T. Brunger, and M. Levitt. "Combining Efficient Conformational Sampling with a Deformable Elastic Network Model Facilitates Structure Refinement at Low Resolution.." *Structure (London, England : 1993)* 15.12 (2007): 1630-41.

Greenfield. D., et al. "Super-Resolution Biomolecular Crystallography with Low-Resolution Data." *Nature* 464.7292 (2010): 1218-22.

Schulmeister, S., et al. "Protein Exchange Dynamics at Chemoreceptor Clusters in Escherichia Coli." *Proceedings of the National Academy of Sciences of the United States of America* 105.17 (2008): 6403-8.

Segall, J. E., M. D. Manson, and H. C. Berg. "Signal Processing Times in Bacterial Chemotaxis.." *Nature* 296.5860 (1982): 855-7.

Shimizu, T. S., and N. Le Novere. "Looking Inside the Box: Bacterial Transistor Arrays." *Molecular microbiology* 69.1 (2008): 5-9.

Skidmore, J. M., et al. "Polar Clustering of the Chemoreceptor Complex in Escherichia Coli Occurs in the Absence of Complete CheA Function.." *Journal of bacteriology* 182.4 (2000): 967-73.

Slocum, M. K., and J. S. Parkinson. "Genetics of Methyl-Accepting Chemotaxis Proteins in Escherichia Coli: Organization of the Tar Region.." *Journal of bacteriology* 155.2 (1983): 565-77.

Smith, R. A., and J. S. Parkinson. "Overlapping Genes at the cheA Locus of Escherichia Coli.." *Proceedings of the National Academy of Sciences of the United States of America* 77.9 (1980): 5370-4.

Sourjik, V., and J. P. Armitage. "Spatial Organization in Bacterial Chemotaxis." *The EMBO journal* 29.16 (2010): 2724-33.

Sourjik, Victor, and Howard C. Berg. "Localization of Components of the Chemotaxis Machinery of Escherichia Coli using Fluorescent Protein Fusions." *Molecular microbiology* 37.4 (2000): 740-51.

Suloway, C., et al. "Fully Automated, Sequential Tilt-Series Acquisition with Leginon.." *Journal of structural biology* 167.1 (2009): 11-8.

Underbakke, E. S., Y. Zhu, and L. L. Kiessling. "Protein Footing in a Complex Milieu: Identifying the Interaction Surfaces of the Chemotaxis Adaptor Protein CheW.." *Journal of molecular biology* 409.4 (2011): 483-95.

Vaknin, A., and H. C. Berg. "Single-Cell FRET Imaging of Phosphatase Activity in the Escherichia Coli Chemotaxis System." *Proceedings of the National Academy of Sciences of the United States of America* 101.49 (2004): 17072-7.

Volz, K., and P. Matsumura. "Crystal Structure of Escherichia Coli CheY Refined at 1.7-A Resolution.." *The Journal of biological chemistry* 266.23 (1991): 15511-9.

Vu, A., et al. "The Receptor-CheW Binding Interface in Bacterial Chemotaxis.." *Journal of molecular biology* 415.4 (2012): 759-67.

Wadhams, G. H., and J. P. Armitage. "Making Sense of it all: Bacterial Chemotaxis.." *Nature reviews.Molecular cell biology* 5.12 (2004): 1024-37.

Wolfe, A. J., B. P. McNamara, and R. C. Stewart. "The Short Form of CheA Couples Chemoreception to CheA Phosphorylation.." *Journal of bacteriology* 176.15 (1994): 4483-91.

Wozniak, Christopher E., Changhan Lee, and Kelly T. Hughes. *T-POP Array Identifies EcnR and PefI-SrgD as Novel Regulators of Flagellar Gene Expression* . 191 Vol. , March 1, 2009 .

Zhang, P., et al. "Direct Visualization of Escherichia Coli Chemotaxis Receptor Arrays using Cryo-Electron Microscopy." *Proceedings of the National Academy of Sciences of the United States of America* 104.10 (2007): 3777-81.

Zhao, Jinshi, and John S. Parkinson. "Mutational Analysis of the Chemoreceptor-Coupling Domain of the Escherichia Coli Chemotaxis Signaling Kinase CheA." *Journal of Bacteriology* 188.9 (May 1, 2006): 3299-307.

CHAPTER THREE

VERSATILE ASSEMBLY OF THE SIGNALING LATTICE ATTRIBUTED TO CHEA P5/CHEW "POLYMERS"

3.1 INTRODUCTION

CheW, the coupling/adaptor protein in the ternary complex, does not have any known enzymatic functions, but has been shown to be critical for the signaling pathway. Cells that lack CheW exhibit extreme smooth swimming bias and cannot respond to stimuli (Parkinson 45-53). Once these cells were complemented with *wt* levels of CheW, normal chemotaxis behavior was restored (Boukhvalova, Dahlquist and Stewart 22251-9).

The role of CheW in tethering CheA to the receptors has been long established. CheW binds to both CheA and MCP with a K_d on the 10 μM scale (Gegner and Dahlquist 750-4; Gegner et al. 975-82). Mutants of CheW that impair the binding of CheW to either CheA or MCP effectively abolish chemotaxis (Boukhvalova, Dahlquist and Stewart 22251-9).

Besides its role as an adaptor, the level of CheW seems to be crucial for chemotaxis. It was found that excessive levels of CheW inhibits the kinase activity and causes defective chemotaxis (Boukhvalova, Dahlquist and Stewart 22251-9; Borkovich et al. 1208-12; Liu et al. 7231-40; Levit, Liu and Stock 6651-8). *In vitro*, excessive levels of CheW cause disassembly of reconstituted stimulatory signaling complexes (Liu et al. 7231-40; Levit, Liu and Stock 6651-8). It was proposed that CheW competes against CheA for binding sites on the MCPs. A recent study proposes that excessive CheW disrupts the MCP trimer-of-dimer formation by competing for the binding sites that

overlaps with the MCP inter-dimer trimerization sites (Cardozo et al. 1171-81). Furthermore, the composition of the ternary complex, especially the stoichiometry of all three components seems to affect the kinase activity. These findings raised the possibility that the role of CheW is more complicated than simply tethering CheA and MCP together.

We established the role of CheW as a scaffolding protein in the rings of alternating CheW/P5 in the signaling lattice (Briegel et al. 3766-71)(described in chapter two). Additionally, we proposed that excessive CheW could replace P5 (hence CheA) in the lattice without disrupting the lattice structure due to the structural similarity of the two proteins. Such a replacement reduces the copies of CheA in the lattice and hence reduces the kinase activity. According to our hypothesis, the resulting lattice, despite being less active, still retains some activity. This remaining activity is in agreement with results from previous biochemical studies (Liu et al. 7231-40; Levit, Liu and Stock 6651-8). The hypothesis that CheW could substitute for CheA and even constitute CheW rings in the lattice (Briegel et al. 3766-71) could also explain why controversial stoichiometries were obtained on the composition of the ternary complex with different preparation techniques (Levit, Grebe and Stock 36748-54; Li and Hazelbauer 3687-3694; Erbse and Falke 6975-6987) and why generally more CheW copies exist than CheA copies do *in vivo* despite the fact that they indeed bind with a 1:1 ratio (Gegner and Dahlquist 750-4).

Because CheA P5 and CheW share a very similar structure and the fact that interactions at the interface between CheA P5 and CheW are mostly hydrophobic in nature, the hetero-oligomerization of CheWs or CheA domains P5 is plausible. For either of the two proteins to substitute for the other in the ring or compose a full ring, one

protein would presumably oligomerize via the same interfaces while retaining its MCP-binding site unoccupied. This chapter is focused on our determination of the crystallographic CheW dimer crystal structure and on the versatile ways to assemble CheW (or P5) into "polymers." Specifically, the construction of the P5-only ring opens up possibilities to versatile ternary complex lattices.

3.1.1 CheW and CheA P5 structures

There is considerable amount of structural information available on CheW. The structures of CheW were determined for *E. coli*, *T. maritima* and *Thermoanaerobacter tengcongensis* by NMR and X-ray crystallography (Park et al. 400-407; Yao, Shi and Liang 1027-32; Griswold et al. 121-5; Li et al. 863-7). Structures of CheW in complexes with other chemotaxis proteins are determined for *T. maritima* (Tm) CheW in complex with TmCheA P4P5, and for Tm CheW in complex with TmCheA P4P5 and the receptor fragment Tm14 (Park et al. 400-407; Briegel et al. 3766-71). The structure of CheV, a chemotaxis protein that consists of a conserved CheW-like domain and a receiver domain is also available (Alexander et al. 494-503). All of the CheW structures share the same fold of two b-barrels. The two intertwined β barrels will be referred to as subunit 1 (N-terminal barrel) and subunit 2 (C-terminal barrel; Fig. 3-1). Each subunit has five β-strands curving around a hydrophobic core. The two subunits are oriented almost perpendicularly to each other and form another hydrophobic core where they interface.

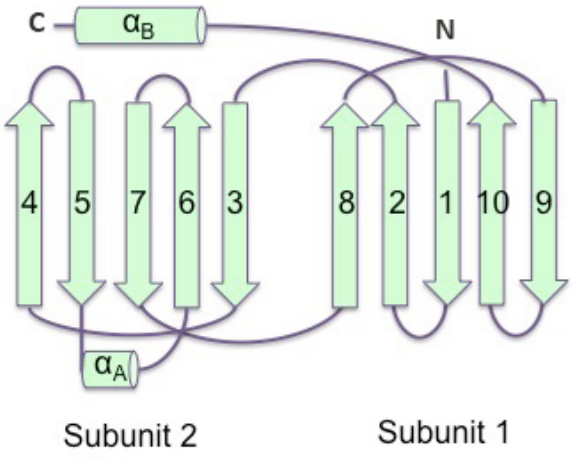

Fig. 3-1. Topology diagram of TmCheW. N- and C- termini are denoted with "N" and "C" in the figure.

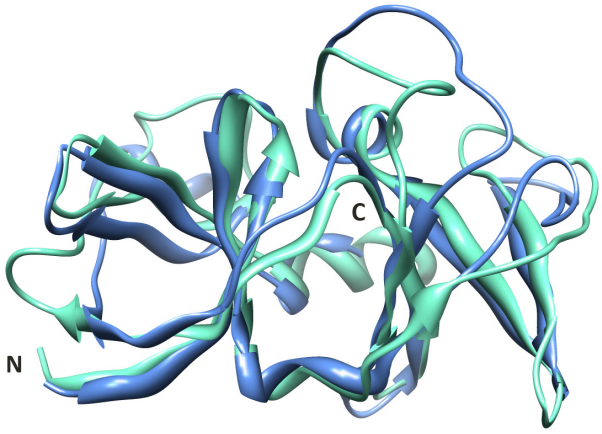

Fig. 3-2 Superposition of TmCheW and TmP5. TmCheW from complex structure of TmCheA P4P5/TmW(PDB: 2CH4) is in green while TmCheA P5 from the same complex structure (PDB: 2CH4) is in blue. The structures of the two proteins are very similar, except for variations in the flexible loop regions and the C-terminus. N- and C- termini are denoted with "N" and "C" in the figure.

As mentioned earlier, the CheA P5 domain is homologous to CheW. Their structures resemble that of each other (Fig. 3-2). The biggest difference between the two structures besides the conformations of the loops is that CheW has a longer C-terminal helix than CheA P5 (e.g. longer by five residues in *T. maritima*).

Among the available crystal structures of CheW, the crystallographic dimer structure of CheW (Fig. 3-3) from *T. tengcongensis* (Yao, Shi and Liang 1027-32) is the only oligomeric structure of CheW molecules. However, in this structure CheW interactions are "face-to-face" (Fig. 3-3) instead of the P5-CheW "head-to-toe" interactions observed in the structures of the complexes (Park et al. 400-407; Briegel et al. 3766-71). Because the "face-to-face" dimer interface overlaps with the MCP binding surface, it is unlikely that CheWs associate with each other in this manner in cells.

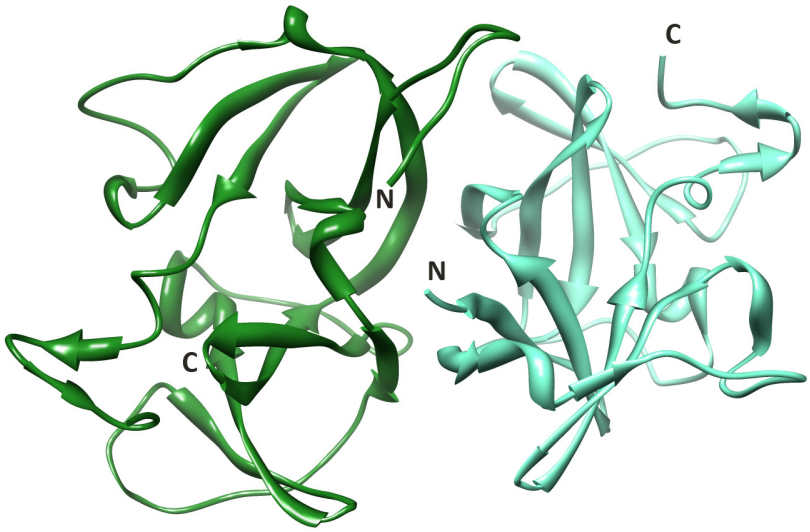

Fig. 3-3 TtCheW dimer crystal structure (PDB: 2QDL) from *T. tengcongensis*. Note that the dimer interface (one molecule colored in dark green, the other colored in light green) in this structure happens to be the interface of CheW/receptor.

3.1.2 CheW (or P5) binding interfaces

As discussed in chapter two, CheW (or P5) binds to MCPs using the cleft region between the two β barrels. The interface between MCPs and CheW/CheAP5 is stabilized mainly by hydrophobic interactions. In terms of CheW-P5 binding, the interactions at the interfaces are also mainly hydrophobic. Each CheA dimer binds to two CheW proteins independently (Gegner and Dahlquist 750-4). The subunit 1 of CheW binds to the subunit 2 of P5 while the subunit 2 of CheW binds to the subunit 1 of P5. We will refer to this type of interaction as "head to toe", subunit 1/ subunit 1 interaction as "head-to-head" and subunit 2/subunit 2 interaction as "toe-to-toe" throughout the chapter.

3.2 MATERIALS AND METHODS

3.2.1 Protein Preparation for Crystallography

The gene encoding for CheW from *T. maritima* was PCR cloned into vector pET28a (Novagen). CheW was expressed with an N-terminal six-Histidine tag in *E. coli* strain BL21 (RIL DE3) (Novagen). *E.coli* cells were inoculated with an overnight culture of the BL21 cells. The cells were harvested after induction of the cells with IPTG at 37 °C at early exponential phase and growth for 7 h. TmCheW was purified from cell lysate with Ni-nitrilotriacetate chromatography, followed by overnight thrombin digestion, and subsequent size-exclusion chromatography (Superdex 75 Hi-load FPLC column in 50

mM NaCl, 100 mM Tris 7.5). Size-exclusion chromatography separated CheW dimers from CheW monomers. For crystallization, only the monomeric CheW fractions were used.

3.2.2 Characterization of CheW by MALS.

Monomeric BSA (Sigma) was first injected onto the size exclusion chromatography (SEC) (Wyatt Technology) that had been equilibrated in gel filtration buffer without glycerol in order to normalize the light scattering detectors and data quality control. Then purified protein samples (1mg/ml to 10 mg/ml) were injected onto the same column. The SEC is coupled to a static 18-angle light scattering detector (DAWN HELEOS-II) and to a refractive index detector (Optilab T-rEX) (Wyatt Technology). Data were collected every second at the flow rate of 1 mL⁄min for 30 mins. The ASTRA program was used for data analysis: the molar weight, the polydispersity of each peak and the molecular weight distributions for the sample were determined.

3.2.3 Crystallization and Data Collection

Rod shaped crystals of TmCheW were grown from 123 μM CheW in the presence of 265 μM Tm14s (107–191), 218 μM CheA Δ289 after 1 month by vapor diffusion from a 2-μL drop [1∶1 mixture of protein and reservoir: 500 μL reservoir of 0.5 M NaAc, 0.05 M $CdSO_4$, pH 5.5]. SDS-PAGE analysis with mass spectrometry analysis confirmed that only CheW is present in these crystals. Most crystals diffracted to 2.8 − 3.5 Å. Crystals were soaked briefly in cryo-protectant consisting of 90/10(vol/vol) reservoir solution with PEG400 prior to data collection in an N_2 cold stream. Diffraction data were collected at 100 K with synchrotron radiation at beamline A1 at the Cornell High Energy Synchrotron Source.

3.2.4 Crystal Structure Determination and Refinement

Diffraction data were processed with HKL2000 (Otwinowski and Minor 307-326). Initial phases were obtained by molecular replacement with PHASER (McCoy et al. 658-674) using one subunit of the CheA Δ354-CheW complex [Protein Data Bank (PDB) 2CH4 chain W] as a search model. Residues 41-51 collided with one other and were therefore removed from the initial model. The residues were later manually built into the resulting electron density maps with XFIT (McRee and Israel 208-13). The modified structure was used as the new probe for molecular replacement with Phenix.

3.3 RESULTS

3.3.1 Oligomerization of CheW

Equilibrium analytical sedimentation showed that CheW exist as a homogenous monomer of molecular weight (MW) of 18 kDa in *E.coli* cells (ref). During size exclusion chromatography of overexpressed CheW, the fractions that correspond to higher oligomers of CheW eluted initially and the majority of the protein eluted later as monomers. Multiple-angle light scattering (MALS) analysis of the supposed CheW monomer peak confirmed its monomeric state, with the expected molecular weight ~18 kDa (Fig. 3-5A). MALS analysis of the oligomerized CheW fractions revealed a mixture of monomers (MW around 20 kDa) and dimers (MW 40 kDa) as well as monomers and dimers in exchange (Fig.3-5B). The existence of a CheW dimer in solution indicates potential specific CheW inter-dimer interactions, but does not exclude the possibility that the dimers are an ensemble of non-specifically bound CheW dimers.

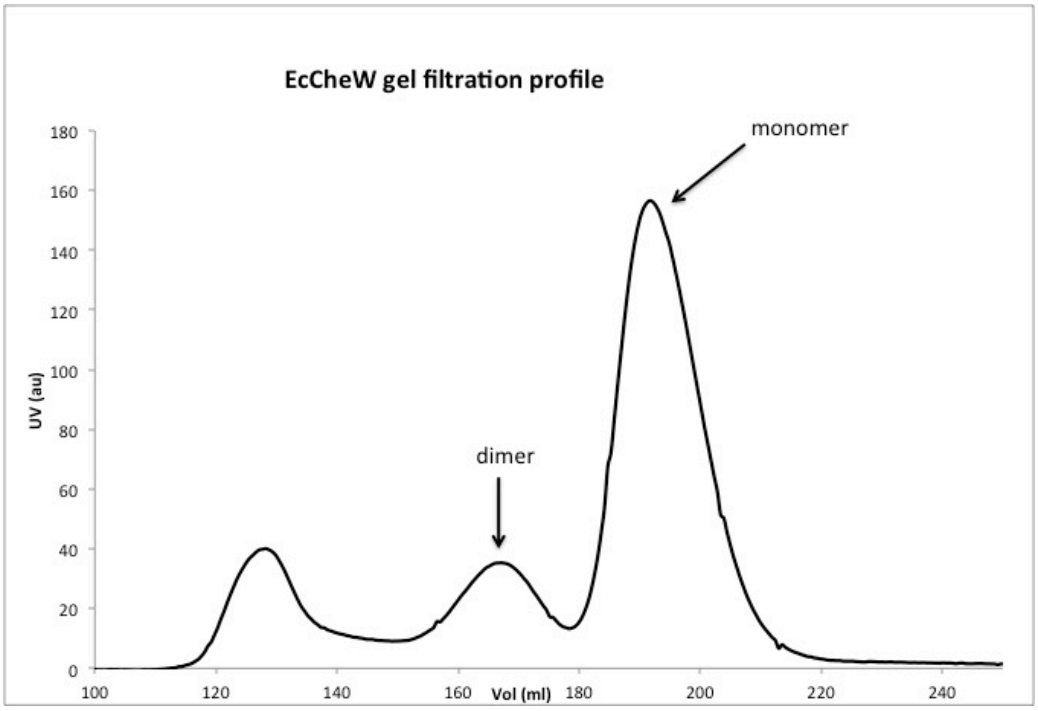

Fig. 3-4 Gel filtration tomography profile of TmCheW. A dimeric form of CheW elutes before the monomeric form of CheW.

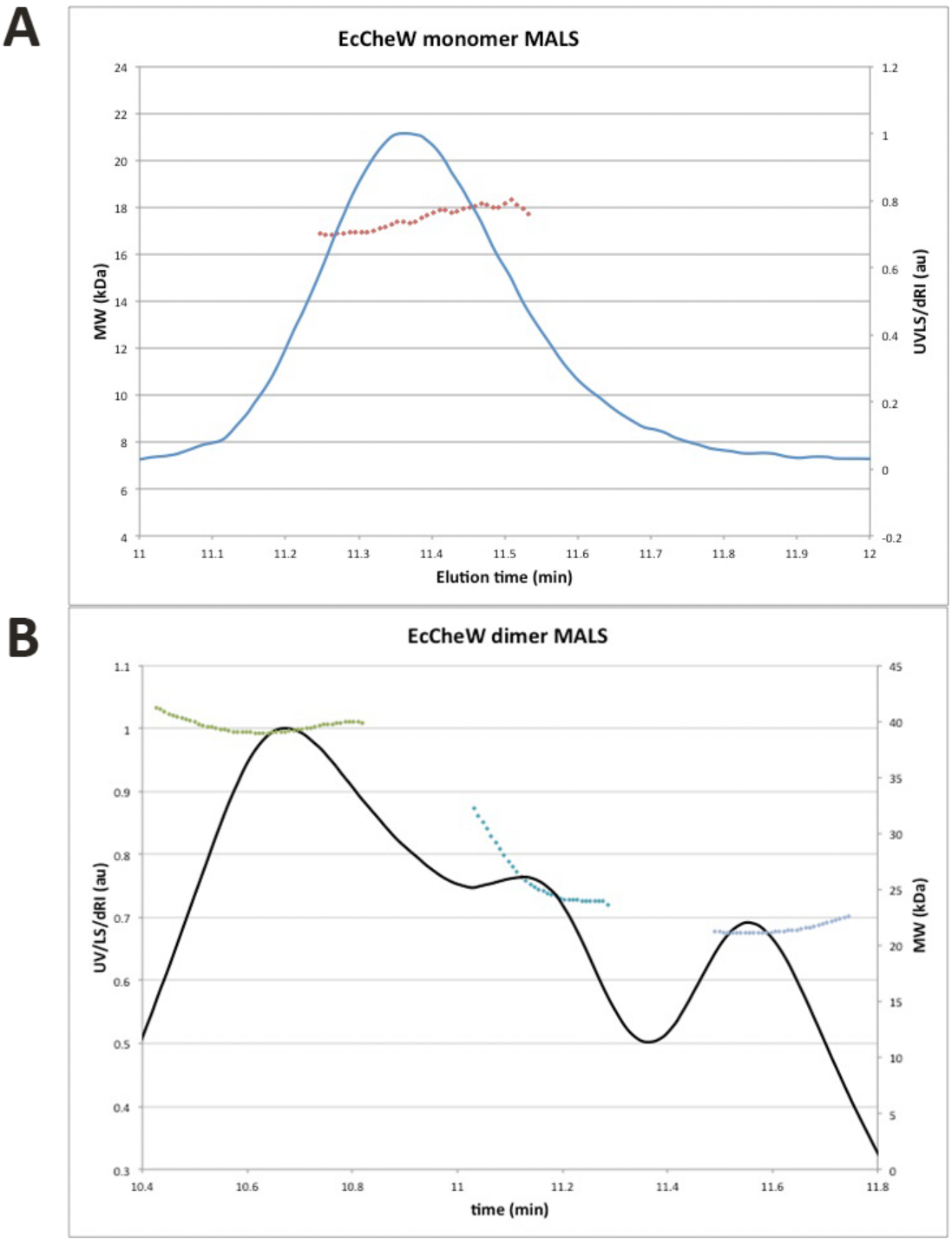

Fig. 3-5 MALS analysis of the two CheW elutes. A. The supposed monomer peak has exclusively monomeric CheW (MW ≈ 17 kDa). B. The supposed dimer peak has a

mixture of dimeric (MW ≈ 40 kDa), monomeric CheW (MW ≈ 22 kDa) and the two forms exchanging equilibrium.

3.3.2 CheW dimer structure

In the newly determined crystallographic CheW dimer structure, the overall structure of CheW remains the same as previously seen in CheW structures. In this structure, the CheW dimers do not interact "head-to-toe", but rather "toe-to-toe," which is more symmetrical than the P5/CheW structure observed in the ternary complex structure. The intra-dimer interface involves β4 and β5 of subunit 2 and the loop between β3 and β4 from both monomers (Fig. 3-6A, Fig. 3-7). The dimer interface interaction is mainly attributed to the hydrophobic interactions as seen in the P5/CheW lattice interfaces and the potential hydrogen bonds between the loops that connect β3 and β4 (Fig. 3-7). Interestingly, the C-terminal helix, which is the most divergent region between P5 and CheW structures, also contributes to the interface. The side chain of Thr146 on the C-terminus helix of one monomer forms a hydrogen bond with Asn54 on the loop between β4 and β5 of the other monomer (Fig. 3-8B).

Due to the "toe-to-toe" conformation of the CheW dimer, if one monomer of the dimer is superimposed with the CheW in the ring of P5/CheW in the ternary complex structure, the other monomer of the CheW dimer has to first be tilted about 30° to fit into the plane of the ring, and then be rotated by 180° around the vertical axis that is orthogonal to the ring plane to be overlaid on the P5 of the P5/CheW ring. The conformation of the CheW dimer positions the MCP binding interface on the opposite side of the dimer surface.

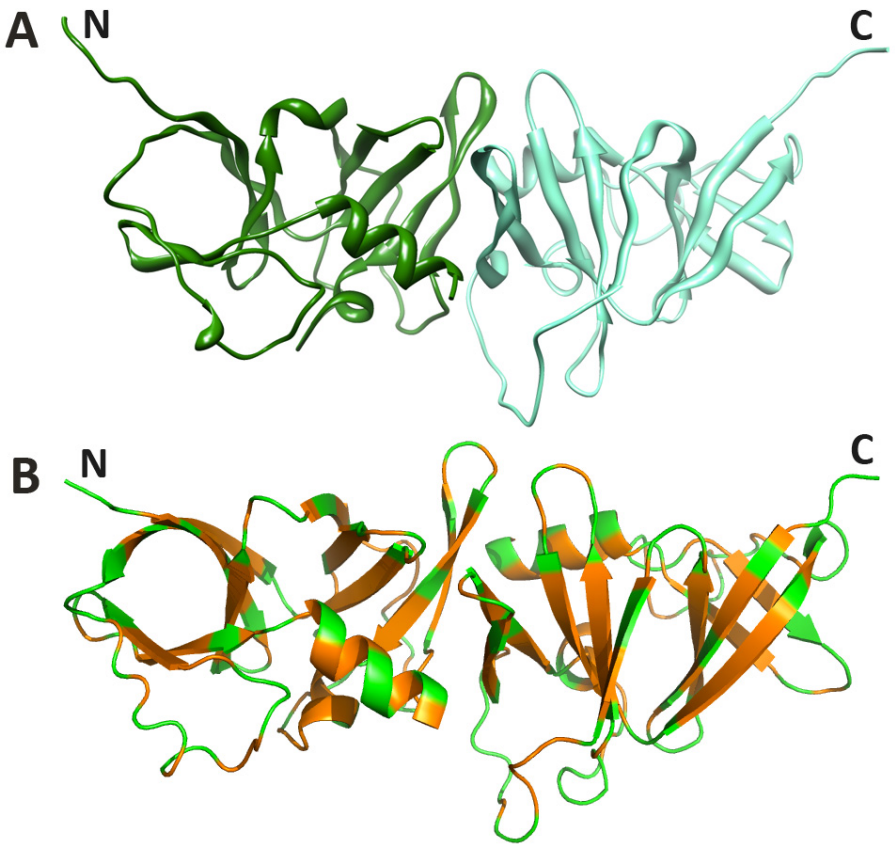

Fig. 3-6 TmCheW crystallographic dimer structure. A. Each monomer of the CheW dimer is colored with different shades of green. B. The hydrophobic residues of the CheW dimers are colored in orange. N- and C- termini are denoted with "N" and "C" in the figure.

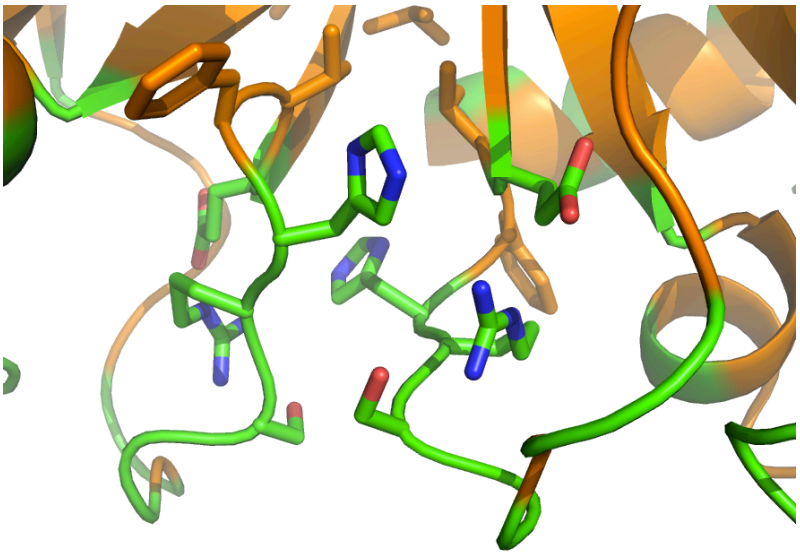

Fig. 3-7 Interaction between loops in the CheW dimer structure. Residues that are predicted to contribute to the interaction by Protein interface surface assembly analysis (PISA) are denoted as stick model on the loop between β3 and β4.

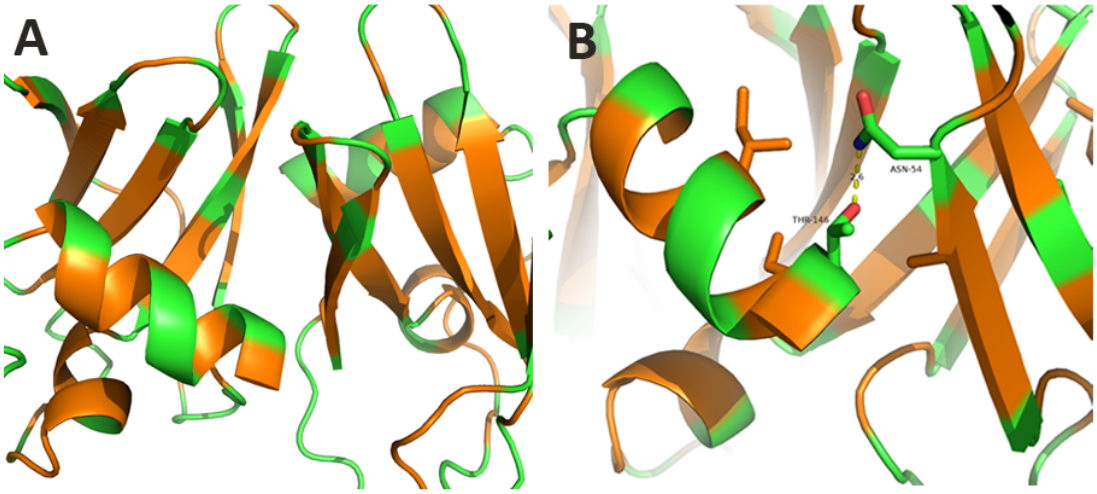

Fig. 3-8 The C-terminus of CheW at the interface. A. Location of the C-terminus of CheW at the interface. B. Hydrogen-bond between the side chain of Thr146 on one monomer to the side chain of Asn54 on the other monomer.

3.4 DISCUSSION

It is not possible to construct a ring of CheW molecules using the CheW dimer structure as a building block. However, we are able to construct a P5-only ring that resembles the P5/CheW ring discussed in chapter two.

Although not being able to form a ring, the CheW dimer can be used to build longer chains with CheA P5 molecules. Although we cannot exclude the possibility that CheW adopts the conformation of the P5 crystallographic dimer and forms a CheW-only ring as predicted in chapter two, the conformation of the CheW dimer gives rise to another hypothesis: An excessive CheW concentration disrupts chemotaxis by competing with CheA for CheW binding site and that leads to the disruption of the CheW/P5 ring.

Fig. 3-9 Crystallographic dimer of CheA P5. TmCheA P5 dimers take a "toe-to-toe" type of interaction. N- and C- termini are denoted with "N" and "C" in the figure.

3.4.1 Construction of P5-only rings

In the crystal complex structure of TmCheA P4P5 and TmCheW that was previously determined in the Crane Group, there are two types of P5 dimers: one non-

crystallographic dimer and one crystallographic dimer. The crystallographic dimer also bears the "toe-to-toe" type of interaction, but the orientation is different than that of the CheW dimer. We superimposed one P5 monomer from the crystallographic dimer onto one P5 of the P5/W ring and applied the same operation to the other two P5 in the P5/W ring. Such operations allowed us to successfully generate a CheA P5 only ring. Amazingly, the one P5 monomer of the dimer (the passively moved one), which was translated only because of the superposition of the other P5 monomer (actively moved one), aligns well with the neighboring CheW in the ring (Fig. 3-10A). More interestingly, the two β barrels of the passively moved P5 align with the opposite subunits of neighboring CheW (Fig. 3-10B&C). Such an arrangement leaves the MCP binding interface of the passively moved P5 on the outside of the ring, on the same side of the P5 dimer surface. The exposure of the MCP binding cleft to the outside of the ring allows P5 rings to bind the hexagonally packed receptors the same way the P5/CheW rings do.

The resulting modeled ring of P5 molecules comprises three crystallographic dimer of P5, resembling the ring of P5/CheW observed in the lattice structure (Briegel et al. 3766-71)(Fig.3-11 A). In this P5 ring, the passively moved monomer of one P5 dimer has an extend loop in subunit 1, which interact with the same loop of the adjacent P5 dimer (Fig. 3-11B). Such "head-to-head" type of interaction has not been observed before. However, due to the similarity of the two β-barrels, it is possible that such an interaction exists and perhaps this interaction involves the loops as seen in the P5-only ring. If such "head-to-head" interaction exists in cells, the composition of the ring would vary from 1:1 as in the P5/CheW ring of the lattice structure because each ring can have stochastic copies of CheA P5 and CheW. The hexagonal array can therefore be packed

with much more versatility than what was proposed in chapter two. Possibly every hexagon of the array could be filled with mixed CheW/P5, P5-only or CheW-only rings.

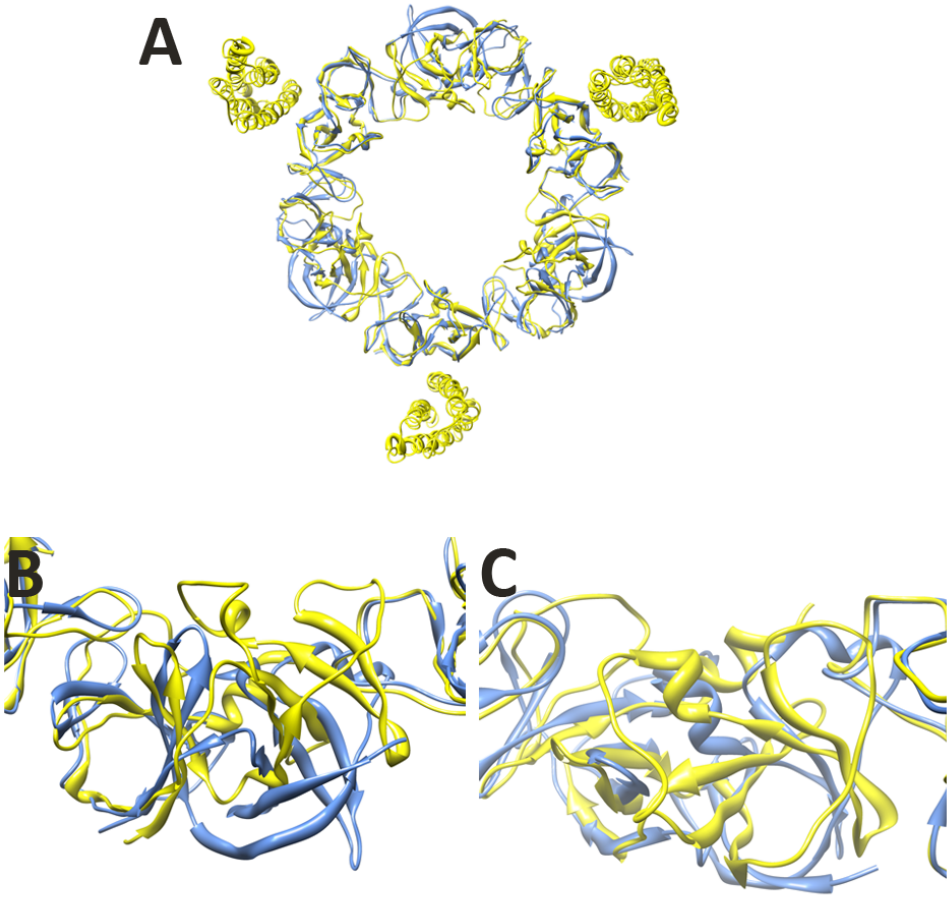

Fig. 3-10 Superposition of the constructed P5 ring (blue) over the CheA P5/CheW ring (yellow). A. One ring from the donut of the ternary complex structure was adopted to construct the P5 ring. B. The passively moved P5 aligning with the CheW in the ring. Top view of the β barrel on the left (subunit 2 of P5, subunit 1 of CheW) of the figure is shown. The other β barrel (subunit 1 of P5, subunit 2 of CheW) is at

almost 90° from the subunit 2. C. Top view of the β barrel on the left (subunit 1 of P5, subunit 2 of CheW).

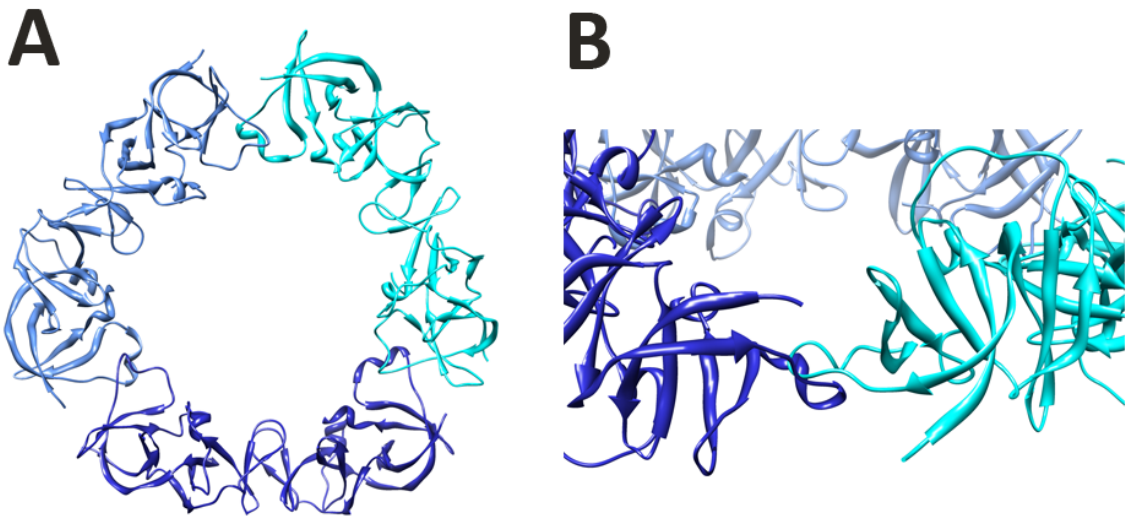

Fig. 3-11 Constructed P5 ring. A. P5 rings composed of three crystallographic dimers. B. The subunit 1 to subunit 1 interaction in the P5 ring.

3.4.2 CheW/P5 and P5 chains

With the CheW dimer and two types of CheA P5 dimers, a few types of chain structures can be generated. Two of them are exemplified in Fig. 3-12. Chain structures cannot be fitted into the MCP lattice in which CheW and P5 alternates to form the ring at the base of the MCPs (Briegel et al. 3766-71) , but they could represent the conformations of the cytosol population of CheW and CheA.

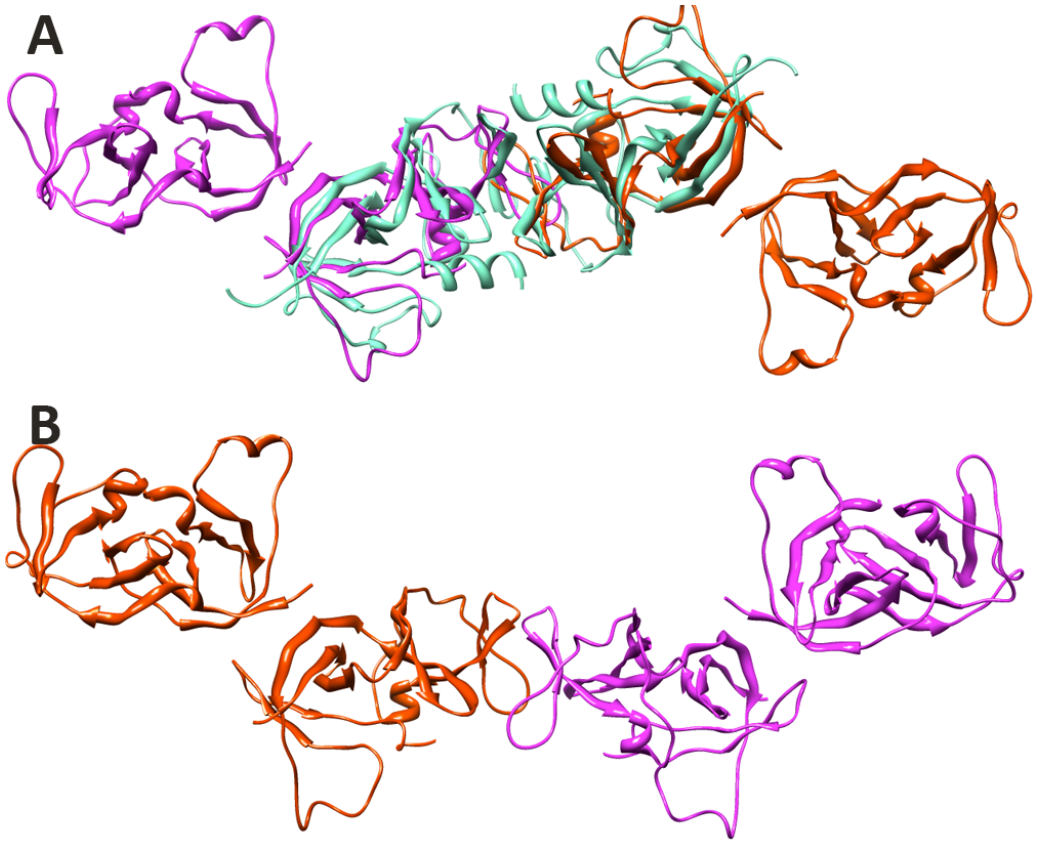

Fig. 3-12 Construction of CheW/P5 and P5 chains. A. CheW/P5 chain. CheW is colored in cyan. Two non-crystallographic P5 dimers are colored in red and magenta, respectively. B. P5-only chain. The centered dimer is the crystallographic dimer, each monomer of which is aligned with a non-crystallographic dimer on both sides.

3.4.3 The role of the C-terminus helix

The truncation of the C-terminus helix increases the binding affinity of CheW to MCP by three-fold despite the fact that the C-terminal helix is not at the MCP/CheW interface. CheW mutant with deletions of the C-terminal residues can also facilitate the incorporation of *wt* CheW into the ternary complex (Zhao and Parkinson 3299-3307; Boukhvalova, Dahlquist and Stewart 22251-9). We observed that the C-terminus of

CheW is involved in the CheW dimer interface. It is possible that CheW with the deletion of the last C-terminus helix mimics the structure of CheA P5 to greater extent than *wt* CheW and can be incorporated into CheW-only rings or have increased copies in the P5/CheW ring. The increase of binding affinity of the C-terminal deletion construct to MCP still requires additional investigation.

Summary

In this chapter, we discussed the structure of the crystallographic CheW dimer from *T. maritima* and proposed that an excess of CheW copies competes with CheA for CheW binding site and hence breaks the ring of P5/CheW, which leads to defective chemotaxis. We also constructed a P5-only ring that resembles the ring structure of P5/CheW and discussed the potentials of having more versatility in the lattice assembly.

REFERENCES

Alexander, R. P., et al. "CheV: CheW-Like Coupling Proteins at the Core of the Chemotaxis Signaling Network.." *Trends in microbiology* 18.11 (2010): 494-503.

Borkovich, K. A., et al. "Transmembrane Signal Transduction in Bacterial Chemotaxis Involves Ligand-Dependent Activation of Phosphate Group Transfer.." *Proceedings of the National Academy of Sciences of the United States of America* 86.4 (1989): 1208-12.

Boukhvalova, M. S., F. W. Dahlquist, and R. C. Stewart. "CheW Binding Interactions with CheA and Tar. Importance for Chemotaxis Signaling in Escherichia Coli.." *The Journal of biological chemistry* 277.25 (2002): 22251-9.

Briegel, A., et al. "Bacterial Chemoreceptor Arrays are Hexagonally Packed Trimers of Receptor Dimers Networked by Rings of Kinase and Coupling Proteins.." *Proceedings of the National Academy of Sciences of the United States of America* 109.10 (2012): 3766-71.

Cardozo, M. J., et al. "Disruption of Chemoreceptor Signalling Arrays by High Levels of CheW, the Receptor-Kinase Coupling Protein.." *Molecular microbiology* 75.5 (2010): 1171-81.

Erbse, A. H., and J. J. Falke. "The Core Signaling Proteins of Bacterial Chemotaxis Assemble to Form an Ultrastable Complex." *Biochemistry* 48.29 (2009): 6975-87.

Gegner, J. A., et al. "Assembly of an MCP Receptor, CheW, and Kinase CheA Complex in the Bacterial Chemotaxis Signal Transduction Pathway.." *Cell* 70.6 (1992): 975-82.

Gegner, J.A., et al. "Signal Transduction in Bacteria: CheW Forms a Reversible Complex with the Protein Kinase CheA.." *Proceedings of the National Academy of Sciences of the United States of America* 88.3 (1991): 750-4.

Griswold, I. J., et al. "The Solution Structure and Interactions of CheW from Thermotoga Maritima.." *Nature structural biology* 9.2 (2002): 121-5.

Levit, M. N., Y. Liu, and J. B. Stock. "Mechanism of CheA Protein Kinase Activation in Receptor Signaling Complexes.." *Biochemistry* 38.20 (1999): 6651-8.

Levit, M. N., et al. "Organization of the Receptor-Kinase Signaling Array that Regulates Escherichia Coli Chemotaxis.." *The Journal of biological chemistry* 277.39 (2002): 36748-54.

Li, M., and G. L. Hazelbauer. "Cellular Stoichiometry of the Components of the Chemotaxis Signaling Complex." *Journal of Bacteriology* 186.12 (2004): 3687-94.

Li, Y., et al. "Solution Structure of the Bacterial Chemotaxis Adaptor Protein CheW from Escherichia Coli.." *Biochemical and biophysical research communications* 360.4 (2007): 863-7.

Liu, Y., et al. "Receptor-Mediated Protein Kinase Activation and the Mechanism of Transmembrane Signaling in Bacterial Chemotaxis.." *The EMBO journal* 16.24 (1997): 7231-40.

McCoy, A. J., et al. "Phaser Crystallographic Software.." *Journal of applied crystallography* 40.Pt 4 (2007): 658-674.

McRee, D. E., and M. Israel. "XtalView, Protein Structure Solution and Protein Graphics, a Short History.." *Journal of structural biology* 163.3 (2008): 208-13.

Otwinowski, Zbyszek, and Wladek Minor. "[20] Processing of X-Ray Diffraction Data Collected in Oscillation Mode." *Methods in Enzymology.* Volume 276 Vol. Academic Press307-326. Macromolecular Crystallography Part A .

Park, S. Y., et al. "Reconstruction of the Chemotaxis Receptor-Kinase Assembly." *Nature structural & molecular biology* 13.5 (2006): 400-7.

Parkinson, J. S. "Complementation Analysis and Deletion Mapping of Escherichia Coli Mutants Defective in Chemotaxis.." *Journal of bacteriology* 135.1 (1978): 45-53.

Yao, W., L. Shi, and D. C. Liang. "Crystal Structure of Scaffolding Protein CheW from Thermoanaerobacter Tengcongensis.." *Biochemical and biophysical research communications* 361.4 (2007): 1027-32.

Zhao, Jinshi, and John S. Parkinson. "Mutational Analysis of the Chemoreceptor-Coupling Domain of the Escherichia Coli Chemotaxis Signaling Kinase CheA." *Journal of Bacteriology* 188.9 (May 1, 2006): 3299-307.

CHAPTER FOUR

CONSTRUCTION OF SOLUBLE CYTOPLASMIC TRIMER-OF-DIMER RECEPTORS TO PROBE COMPLEX CONFORMATION IN KINASE ACTIVATION

4.1 INTRODUCTION

4.1.1 Trimeric arrangement of the MCP dimers

One of the first significant findings critical for the determination of the oligomeric state of MCP homodimers was the crystal structure of the *E.coli* serine sensing MCP Tsr in 1999(Kim, Yokota and Kim 787-92). The MCP cytoplasmic fragment crystalized in a trimer-of-dimer arrangement in which the three dimers relate to each other in the structure by three-fold crystallographic symmetry. However, the construct the authors applied in this study has a N-terminal helix that is 40 residues shorter than the C-terminal helix and resulted in unwounded coiled coils that were thought to potentially contribute to the trimer-of-dimer arrangement. Nonetheless, the burying of the 970 $Å^2$ surface area in the trimer-of-dimer arrangement and the extensive interaction among dimers in the conserved tip region underscores the possibility and underlying driving force for such an arrangement. This structural work has lead to further investigations of the trimeric states of the receptor homo-dimers.

The supposed MCP trimer-of-dimer interfaces as predicted by the Tsr crystal structure appeared to be crucial for signaling. Mutants of the supposed trimer interaction sites on MCPs were examined for receptor clustering and function(Ames et al. 7060-7065). These mutants can abolish cluster formation and/or block the signaling depending on the nature of the mutants.

Crosslinking experiments on the periplasmic and the cytoplasmic domains of MCP also supports the trimer-of-dimer arrangement. *In vivo* crosslinking of the periplasmic domain of MCP resulted in higher-order aggregates, some of which corresponds to the size of trimer of dimer MCPs (Homma et al. 3462-3467). Crosslinking efficacy is higher in the presence of CheA/CheW than in their absence. Interestingly, attractant binding seems to decrease the formation of crosslinked oligomers. The crosslinking of site-directed cysteine mutants *in vivo* by a tri-functional thio-specific agent Tris-(2-maleimidoethyl)amine (TMEA) at the cytoplasmic domain indicates that MCP trimer-of-dimers (mixed and homogenous) exist in living cells(Studdert and Parkinson 2117-22). In this study, neither CheA/CheW or CheR/CheB affects the level of crosslinked trimer-of-dimers, which implies that the cytoplasmic trimer-of-dimer formation is independent of whether the MCPs are in complex with CheA/CheW or their methylation levels. However, it is still unclear why the crosslinked trimer is only observed *in vivo*, but not in cell membranes when they are treated with TMEA.

EM enables direct visualization of the cells and reveals a commonly preserved arrangement of the MCPs in higher-ordered lattices in cells, in which MCPs reside at the vertices of hexagons that are extended into honeycomb-like arrays (Briegel et al. 30-41; Zhang et al. 76-83; Zhang et al. 3777-3781; Briegel et al. 17181-17186; Liu et al. E1481-8) . Interestingly, the trimer-of-dimers of MCPs can be fitted into the electron density at the vertices of the hexagons. Improved resolution of ECT confirms the trimer-of-dimer MCPs at the vertices of the signaling lattice and resolves individual dimers within the trimer-of-dimers (Briegel et al. 3766-71) .

4.1.2 Impact of oligomerization on kinase activation

The application of nanodisks to incorporate full-length MCPs gave the first clue of the effect of the trimer-of-dimer arrangement of MCPs has on kinase activation (Boldog et al. 11509-11514) . Nanodisks are phospholipid bilayers surrounded by amphipathic scaffold proteins(Nath, Atkins and Sligar 2059-69). Nanodisks mimic the natural environment of a membrane, and the application of nanodisks on studying membrane proteins circumvents the problems involved in solubilizing proteins using detergents. Due to the defined size of nanodisks, they were used to isolate a designated number of MCPs in one nanodisk (Boldog et al. 11509-11514). Although the nanodisks with one MCP dimer is able to bind to ligand, transduce signal across membrane and be modified by methylation enzymes, they are not able to stimulate the kinase. On the contrary, nanodisks with at least three parallel dimer MCPs were able to initiate kinase activation (Boldog et al. 11509-11514). This study underscores the role of trimer-of-dimer arrangement in the MCP-dependent regulation of the kinase. A more recent study with nanodisk incorporated MCPs proposed that the kinase activation requires the specific stoichiometry of two MCP trimer-of-dimers: one CheA dimer: two CheW(Li and Hazelbauer 9390-9395).

4.1.3 Trimerization motifs

With the exception of the Tsr crystal structure, all of the trimer-of-dimer MCPs were observed or studied in the membrane or a membrane-like environment. The manipulation of membrane proteins involves multi-step preparation, and the existence of vesicles, detergents or nanodisks complicates data analysis. We aimed to rationally design soluble MCP or MCP fragments that oligomerize into trimer-of-dimers to eliminate these known complications.

There are naturally existing protein trimerization motifs that are known to facilitate the trimerization of their attached domains/proteins. We explored two trimerization motifs: the foldon domain from bacteriophage T4 fibritin (Tao et al. 789-98) and synthetic trimeric coiled coils (Schneider, Lombardi and DeGrado R29-40) in our studies. Foldon is the C-terminal trimerization domain from bacteriophage T4 fibritin that is essential for the fibritin's trimeric structure (Tao et al. 789-98) . Foldon, despite of its small size, can form a stable β propeller with three β hairpins from three protomers. Each β hairpin has only five amino acids per β strand, but extensive hydrogen bonding among the β hairpins together with the hydrophobic interactions among the 3_{10} helices flanking the β hairpins are accounted for by the extremely stable trimeric structure (Tao et al. 789-98; Habazettl, Reiner and Kiefhaber 103-14) (Fig. 4-1). It was shown previously that the foldon domains does not only trimerize rapidly and form stable trimers themselves, but also facilitates the trimerization of other proteins once they were fused onto them (Bhardwaj et al. 1475-85) . Specifically, the foldon domain fused bacteriophage P22 needle gp26 chimera protein self-assembles into trimers which exhibit high stability and refold simultaneously after being removed from denaturation conditions (Bhardwaj et al. 1475-85) .

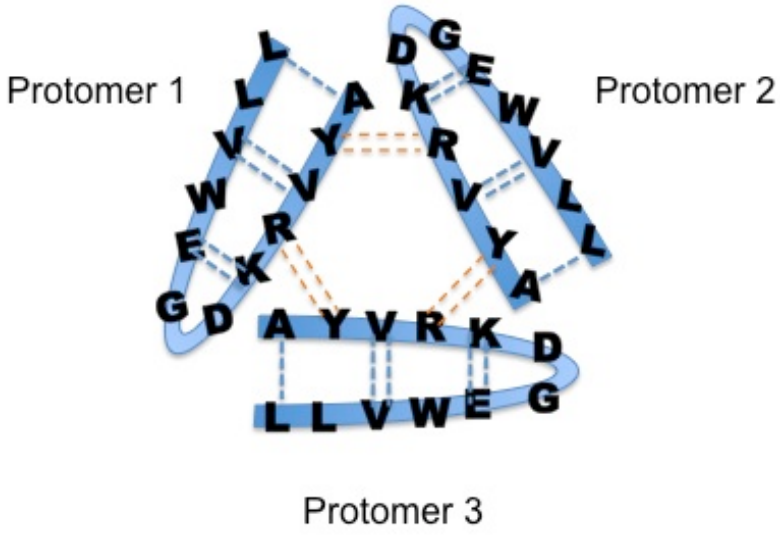

Fig. 4-1 Three protomers of the foldon motif forms a β-propeller. The small foldon motif has extensive hydrogen bonds, mainly between main chain amino groups and carbonyl groups. Intra-molecular hydrogen bonds are depicted in blue dash lines and inter-molecular hydrogen bonds are in orange.

The other trimerization motif we applied is the trimeric coiled coil. Trimeric coiled coils are ubiquitous in nature; they are found in transcription factors, fibrous proteins and cell surface receptors (Coiled coil database http://coiledcoils.chm.bris.ac.uk/ccplus/search/)(Schneider, Lombardi and DeGrado R29-40). Parallel trimeric coiled coils have been identified and investigated in viral fusogenic proteins that mediate attachment of the virus to its cellular host, including HIV, Moloney murine leukemia virus (Gruber and Lupas 679-85; Lupas and Gruber 37-78) . The study of trimeric coiled coils has attracted many researchers and the design of synthetic trimeric coiled coil has expanded (Gruber and Lupas 679-85) . In our study, we applied the repetitive heptads of a synthetic coiled coil sequence EIAAIKQ (gabcdef) that is known to trimerize (personal communications with Dr. Dek Woolfson from Bristol University).

In the heptad repeats, isoleucine residues are the hydrophobic core residues while glutamate and lysine residues form inter-helical electrostatic interactions.

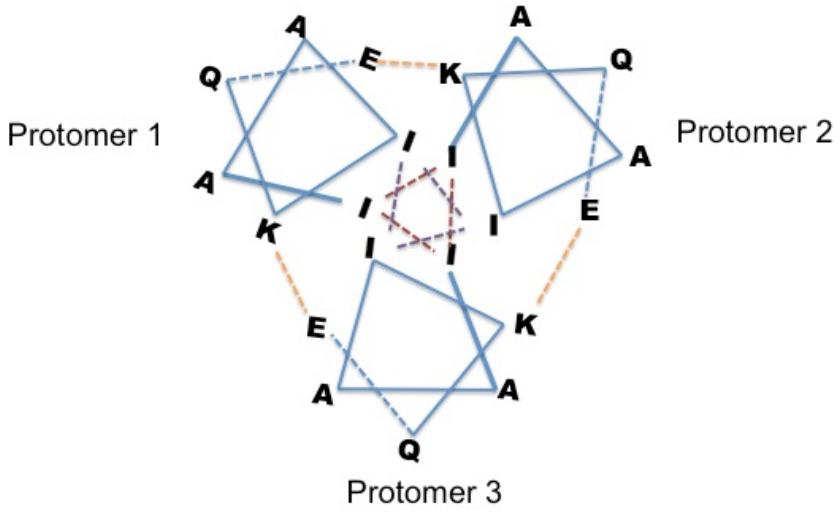

Fig. 4-2 Helical wheel scheme of the parallel trimeric coiled coil. Inter-molecular interactions are shown in dashed lines. Electrostatic interactions are in orange. Hydrophobic interaction among residues are in dark red.

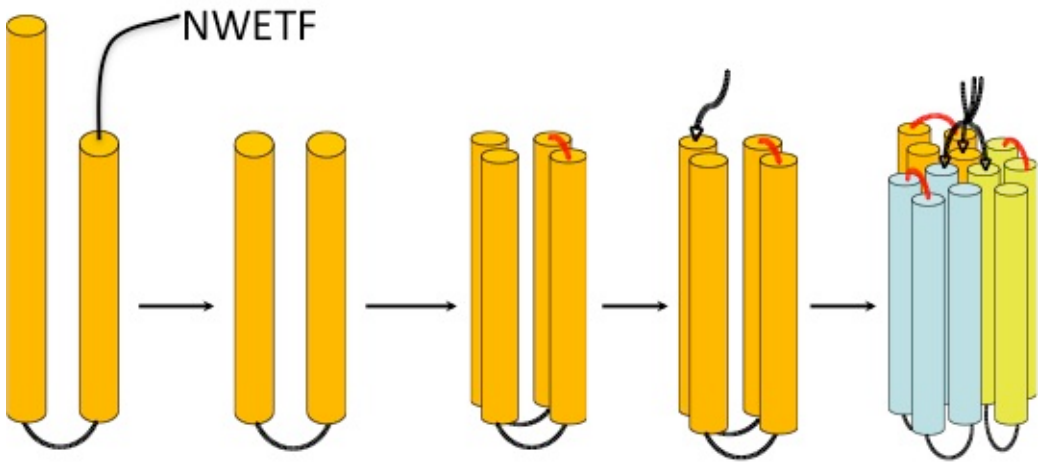

Fig. 4-3 Schematic of the step-by-step construction of the foldon-fused MCP single-chain dimer.

A previous study from the Crane Group investigated the conformation of an inhibitory ternary complex from distance restraints acquired by DEER spectroscopy (Bhatnagar et al. 3824-41) . The goal of this study is to probe the conformation of the stimulatory complex and compare it with that of its inhibitory counterpart (Bhatnagar et al. 3824-41) . We aimed to study the stimulatory complex by DEER spectroscopy for a direct comparison of the results obtained for the inhibitory complex. The starting point was to obtain a soluble construct of the MCP that activates the kinase when in complex with it, since the truncated cytoplasmic domain of the MCP in solution does not activate the kinase. If trimerization is required for MCP to activate the kinase, a MCP trimer-of-dimers is plausible to form a stimulatory complex with CheA coupled by CheW. In this chapter, it will be discussed how we rationally designed and constructed soluble trimer-of-dimer MCP constructs and characterized their binding affinity and activation of the kinase.

4.2 MATERIALS AND METHODS

4.2.1 Constructing the soluble trimer-of-dimer MCPs

We truncated the cytoplasmic domain of the MCP (MCP_c) to be symmetrical by eliminating the HAMP domain and the C-terminal loop. With the symmetrical MCP monomers, we engineered so-called single-chain dimers (sc-dimers) by joining the C-terminus of one monomer with the N- terminus of a second monomer using a seven residue linker. We then fused the trimerization motif onto either the N-terminus or the C-terminus of the sc-dimers.

4.2.2 Cloning of the soluble trimer-of-dimer MCPs

The cytoplasmic region of the aspartate receptor Tar plus a sequence that codes for a seven amino acid peptide GASGGTG at the 3' end was cloned into pET28 with restriction sites. Then a second monomer (can be the same or different than the first monomer) of Tar was cloned into the same vector with restriction sites. The trimerization motif was also introduced into the vector with restriction sites (Fig. 4-6). When a stop codon is cloned at the 3' end, the clone is for sc-dimers. The number of restriction sites that can be used is limited because many restriction sites are encoded in the inserts.

The foldon domain was first cloned into pET28 from the vector GP67 from the Whittaker Lab by Joanne Widom of the Crane Group. The 6-His tag and thrombin cleavage site was cloned before the foldon domain in pET28. When the foldon domain was to be fused onto the C-terminus of the sc-dimers, the foldon domain was recloned into pET28 with deletion of the sequences coding for the 6-His tag and the thrombin cleavage site plus addition of the stop codon on the 3' end. The trimeric coiled coil motif was designed to be fused onto the N-terminus of sc-dimers. Residues 263-515 of Tar correspond to the coiled coil signaling module that was mentioned in chapter one. We varied the starting and ending residues of each monomer in order to introduce changes of the length and identity of the linker (Table 3).

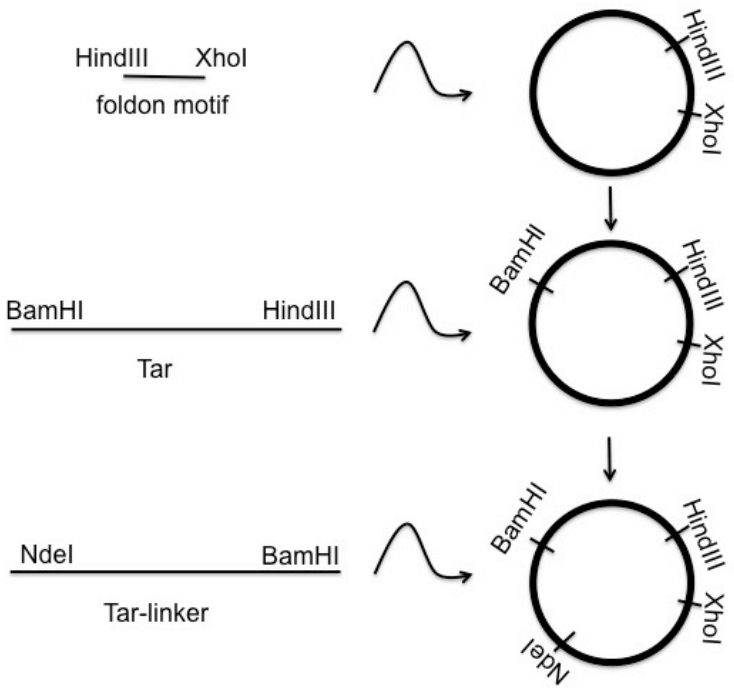

Fig. 4-4 Schematic on the cloning of Tar4Qsc-Cfoldon. Note that the scale of the insert is expanded for clarity and it is not the same scale as the vector.

4.2.3 Modification of linker regions

We optimized the design of the timer-of-dimer MCPs to improve their expression and stability: variation of the linker between the two receptor monomers was completed to achieve optimal conformations of the dimer; variation of the linker between the sc-dimer and the foldon domain was tested to ensure that the tight interactions within the foldon domain and the resulted geometry of the foldon domain do not interfere with the optimal conformations of the trimer-of-dimers and inter-dimer interactions; variation of the C-terminus of the second monomer was completed to study whether the methyltransferase binding site of the MCP affects its stability. The constructs with varied linkers exhibited different expression levels and tendencies toward proteolysis. The

constructs with the trimeric coiled coil motif exhibited lower expression than the constructs with foldon motif, although both trimerization motifs facilitated trimerization. Despite of the effort made to vary the length and identities of the stutter between the trimeric coiled coil motif and the sc-dimers, nothing seemed to improve their expression. Therefore we proceeded only with the constructs with the foldon motif. Among the constructs with the foldon motif (Table 3), one construct with residues 257-521 for the first monomer, residues 257-515 for the second monomer and the foldon motif on the C-terminus (the construct is referred to as Tar-foldon) showed the best expression level and stability, so we focused on this construct in the following studies.

4.2.4 MCP mutants

4.2.4.1 Modification of methylation states of receptors

We changed the modification levels of the MCPs in order to acquire MCPs with higher kinase activation ability. It has been shown that methylated MCPs have enhanced ability of kinase activation (Borkovich, Alex and Simon 6756-60; Sourjik and Berg 437-41; Li and Weis 357-65) . The reversible methylation at specific glutamate residues changes the net charge of the receptors and affects the density of the receptor clusters. The change in density could be one factor that affects the kinase activation level (Besschetnova et al. 12289-12294) . Mutation of the methylation sites on the receptors from Glu to Gln (E302Q, E491Q) mimics the methylated state of the receptors. We made the sc-dimer mutants with four consecutive Gln (4Q) receptors (referred to as Tar4Q sc) to optimize the ability of the constructs to activate the kinase. We also made the 4Q verion of Tar-foldon with the same method as we made the unmodified foldon-fused receptor dimers (the 4Q version of Tar-foldon is referred to as Tar4Q-foldon).

Table 2 Constructs of the foldon-domain fused chimera MCPs

	Methylation states	N-/C-foldon	1st Tar residue numbers	2nd Tar residue numbers
1	QEQE	n/a	257-521	257-521
2	QEQE	N	257-521	257-521
3	QEQE	N	263-515	263-553
4	QEQE	N	263-515	263-515
5	QEQE	N	GGGGG 263-515	263-515
6	QEQE	N	263-515	263-515-NWETF
7	QEQE	C	GGGGG 263-515	263-515
8	QEQE	C	263-515	263-515
9	QEQE	C	263-515	263-521
10	QEQE	C	257-521	263-515
11	QEQE	C	257-521	257-521
12	QEQE	C	257-521	257-515
13	QQQQ	n/a	257-521	257-521
14	QQQQ	C	257-521	257-515
15	QQQQ	C	257-521	257-521
16	QQQQ	C	257-521	257-528

4.2.4.2 Site-specific mutagenesis for DEER labeling

For DEER distance measurement of the trimerization motif fused chimera proteins, each individual labeling site introduced would produce three labeling sites in proximity because of the trimeric state of the chimera protein. To simplify the distance profile, only one labeling site was introduced into one monomer of the chimera protein. Quick-change mutation to Cys residues was carried out on E389 of the first Tar monomer. Then the mutant was ligated into the plasmid that contains the second Tar monomer and the C-terminal foldon motif.

4.2.5 Characterization of C-foldon constructs by MALS.

Monomeric BSA (Sigma) was injected onto the SEC (Wyatt Technology) that had been equilibrated in gel filtration buffer without glycerol in order to normalize the light scattering detectors and data quality control. Then purified protein samples (1mg/ml to 10 mg/ml) were injected onto the same column. The SEC is coupled to a static 18-angle light scattering detector (DAWN HELEOS-II) and a refractive index detector (Optilab T-rEX) (Wyatt Technology). Data were collected every second at the flow rate of 1 mL⁄min for 30 mins. The ASTRA program was used for data analysis, including the molar weight, the polydispersity of each resolved peak and the molecular weight distributions for the sample.

4.2.6 Binding affinity assay

Binding affinity of the Tar4Q-sc to both the co-purified TmCheA and TmCheW, and TmCheW alone were tested. The 6His-tag of Tar4Q-sc was cleaved with thrombin. Co-purified TmCheA and TmCheW, and TmCheW alone have 6His-tag at their N-termini. Proteins to be tested were incubated together with 50 μl Ni^{2+}-NTA resin

(equilibrated with 25 mM HEPES pH 7.5, 500 mM NaCl, 5 mM imidazole, 10% glycerol) for 1 hr at room tempature before rigorously washed by buffer (25 mM HEPES pH 7.5, 500 mM NaCl, 20 mM imidazole, 10% glycerol) to remove non-specifically bound proteins. Then 20 μl of the resin was loaded onto the denaturing Nu-PAGE gel and subject to gel electrophoresis.

4.2.7 Phosphorylation assay

Proteins (CheA, CheW and the MCP constructs) were mixed and incubated together at 4 °C overnight (12 hrs) before carrying out the phosphorylation assay. In the assay, 2μl of the mixture of 1 mM non-radioactive ATP and the radioactive ATP was added to a total reaction volume of 25 μl to initiate the phosphorylation reaction. The reaction was quenched with equal volume of 2×SDS PAGE dye plus 50 mM EDTA at designated time points. Then 40 μl of the quenched reaction mixture was loaded onto a Tris-Glycine gel and subjected to electrophoresis. The radioactivity was measured with a Storm phosphoimager (GE Healthcare).

4.2.8 ATPase coupled assay

The ATPase coupled assay was carried out as described before (Ninfa et al. 9764-9770) . A mixture of 0.6 μM CheA, 1 μM CheW, 13 μM CheY and various concentrations of MCPs were incubated at 0°C for 15 min before ATP was added to initiate the reaction. The coupled reaction was monitored at 340 nm for 15 min or until the consumption of all NADH was visibly completed.

4.2.9 Intra-dimer distance measurement by DEER

CheA or CheA P3P4P5 (d289) was expressed, purified and spin-labeled as described in chapter two. The Tar4Q-foldon was purified and spin-labeled as described in

chapter two followed by subsequent incubation with thrombin to remove the 6His-tag, as the 6His-tag could possibly interfere with the inter-molecular interactions of the foldon domain.

4.3 RESULTS

4.3.1 Characterization of the trimer-of-dimers

Different constructs of trimer-of-dimer MCPs exhibited different expression level and vulnerability towards proteolysis.

Although the expression levels of different constructs vary, all of the chimera protein constructs were determined to exist as trimer-of-dimers by MALS with trace of higher molecular weight (MW) aggregates.

Specifically, the MW of Construct No. 5 in Table 3 corresponds to the MW of three MCP sc-dimers (3×59 = 177 kDa). A total of 88% of calculated mass has an average MW of 168 kDa, roughly the molecular weight of the trimer-of-dimers (Fig. 4-5B). Whereas 11% of the calculated mass has average MW of 209 kDa, which may be attributed to bigger aggregates.

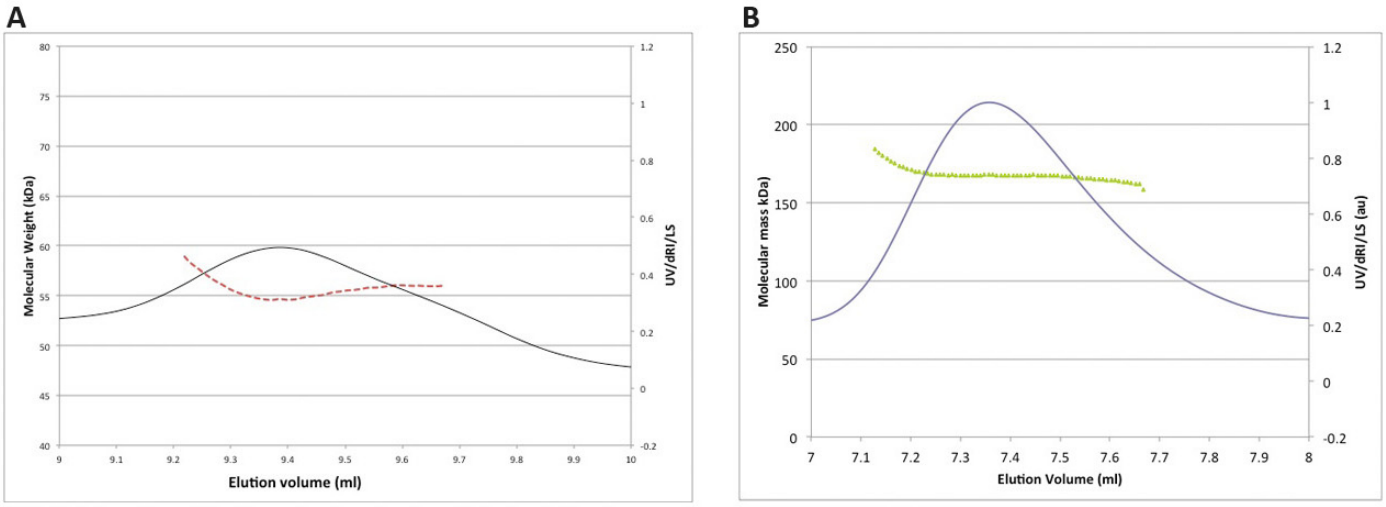

Fig. 4-5 MALS analysis of the oligomerization state of Tar4Q-sc and one foldon-fused sc-dimers. A. The MW of Tar4Q-sc is around 58 kDa. B. The MW of one foldon-fused sc-dimers is 59 kDa. The corresponding MW of the peak is 168 kDa, about three times the MW of a sc-dimer.

4.3.2 Binding ability of Tar4Q single-chain with CheA and CheW

To compare the conformation of CheA in the ternary complexes in different states, CheA with the same labeling sites as in the inhibitory complex(Bhatnagar et al. 3824-41) was applied in the study of the stimulatory complex. The inhibitory complex is comprised of Tm14, TmCheA and TmCheW. The complex that was tested herein was a hybrid complex of CheA/CheW from *T. maritima* with Tar4Q-sc made from the aspartate sensing MCP Tar from *E. coli*. Given that the signaling module of the receptors is highly conserved, the interactions between TmCheA/TmCheW and the Tar4Q-sc should represent those in native complexes.

The binding affinity assay shows that 6His-tagged CheA/CheW and CheW can pull down untagged Tar4Q-sc from the complex solution, which indicates reasonable binding affinity (Fig. 4-6).

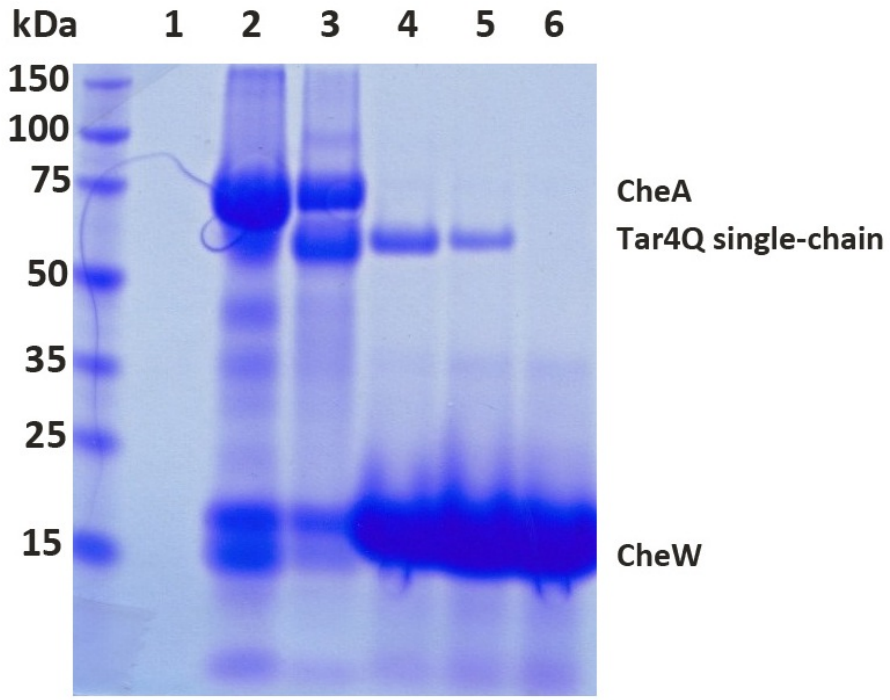

Fig. 4-6 Affinity chromatography of Tar 4Q single-chain with CheA and CheW. Lane 1 to Lane 6: Tar 4Q single-chain only; copurified 6His-CheA/6His-CheW; copurified 6His-CheA/6His-CheW + Tar4Q single-chain; 6His-CheW + Tar 4Q single-chain; 6His-CheW. The protein ladder is shown on the left side of the gel. 6His-CheA denotes CheA with 6His-tag.

4.3.3 Activation of the kinase by the sc-dimers and the foldon fused sc-dimers

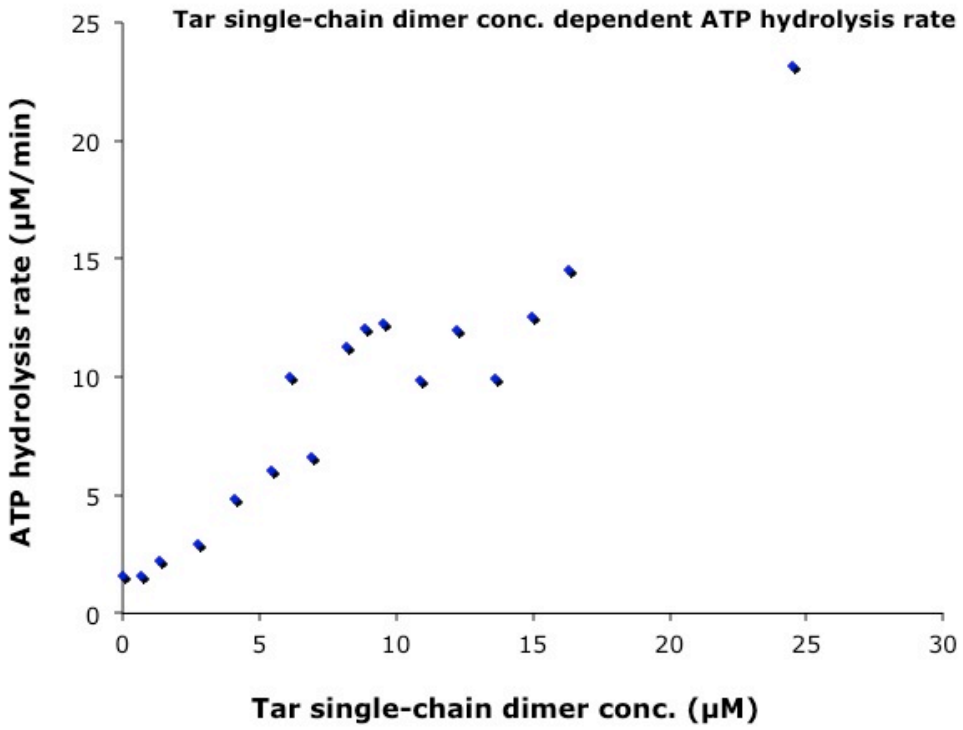

Fig. 4-7 Titration of Tar single-chain on the measurement of its kinase activation ability by the ATPase coupled assay.

Tar sc-dimer can activate the kinase up to ≈ 20-fold as measured in the coupled assay (Fig. 4-7). In the phosphorylation assay where the stoichiometry of the complex proteins is closer to expressed cellular numbers, Tar4Q-sc and Tar4Q-foldon both inhibit the kinase when the MCP dimer/CheA dimer ratio is less than 6, and starts to activate the kinase when the ratio is around 6 (Fig. 4-8C). This effect is CheW dependent: in the absence of CheW, the kinase activity is inhibited with MCP dimer concentration 6 times that of CheA dimer concentration.

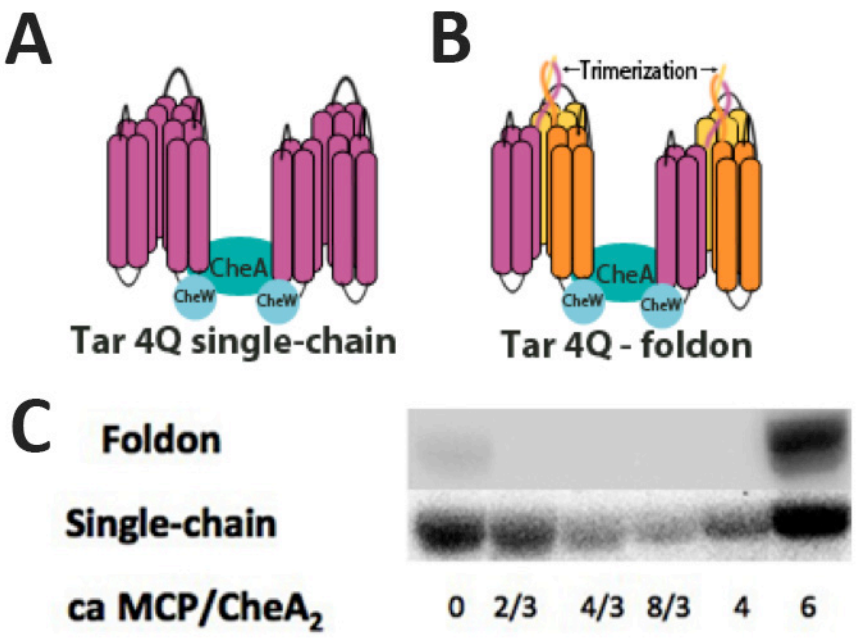

Fig. 4-8 Kinase activation stimulated by single-chain MCP dimers and trimer-of-dimer MCP constructs. A. Schematic of Tar4Q-sc in a stimulatory complex with CheA and CheW. B. Schematic of Tar4Q-foldon in a stimulatory complex with CheA and CheW. C. Phosphorylation assay of Tar4Q-sc and Tar4Q-foldon.

4.3.4 Conformation change in the stimulatory complex by DEER spectroscopy

4.3.4.1 P1 domain

In the inhibitory complex(Bhatnagar et al. 3824-41), the P1 domain of CheA samples a variety of orientations and is believed to be mobile. The P1 domain of unbound CheA also behaves similarly. In the stimulatory complex, the intra-dimer distance of E12 on the P1 domain is still broadly distributed. This result confirms that the P1 domain is still mobile even in the stimulatory complex. The only difference observed in the experiments is that there also exists shorter distance in the P1 domain intra-dimer distance, which

indicates that P1 domains of CheA dimers come into vicinity during the activation of CheA that is regulated by the receptors. We compared the distance profile in the presence and in the absence of ATP and found there is no change in the distance distribution. There seems to be no correlation between the activation states of the kinase and the general mobility of the P1 domain.

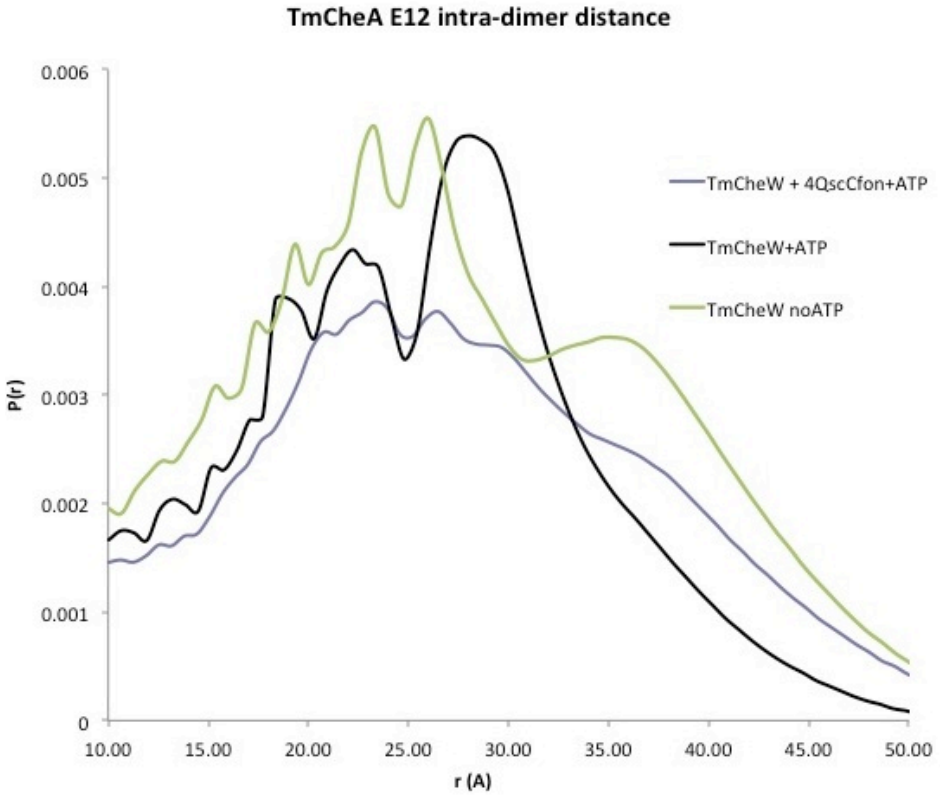

Fig. 4-9 Intra-dimer distance between E12 of P1 domain as measured by DEER. The intra-dimer distance distribution for CheA with CheW in the absence of ATP is shown in green; for CheA with CheW in the presence of ATP is shown in black; for CheA, CheW with Tar4Q-foldon is shown in purple.

4.3.4.2 P4 domain

The kinase domain also exhibits the same behavior as the P1 domain. The intra-dimer distance distribution between the labeled E401 sites is also broad in the presence and

absence of receptors, regardless of whether the receptors are activating or inhibiting the kinase.

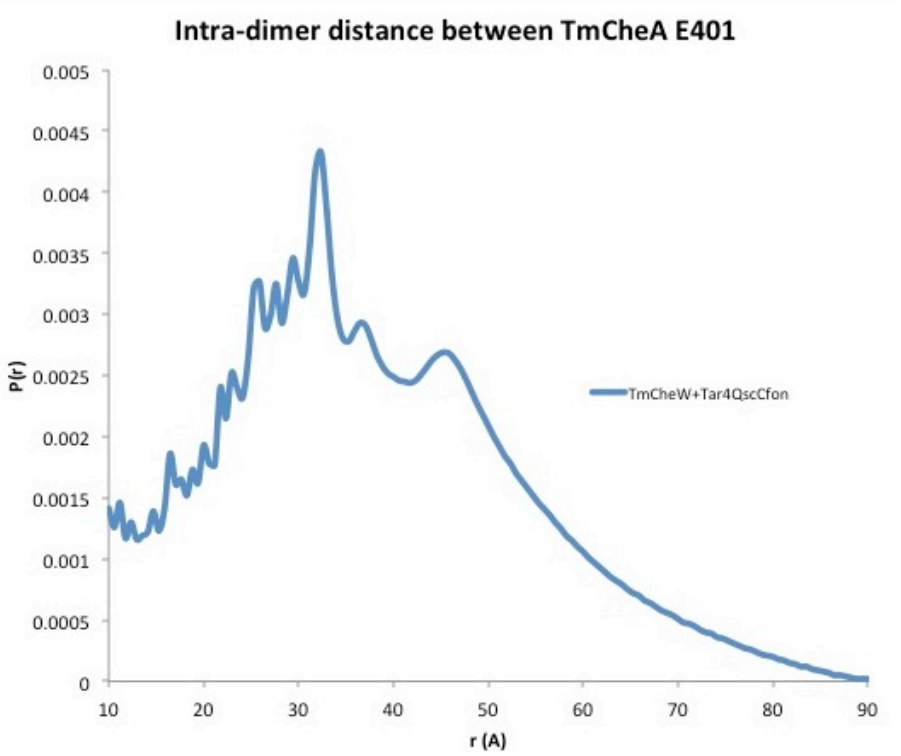

Fig. 4-10 Intra-dimer distance between E401 of P4 domain as measured by DEER. In this sample, the intra-dimer distance measured is of CheA in complex with CheW and Tar4Q-foldon.

4.3.4.3 P5 domain

The only significant difference we observed between the stimulatory and inhibitory complexes is on P5 domain. The intra-dimer distance of the Q545 in the inhibitory complex is bimodal; one of the distances of maximum probability is 36 Å. In the unbound CheA, P5 Q545 has a broader distribution, which is similar to that of the stimulatory complex.

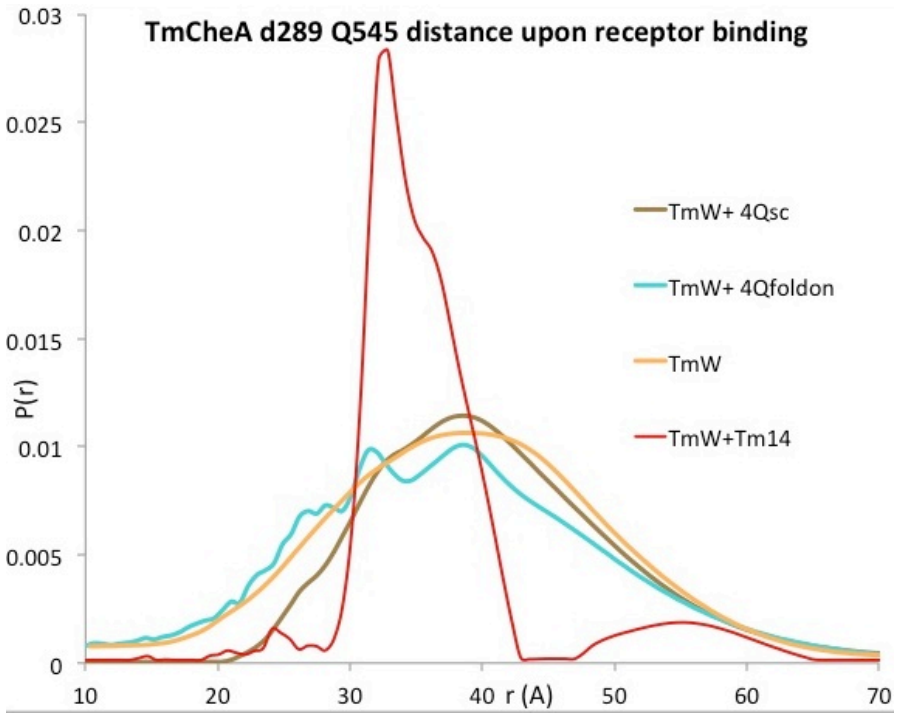

Fig. 4-11 Intra-dimer distance distribution between Q545 on P5 domain upon receptor binding. The intra-dimer distance measured is of CheA in complex with CheW only (orange); CheW and Tm14 (red); CheW and Tar4Q single-chain (brown); CheW and Tar4Q-foldon (cyan).

4.4 Discussion

The construction of soluble trimer-of-dimer MCPs using the trimerization motif proved to be successful. The chimera proteins were characterized with MALS, which confirms the trimeric state of the proteins. The length and identity of the linker which is between the monomers did not affect the expression level or the association of proteins into trimeric state. However, the length and identity of the linker which is between the sc-dimer and the C-terminal foldon domain seems to affect the stability of the protein, with longer linker more susceptible to proteolysis. The chimera proteins with the trimeric

coiled coil motif also trimerize as confirmed by MALS data. But since they did not express well, they were not subject to further characterization.

The chimera construct that exhibited the best expression level and stability was modified on specific glutamate residues to mimic the highly methylated state of the MCP by mutagenesis. The high-methylation-level mimicking (4Q) protein was analyzed by MALS and found to exist as a trimer-of-dimer. This agrees with previous findings that methylation does not change the oligomeric state of the MCPs (Ames et al. 7060-7065) . Subsequently, the high-methylation-level mimicking protein was subjected to affinity chromatography and was confirmed to bind to both TmCheW and TmCheW in complex with TmCheA (Fig. 4-6), indicating the chimera protein forms the ternary complex with CheW and CheA. Given that the signaling module of the MCP is highly conserved among bacteria and archea, the ternary complex formed herein is likely to represent the common features of ternary complexes in its associated activation state.

ATPase coupled assay was carried out to measure the kinase activation ability of the proteins. At the experimental conditions, Tar single-chain showed kinase activation up to ≈ 20 fold (Fig. 4-7). Tar4Q single-chain and Tar4Q-foldon also showed kinase activation measured by this assay. But the proteins were not stable in the assay conditions and tended to aggregate, so only Tar single-chain was examined by this assay. Moreover, because of the sensitivity of the coupled assay and the complication introduced by the presence of other coupled proteins in this assay, we were not able to deduce useful information on the stoichiometry of the stimulatory ternary complex. The phosphorylation assay was subsequently carried out on the Tar4Q single-chain and the Tar4Q-foldon. Interestingly, the kinase activity initially decreased from the basal level of

un-complexed kinases, and not until the ratio of MCP dimer to kinase dimer reached approximately 6:1, did the kinase boost to higher levels. This ratio of 6:1 agrees with the findings of the minimum ratio of MCP dimers required per CheA dimer that was determined by the nanodisk study (Li and Hazelbauer 9390-9395) and the stoichiometry predicted by the lattice model in chapter two. We believe that both Tar4Q-sc and Tar4Q-foldon assemble into a stimulatory ternary complex with CheA and CheW. The resulting complex bears a basic unit of two MCP trimer-of-dimers, two CheW and one CheA dimer (Fig. 4-8A&B).

With site-specific labeling, we were able to measure intra-dimer distance of specific CheA residues in the stimulatory complex with either Tar4Q single-chain or Tar4Q-foldon. The preliminary results indicate that CheA P1 domain and P4 domain undergo little restricted movements regardless of whether CheA is associated in complexes or is by itself. CheA P5 domain has the most different conformations between the inhibitory complex and the stimulatory complex. In unbound CheA which retains basal kinase activity and CheA in the stimulatory complex which has a elevated kinase activity, the intra-dimer distance between Q545 of CheA P5 domain samples a broader distance distribution than the CheA in the inhibitory complex (Fig. 4-11). The intra-dimer distances of maximum probability for the two categories also differs by ≈ 5 Å, with the intra-dimer Q545 distance of the inhibitory complex exhibiting a closer distance ≈ 36 Å than that of stimulatory complex ≈ 40 Å. It should be noted that the intra-dimer distance of Q545 C_α in the signaling lattice structure that is predicted in chapter two is ≈ 41 Å. The differences in the distance distribution of the P5 domain residue suggests different mode of motions of the P5 domain in the active and inactive states. The switch of states

of CheA may be propagated from P5 domain to P1 and P4 domains, which requires further investigation.

Summary

We rationally designed and successfully constructed soluble trimer-of-dimers of the cytoplasmic domain of *E. coli* aspartate sensing MCP Tar. The high-methylation-level-mimicking construct Tar4Q single-chain can bind to CheA and CheW to form the ternary complex and exhibited kinase activation ability. The ratio of the MCP construct to CheA dimer in the stimulatory complex is 6:1, which agrees with previous findings. The intra-dimer distance measurement determined by DEER spectroscopy on specific labeling sites on CheA that is coupled in the stimulatory complex with the MCP construct Tar4Q-foldon indicates relatively free P1 and P4 movement in the CheA activation state and a more dynamic P5 in the stimulatory complex than in the inhibitory complex. The dynamic behavior of P5 in the stimulatory complex may be important to propagation of the signal to P4 or P1 domain, or provide restraints on P1 and P4 domains. Further investigation on the stimulatory complex is required for elucidating the regulation of CheA by MCPs.

REFERENCES

Ames, Peter, et al. "Collaborative Signaling by Mixed Chemoreceptor Teams in Escherichia Coli." *Proceedings of the National Academy of Sciences* 99.10 (2002): 7060-5.

Besschetnova, T. Y., et al. "Receptor Density Balances Signal Stimulation and Attenuation in Membrane-Assembled Complexes of Bacterial Chemotaxis Signaling Proteins." *Proceedings of the National Academy of Sciences of the United States of America* 105.34 (2008): 12289-94.

Bhardwaj, A., et al. "Foldon-Guided Self-Assembly of Ultra-Stable Protein Fibers.." *Protein science : a publication of the Protein Society* 17.9 (2008): 1475-85.

Bhatnagar, J., et al. "Structure of the Ternary Complex Formed by a Chemotaxis Receptor Signaling Domain, the CheA Histidine Kinase, and the Coupling Protein CheW as Determined by Pulsed Dipolar ESR Spectroscopy.." *Biochemistry* 49.18 (2010): 3824-41.

Boldog, T., et al. "Nanodiscs Separate Chemoreceptor Oligomeric States and Reveal their Signaling Properties." *Proceedings of the National Academy of Sciences of the United States of America* 103.31 (2006): 11509-14.

Borkovich, K. A., L. A. Alex, and M. I. Simon. "Attenuation of Sensory Receptor Signaling by Covalent Modification.." *Proceedings of the National Academy of Sciences of the United States of America* 89.15 (1992): 6756-60.

Briegel, A., et al. "Universal Architecture of Bacterial Chemoreceptor Arrays." *Proceedings of the National Academy of Sciences of the United States of America* 106.40 (2009): 17181-6.

Briegel, A., et al. "Bacterial Chemoreceptor Arrays are Hexagonally Packed Trimers of Receptor Dimers Networked by Rings of Kinase and Coupling Proteins.." *Proceedings of the National Academy of Sciences of the United States of America* 109.10 (2012): 3766-71.

Briegel, A., et al. "Location and Architecture of the Caulobacter Crescentus Chemoreceptor Array.." *Molecular microbiology* 69.1 (2008): 30-41.

Gruber, M., and A. N. Lupas. "Historical Review: Another 50th Anniversary--New Periodicities in Coiled Coils.." *Trends in biochemical sciences* 28.12 (2003): 679-85.

Habazettl, J., A. Reiner, and T. Kiefhaber. "NMR Structure of a Monomeric Intermediate on the Evolutionarily Optimized Assembly Pathway of a Small Trimerization Domain.." *Journal of molecular biology* 389.1 (2009): 103-4.

Homma, Motohiro, et al. "Attractant Binding Alters Arrangement of Chemoreceptor Dimers within its Cluster at a Cell Pole." *Proceedings of the National Academy of Sciences of the United States of America* 101.10 (2004): 3462-7.

Kim, K. K., H. Yokota, and S. H. Kim. "Four-Helical-Bundle Structure of the Cytoplasmic Domain of a Serine Chemotaxis Receptor.." *Nature* 400.6746 (1999): 787-92.

Li, G., and R. M. Weis. "Covalent Modification Regulates Ligand Binding to Receptor Complexes in the Chemosensory System of Escherichia Coli.." *Cell* 100.3 (2000): 357-6.

Li, M., and G. L. Hazelbauer. "Core Unit of Chemotaxis Signaling Complexes." *Proceedings of the National Academy of Sciences of the United States of America* 108.23 (2011): 9390-5.

Liu, J., et al. "Molecular Architecture of Chemoreceptor Arrays Revealed by Cryoelectron Tomography of Escherichia Coli Minicells.." *Proceedings of the National Academy of Sciences of the United States of America* 109.23 (2012): E1481-8.

Lupas, A. N., and M. Gruber. "The Structure of Alpha-Helical Coiled Coils.." *Advances in protein chemistry* 70 (2005): 37-78.

Nath, A., W. M. Atkins, and S. G. Sligar. "Applications of Phospholipid Bilayer Nanodiscs in the Study of Membranes and Membrane Proteins.." *Biochemistry* 46.8 (2007): 2059-69.

Ninfa, E. G., et al. "Reconstitution of the Bacterial Chemotaxis Signal Transduction System from Purified Components." *Journal of Biological Chemistry* 266.15 (1991): 9764-70.

Schneider, J. P., A. Lombardi, and W. F. DeGrado. "Analysis and Design of Three-Stranded Coiled Coils and Three-Helix Bundles.." *Folding & design* 3.2 (1998): R29-40.

Sourjik, V., and H. C. Berg. "Functional Interactions between Receptors in Bacterial Chemotaxis.." *Nature* 428.6981 (2004): 437-1.

Studdert, C. A., and J. S. Parkinson. "Crosslinking Snapshots of Bacterial Chemoreceptor Squads.." *Proceedings of the National Academy of Sciences of the United States of America* 101.7 (2004): 2117-22.

Tao, Y., et al. "Structure of Bacteriophage T4 Fibritin: A Segmented Coiled Coil and the Role of the C-Terminal Domain.." *Structure (London, England : 1993)* 5.6 (1997): 789-9.

Zhang, P., et al. "Direct Visualization of Escherichia Coli Chemotaxis Receptor Arrays using Cryo-Electron Microscopy." *Proceedings of the National Academy of Sciences of the United States of America* 104.10 (2007): 3777-81.

Zhang, P., et al. "Direct Visualization of Receptor Arrays in Frozen-Hydrated Sections and Plunge-Frozen Specimens of E. Coli Engineered to Overproduce the Chemotaxis Receptor Tsr." *Journal of microscopy* 216.Pt 1 (2004): 76-83.